To the Graduate Council:

I am submitting herewith a thesis written by Arun Balasundaram entitled "Study of Hydrogel Properties and Immobilization of a Bioluminescent Bioreporter". I have examined the final electronic copy of this thesis for form and content and recommend that it be accepted in partial fulfillment of the requirements for the degree of Master of Science, with a major in Engineering Sciences.

Anthony English

Major Professor

We have read this thesis and recommend its acceptance:

Gary S. Sayler

Mohamed Mahfouz

Accepted for the Council:

Anne Mayhew

Vice Chancellor and Dean of Graduate Studies

(Original signatures are on file with official student records)

Study of Hydrogel Properties and Immobilization of a Bioluminescent Bioreporter

A Thesis

Presented for the

Master of Science

Degree

The University of Tennessee, Knoxville

Arun Balasundaram

May 2006

Dedication

I dedicate this work to my family and thank you for your continuous love, encourage and motivation. This would not have been possible without their support.

Acknowledgements

I would like to thank Dr. Anthony English for his patience, guidance and support throughout my Master's Program at the Mechanical Aerospace and Biomedical Engineering department. I would also like to thank Dr. Gary Sayler for providing me the opportunity to work in one of his challenging real-time projects. I am grateful to my committee member Dr. Mohamed Mahfouz for his valuable suggestions and assistance during the thesis work.

In addition, I would like to acknowledge Dr. John Dunlop, at the electron microscopy department for his assistance with the microscopic imaging sessions. I am really thankful to graduate student Ms. Elizabeth Mitchell and Dr. Steve Ripp at the center for environmental biotechnology for training me in basic microbiological tests and sharing their valuable opinions on more than just my thesis project.

I would like to thank everyone at the MABE dept and Tissue engineering lab for their support and assistance throughout my time at UT.

Abstract

The past decade has witnessed the development of a novel class of sensors; Bioluminescent Bioreporter Integrated Chip biosensors, designed to accurately measure small physical changes in the atmosphere using genetically engineered micro-organisms (bioreporters). The major challenge that now remains is to design a suitable matrix that can hold the bioreporters functionally active over a period of time. The project is an effort to develop and demonstrate alternative methods to favorably immobilize bioreporters without affecting its metabolic functions. The wide collection of literature indicates the successful use of hydrogels for cellular immobilization over the past few years. Hydrogels are inexpensive, easy to fabricate in laboratory conditions, chemically inert, biocompatible, structurally stable, optically transparent and more importantly permeable to target analytes. The equilibrium swelling properties and membrane potential of the hydrogels were studied to gain sufficient insight into its characteristic response over long periods. The knowledge was then used to control the mechanical properties such as stiffness, porosity and surface charge of the hydrogel scaffolds to exactly meet the design criteria of an ideal immobilization matrix. The study particularly involved tests to immobilize cells of *Pseudomonas fluorescens 5RL*, a genetically engineered bioluminescent bioreporter in the volume and surface of charged polyelectrolyte hydrogels and alginate gels. The bioluminescent light assays, Live dead assays, Electron microscopy were used to verify the viability of the immobilized bioreporters. The tests demonstrate the ability of the hydrogels in immobilizing the microorganisms without significantly affecting the physiology of the cells. The results indicate tremendous potential and a major role that hydrogels can play in the immobilization of

microorganisms. Such successful techniques integrated with large scale commercialization could change the face of the conventional sensor technology in every possible areas like waste water remediation, medical diagnostics, sealed room gas analyzers in space shuttles and many more.

Table of Contents

List of Tables

List of Figures

Chapter One

HYDROGELS AND WHOLE CELL BIOSENSORS

INTRODUCTION

The best approach to detect the chemical pollutants in the environment involves long and elaborative experimental protocols, necessitating specialized test conditions and equipments. These complex analyses yield accurate results, but come at a high price of time and money. In addition, it does not provide any information on the bio-availability of the pollutants, their effects on living organisms and their behavior in mixtures [1]. In the light of these technical difficulties there have been serious quests for newer sensor technologies that are simple, robust, inexpensive requiring minimum maintenance. The past decade has witnessed the development of new class of whole cell sensors, incorporating genetically engineered microorganisms. These modified microbial cells better known as bioreporters are specifically designed to detect changes in the environmental conditions and produce a measured response, which is amplified and recorded for appropriate control action. Based on this concept several bioreporters biosensors have been developed for target analyte detection [2-7]. More recently advances in this field have developed bioreporters with multicolored fluorescent proteins and extended them to cyanobacteria, fungi and yeast. The whole cell based Bioluminescent Bioreporter Integrated Chip (BBIC) with a low intensity CMOS microluminometer developed at the University of Tennessee and Oak Ridge National Laboratory is probably the first integrated whole cell biosensor [8-11]. The success of the

bioreporter technology has set the stage for incorporation of whole cells on silicon chips, optical fiber and other configurations. The future seems bright for such simple, yet arguably efficient sensors.

REVIEW OF LITERATURE

A. Biosensors

The technical definition for biosensors is the coupling of biological agents to microelectronic system or device to enable rapid, accurate and low level detection of various substances in body fluids, air or water [13]. The biosensors have been based on the specific interactions between enzymes and their substrates, the recognition between antibodies and antigens, accessibility of specific target molecules to their receptors, the high affinity of nucleic acid strands to their complementary sequences or the whole live cells. The use of a particular kind of a biological agent is case specific. The biosensors differ from each other in the type of the bioreporter system - the method of response used to indicate the detection of target analytes. Accordingly they are classified as whole cell, DNA, enzymatic or antibiotic in Table 1 [14, all tables are in Appendix]. The merits and demerits of the different bioreporter systems are indicated in Table 2 [15]. The parameters such as bioavailability, toxicity and genotoxicity can be more easily assayed using whole cell. This is the primary reason the whole cell array based biosensors have attracted a lot of attention recently. The main components of a biosensor are the biological agent, the encapsulation matrix, the signal processing circuitry which includes a transducer and an amplifier.

B. Bioluminescent Bioreporter Integrated Chip – Biosensors

Bioluminescence. Some species in prokaryotic organisms particularly in the genera *Vibrio*, *Photobacterium*, and *Photorhabdus*, are found to activate a *lucCDABE* genecluster to produce the enzymes required for bioluminescence [9, 21, 22, 23]. Typically the use of the eykaryotic genes in foreign hosts requires the exogenous addition of the luciferin to generate light response. The lux A and B code for heterodimeric luciferase (monooxygenase), the luxC gene for a reductase, the luxD for a transferase, and the luxE for a synthetase. The reductase, transferase, and sythetase form a complex to convert a fatty acid in an acyl carrier protein to an aldehyde at the expense of an ATP and an NADPH molecule. In the presence of oxygen, both the aldehyde and an $FMNH_2$ molecule are co-substrates that are oxidized by the luciferase to generate light (Eq.1)

$$\mathbf{FMNH_2 + R\text{-}CHO + 0_2 \rightarrow FMN + R\text{-}COOH + H_2O + LIGHT}$$

Bioreporters, using the *luxCDABE* cluster are naturally occurring environmental isolates, genetic constructs with constitutive promoters (always expressed), constructs with promoter-lux fusions for specific stress-related responses, constructs with gene regulator systems that are specific for certain analytes or classes of analytes and multiple contructs with different promoters functioning in a genomic-wide array [9].

Bioreporter. A bioreporter is a living microorganism used as a biological agent in a biosensor, integrated with reporter gene fusion to specifically detect and quantify numerous chemical, biological and physical agents [1,18]. It typically contains a gene(transcriptional) regulatory system coupled to a reporter gene that encodes for reporter protein responsible for that signal. Such a system is usually achieved through a genetic transformation to customize the desired response and in cases where it is not native to the cell. Generally a transcriptional regulatory system includes a regulatory gene(s), its expressed regulator protein(s), as well as the promoter/operator DNA sequence that controls the expression of a downstream gene(s) [7]. These elements work together to detect the physical or chemical changes in the environment and control the expression of the gene. The analyte – the target chemical/toxin act as the inducer forms a complex with the regulator protein. This complex interacts with the promoter to initiate the binding of RNA polymerase and the transcription of downstream genes. The bioreporter is tuned to harness the native transcriptional regulator system by fusing the native promoter to the reporter gene(s) and inserting the fusion into a host cell. This enables to signal that the native protein is being expressed and/or the corresponding chemical or physical changes has occurred [9]. Several reporter genes have been isolated from a variety of naturally occurring organisms (Daunert et.al., 2000) and have categorized by the means of detection (Keane et.al., 2002 and Kohler et.al., 2000). There are several reporter genes coding for proteins that produce color changes, fluorescent molecules, electro active species, or bioluminescence, which can be detected and recorded using conventional analytical measuring devices. Some of the calorimetric and fluorescent signaling products also can remain active for long periods of time (even after

cell death), and thus are not suitable for dynamic *in situ* real time monitoring. The mode of signaling incorporated into the bioreporters is typically case specific, but commonly a system is adopted wherein it requires no exogenous addition of substrates for producing the required response. The bioluminescence based systems does not require any additional external source of radiation, since the light producing reaction is biochemical in nature. The strategy also minimizes the background noise and requires no wavelength discrimination [8]. The merits and demerits of the different reporter systems used are listed on Table 2 [2, 7, 15, 16, and 17]. King et.al successfully constructed a bioluminescent bioreporter by insertion of the constitutively expressed *luxCDABE* genes into a *Pseudomonas fluorescens 5RL* strain 5R via the lux transposon Tn4431 carried on a suicide vector pUCD623 [24]. *Pseudomonas fluorescens 5RL* is an environmental strain isolated from contaminated Gas Plant soil. Strain 5R carries a catabolic plasmid (pKA1) based on the model plasmid pNAH7, found in certain organisms equipped with natural naphthalene degradation mechanisms such as *Pseudomonas putida*. A bioluminescent construct was then selected and characterized by inserting the lux cassette into nahG. The luc cassette disrupts the lower operon and prevents the 5RL from converting the salycylates into pyruvate and acetaldehydes and as a result there is a strong induction of the upper pathway leading to a highly luminescent reporter system. The *Pseudomonas fluorescens 5RL* bioreporter has a tetracycline resistant gene, can be grown easily at room temperature, gives a high level of bioluminescence on induction with salycylate and also has a well characterized mechanism of induction [25].

Detection of Bioluminescence. The laboratory testing of the bioreporter system could be performed using a liquid scintillation counter (Wallac). The cultures of bioluminescent bacteria are mixed with appropriate toxic reagent and the response was then recorded. The bioluminescence recorded was then compared to that from a control sample and corresponding magnitude of the decrease is calculated to quantify the level of toxicity. In order to achieve *in situ* real-time monitoring of toxins in a controlled environment, Simpson et.al, conceived and developed a CMOS (Complimentary Metal Oxide Semiconductor) imager chip [8]. The chip measuring 2 x 2 mm approximately included a photodiode and the signal conditioning circuitry mainly to accomplish a current to frequency conversion. The circuit included a gated integrator which allows the collection of photo current and dark current (absence of bioluminescence) onto a capacitor (on-chip) until a threshold voltage is exceeded, after which it resets the input gated integrator by closing the switch across the capacitor. The switch is then opened and process continues to produce pulses that may be timed to obtain pulse interval measurements (inversely proportion to current). The pulse can also be measured for a fixed time interval to provide frequency data that is proportional to the current. The chip demonstrated a large dynamic range, could be exposed to high and low light levels without significant memory effect. The microluminometer could be exposed to room light without significant damage unlike PMT based systems. The CMOS chip tested with TV8 cells (*Pseudomonas putida*) induced to toluene vapors and the bioluminescence was recorded indicating the success of the same [8].

C. Hydrogels

Hydrogels are networked structures of polymer chains cross linked with each other surrounded by an aqueous solution. The polymer chains have acidic or basic groups attached to them. Ionic polymer gels are composed of a solid and a liquid phase. The solid portion of the gel consists of a cross-linked polymer network with acidic or basic group bound to the polymer chains. When immersed in a suitable solvent, the chains in the network become solvated. Crosslink's prevent complete mixing of the polymer chains and the solvent by providing an elastic restoring force that counters the expansion of the network.

MOTIVATION

Naphthalene is a Persistent Bioaccumulative and Toxic (PBT) chemical that does not break down easily in environment, difficult to metabolize in human or ecological food chains through consumption or uptake and may be hazardous to human health or the environment. A PBT chemical, once released to the environment, may present increasing long-term toxic effects to human health and the environment, even if the release was of a small amount. The U.S. Environmental Protection Agency (U.S. EPA) has created a priority in its hazardous waste minimization program to reduce the presence of PBT chemicals, promote pollution prevention and avoid the transfer of PBT chemicals across environmental media. Naphthalene is a high priority PBT chemical. The Agency for Toxic Substances and Disease Registry (ATSDR) reports naphthalene to be found in seventy sites overall thirty seven in the national priorities list and ranks it thirty sixth in the environmental pollutants list. The Environmental Protection Agency categorizes

Naphthalene in-group C as a possible carcinogen in humans. Exposure to Naphthalene may cause irritation and inflammation in eyes, nose and throat. Inhalation or naphthalene intake through skin in large amount destroys red blood cells and causes hemolytic anemia in children. The other symptoms include loss of appetite, sleeplessness, fatigue, nausea, vomiting, diarrhea and blood in urine. These effects can also be passed on from a mother to an unborn child. As a result of these undesirable effects of naphthalene exposure, it would be in the best interest if such harmful chemicals could be detected and eliminated completely if possible.

PROBLEM STATEMENT

Bioluminescent Bioreporter Integrated Chip (BBIC) sensors are a novel class of microbial sensors that produces a measured light signal in response to a target analyte. The low intensity light signal is measured by a CMOS chip and processed for effective detection of the target analyte of choice. Bioreporters can be developed for any known environmental toxin. The major hurdle in the commercialization of such a sensor is to interface the bioreporters to the silicon chip while preserving the viability of the bioreporters over a period of time. Thus a simple, compact and inexpensive immobilization system has to be designed that can hold the bioreporter cells close to the chip, functionally viable over a long period. The immobilant should be chemically inert and permeable to target pollutant with minimum maintenance concerns while maintaining the viability. One of the major design criteria is to keep the bioreporters right next to the chip and electronic circuitry to efficiently measure the bioluminescence on detection of any toxin. The system has to effectively block out any external light signals that can

interfere with the measurement of the low intensity bioluminescent signal, to prevent any false detection. The most challenging part is to design an immobilization system that can optimally feed the bioreporters for it survival and hold them functionally interactive to target analytes. It would be ideal if the system could be designed to maintain the number of immobilized cells, without any further growth to avoid any calibration problems that could arise as a result of the difference in the amount of the bioluminescence detected to the actual change in the concentration of the pollutant. The system should also have the ease of being replaced in the event of any malfunction. The successful system has to be designed to withstand the rugged operating conditions for one to six months.

Chapter Two

MATERIALS AND METHODS

GROWTH MEDIUM

LB (Luria Bertani), a rich medium is used for cell culture. It is a mixture of 10 g of Tryptone, 5 g of yeast extract and 10 g of sodium chloride in a liter of de-ionized water. The pH of the solution is adjusted to 7.5. The medium is then transferred into 100 ml culture flasks and sterilized for 25 minutes (fluid cycle).

MINIMAL SALT MEDIA (MSM)

The MSM is a medium with accurate quantity of the salts required to keep the cells functional. It is a mixture of 2g NaNO3, 0.75g KH2PO4, 0.003g FeCl3, 0.1g MgSO4, 0.005g CaCl2, 0.25g Na2HPO4, 1L-deionizedwater. MSM is used for all the experiments except for the cell culture as it is not a rich medium. MSM is also adjusted to a pH of 7.5 and sterilized before use.

CELL CULTURE

All experiments were performed with *Pseudomonas fluorescens 5RL*. The media used for growth of 5RL cells was Luria Broth (LB) (10g tryptone, 5g yeast extract, 10g NaCl, 1L de-ionized water) supplemented with 14 µl/ml tetracycline (Fisherbrand). A stock solution of tetracycline was prepared with 14 mg tetracycline in 5ml of sterile water and 5ml of ethanol and stored at -20°C in a light safe container. During experiments Minimal Salts Media (MSM) was utilized (2g $NaNO_3$, 0.75g KH_2PO_4, 0.003g $FeCl_3$, 0.1g $MgSO_4$, 0.005g $CaCl_2$, 0.25g Na_2HPO_4, 1L-deionized water). All media is sterilized in a autoclave

at 250°C and 20 PSI for 20 min before use. Tetracycline was added after sterilization of the culture medium.

Choice of monomers

In the experiments conducted, 2-hydroxyethyl methacrylate (HEMA) is used as the neutral monomer and 2-methacryloxy ethyltrimethyl ammonium chloride (MEATAC) was used as the strong basic monomer while N,N-dimethyl aminomethyl methacrylate (DMAEM) was used as the weak basic monomer (Figure 2.1). Combination of these monomers yields biocompatible polymer networks.

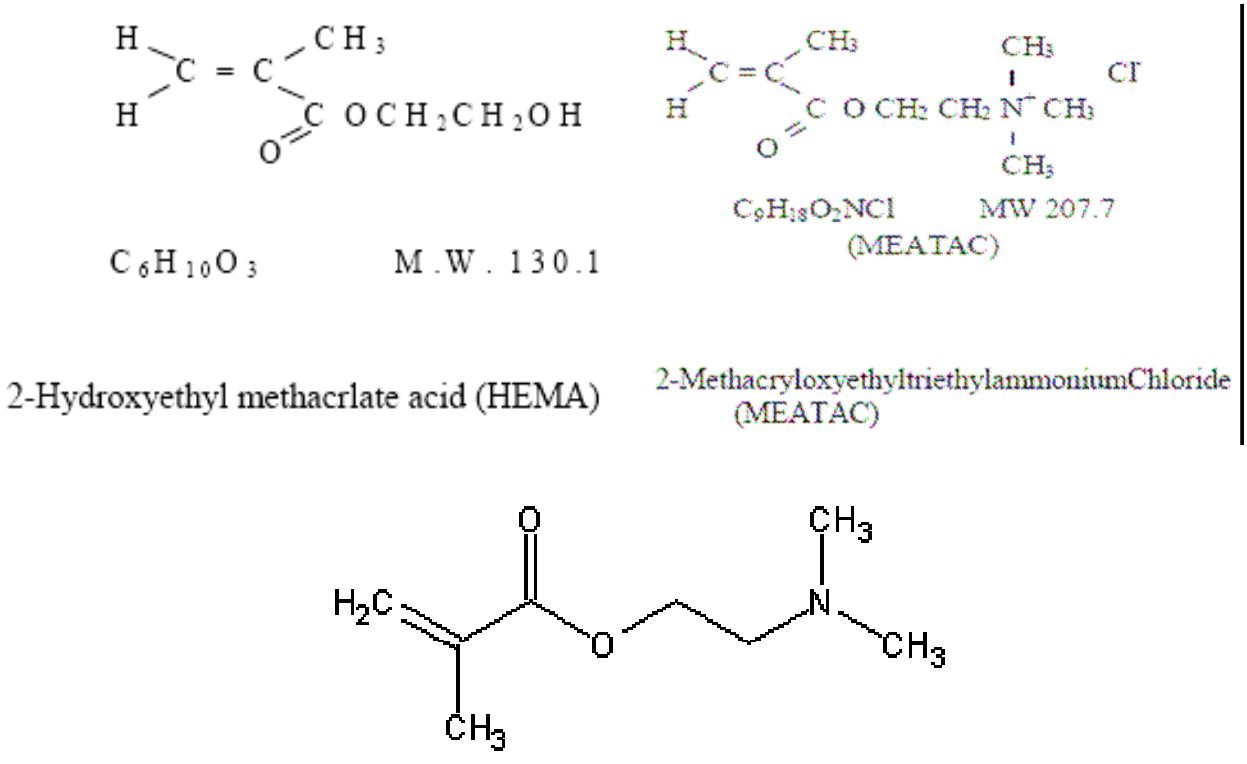

Figure 2.1 Structural formulae of monomers used in hydrogel fabrication

HYDROGEL PREPARATION

Weak basic polyelectrolyte hydrogels can be prepared using tertiary amine monomers such as dimethyl aminomethyl methacrylate (DMAEM). Tertiary amines such as dimethyl aminomethyl methacrylate (DMAEM) become charged when the amine functional group is protonated. Strongly basic polyelectrolyte hydrogels are prepared using the quaternary ammonium salts like 2-methacryloxy ethyltrimethyl ammonium chloride (MEATAC). The copolymer hydrogels were fabricated according to techniques established in this laboratory. An aqueous solvent with 40% ethylene glycol (EG) was also used for each stock solution. The polymerization reactions were initiated with 1.76 mM ammonium persulfate (APS). The DEGDMA cross-linker, APS initiator, and EG solvent were all purchased from Aldrich Chemical Company. The chemical concentrations used to prepare stock solutions of HEMA, DMAEM and MEATAC and concentration of the negatively charged monomer (Monoacryloxyethyl phosphate) are given in Tables 2.1, 2.2, 2.3, 2.4 (Appendix). A specific range of concentrations was chosen to avoid phase separation thereby making the copolymers either too brittle and hard or too soft and weak. All hydrogel samples were degassed under a vacuum since oxygen interferes with the polymerization process. These were then saturated using nitrogen gas to help reduce the re-uptake of oxygen. After the stock solutions were degassed, the appropriate proportions of ionic stock solutions were added to aliquots of the neutral stock solutions to produce six 10mL sample solutions with concentrations of 0, 40, 80, 120, 160, and 200 mM. Hydrogel membranes were formed by casting several milliliters of the pre-gelation solution between two glass plates separated by a thin Teflon film spacer. Small metal binder clips were used to form a tight seal between the two

plates. Test tubes containing the remaining solutions were each filled with several 100 μL micropipettes with inner diameters of 1293 μm. Since basic hydrogels tend to adhere to glass surfaces because of their positive charge, the micropipettes were first coated with a glass repellent consisting of a 20 g/L solution of dimethyldichlorosilane in 1,1,1-trichloroethane from Pharmicia (Repel-Silane) and washed with distilled deionized water thoroughly to remove all chemicals not affixed to the glass. These micropipettes were then blown dry and placed within the test tubes. This completed, all samples were allowed to polymerize at 25C for 24 hours.

EQUILIBRIUM SWELLING MEASUREMENTS

After the polymerization is complete, the samples are placed in de-ionized water, with the water replaced every day continuously for two weeks, to remove any residual non-polymerized chemicals from the samples. The samples were then removed from the glass pipettes by carefully crack opening with a glass cutter. The samples were cut into 2-3 mm specimens and then placed into glass holders and washed continuously and in parallel with distilled de-ionized water for two more weeks. The DI water was then replaced with NaCl solutions (1.54 mM) and washed until the samples were equilibrated. The process was repeated successively with 1X - PBS (Phosphate Buffer Solution). The diameter of the specimens was then measured using a light microscope equipped with a CCD camera.

MEMBRANE POTENTIAL MEASUREMENTS

The equipment used for this experiment to measure the steady state potential is the EVC-4000 Multi-Channel Voltage/Current Clamp instrument (World Precision Instruments, FL). A four-channel Voltage/Current clamp apparatus, the EVC4000 employs the voltage clamp technique to monitor membrane permeability as a function of membrane voltage or applied chemicals. Each module, with its companion preamplifier, can operate independently in one of three different modes: Voltage Clamp (VC), Current Clamp (CC), or Open Circuit Potential (PD) measurement.

Voltage Clamp

Panel Setting Range - ± 200 mV, Clamp V. per Volts Applied Ext - 100 mV per volt

Max.Voltage Range of Current Electrodes - +32 Volts

Max. Clamp Voltage - ± 100 mV, Fluid Resistance Compensation - 0 to 1000 Ohms

Current Clamp

Maximum Clamp Current - ± 1 milliampere,

Current per Ext volts Applied - 1 μA per millivolt

The polyelectrolyte hydrogel is placed in the "Ussing chamber" - a perfusion chamber made from solid acrylic with port entries for fluid lines, electrodes or bridges. The chamber essentially holds the specimen (membrane) under study, separating it from the fluid compartments on its either sides. Two voltage electrodes and the corresponding two current electrodes are inserted on either side of where the membrane is normally located. The solution in the first chamber is continually changed with varying concentrations of NaCl ranging from 1.54mM, 4.87mM, 15.4mM, 48.7mM, 154mM, 487mM and finally

1.54M. The second chamber is filled with 154mM NaCl and is fixed at that level so as to serve as a reference. Care should be taken to set the electrode offset adjustment controls on the preamplifier to zero before beginning each measurement case i.e. when concentration of electrolytes on both sides is 154mM, the potential difference should be zero. By controlling the offset to zero, we help reduce the related errors. The sequence of basic Polyelectrolyte hydrogels with the charges 0mM, 40mM, 80mM, 120mM, 160mM, 200mM are used as the anion exchanging membranes separating the two compartments of the oozing chamber. The 0mM Polyelectrolyte gel membrane is aligned in between the two chambers and the first compartment is filled with 1.54mM of NaCl solution while the second chamber stays fixed at 154mM of NaCl for the entire duration of the experiment. The electrolyte in the first compartment is then replaced with a higher concentration of the same, starting from 4.87mM, 15.4mM and so on until 1.54M is reached. For each concentration, note the steady state potential. Once a sweep of electrolyte concentrations is completed, the Polyelectrolyte gel membrane is replaced with a higher charged one and the same procedure as was followed for the "0" mM is to be repeated. This ranges from 8.66mM up to 866mM for both PEG-MAETAC and PEG-DMAEM in this experiment. The steady state potentials are then tabulated.

HEMA-DMEAM HYDROGELS FOR BIOREPORTER IMMOBILIZATION

A 10ml stock solution of the pre-gel solution is made up by mixing 3.414 ml of N,N-dimethyl aminomethyl methacrylate (DMAEM - Weak base), 4 ml of Ethylene Glycol (solvent), 40 of Ethylene Glycol dimethacrylate (EGDMA- Cross linker). The rest of the solution is filled with water or bacterial cell solution. The initiator used here is 4 pt.wt

solution of Ammonium Persulphate (1% of total volume of the pregel stock). The pregel solution, cell suspension and a neutral monomer Polyethylene glycol dimethacrylate (PEGDMA) is mixed in equal proportions and injected into glass cast with a Teflon spacer. A thin membrane of cells encapsulated in the gel is obtained after the polymerization process, which takes about 5-7 minutes. The membrane is then rinsed well in Minimal Salt Medium to wash off the byproducts. Circular specimens of the membrane are cored out using cylindrical metal cutters for bioluminescence measurement and other tests. Table 2.5 lists the recipe for the preparation of 10 ml stock solution for DMAEM hydrogels. The DMAEM hydrogels were used in the encapsulation of bioreporter cells.

ALGINATE BEADS

The bioreporter culture is grown in LB medium to OD_{546} = 0.60. The culture is then centrifuged at approximately 3000 x g for 10 minutes and washed with an equal amount of saline. It is then re-centrifuged and again re-suspended in saline or Minimal Salt Medium. The mixture is held in an ice pack until it is used. A stock solution of 3.5% low viscosity alginic acid (Sigma-Aldrich) solution is prepared by stirring overnight and sterilized the next day. One part of the cell suspension is gently mixed with two parts of alginic acid and held in an ice pack until required. A stock solution of 0.1M strontium chloride ($SrCl_2$) in water is prepared, sterilized and refrigerated. The cell-alginic acid mixture is transferred into a syringe and the mixture is pushed gently through the needle in a dropwise fashion, allowing the drops to fall into cold strontium chloride solution stirred on a stir plate. Drops solidify immediately on contact. To ensure complete

solidification the beads are allowed to stir in the solution for approximately 45 minutes. The beads are then removed with sterile cheesecloth. The beads can then be stored at 4^0 C for up to three months.

SURFACE INOCULATION

The cored out discs of the gel were transferred into a Falcon glass 4x6 multiwell along with 1.5 ml of MSM in each well to prevent desiccation of gels. The gels in each well were then inoculated with 500 µL of harvested cell suspension. The gels were left 10 – 12 hours and then transferred into a Greiner 4x6 well Black plate. One of the samples in each category was rinsed well to remove the loosely adhered cells. Each well was then filled with 2 ml of MSM with 30 ppm of sodium salycylate (Bioluminescence inducer) and sealed with the Topseal™. The plate was mounted into a 1450 MicroBeta™ PLUS Liquid scintillation counter (Wallac, Finland) for monitoring the luminescence over the next 24 hour period.

CELLULAR ENCAPSULATION AND BIOLUMINESCENCE MEASUREMENT

The pregel solution was prepared according to the protocol given above. A uniform mixture of the bacterial cell suspension and the pregel solution was either cast into a thin polymer membranes or small beads depending on the type of the gel. The encapsulated cells were stored at 4^0 C along with MSM until required for testing. The beads were stored in a dry, sterile and sealed test tube. The encapsulated cells were later induced artificially with 20-30 ppm of sodium salycylate solution. The bioluminescent activity of the encapsulated cells was measured in a liquid scintillation counter.

TRANSMISSION ELECTRON MICROSCOPY

A Transmission electron microscope (Hitachi H800) was used to image the hydrogel samples with embedded bioreporter cells to investigate the effect of encapsulation on the physiology of the encapsulated cells. The samples had to undergo two rounds of fixation before it can be imaged. For the primary fixation the gels were cut to measure 2 X 2 mm approximately and fixed for a hour in a 3% glutaraldehyde buffer, which is a mixture of 1ml of 25% glutaraldehyde, 3.2ml of De-ionized water and 4.2ml of 0.2M Cacodylate buffer. The samples were then washed with the cacodylate buffer to remove glutaraldehyde. For the secondary fixation the samples were then fixed with 5ml of 4% OsO4 and 5 ml of the buffer for a hour. After fixation the samples were dehydrated with ethanol and embedded in Spurr's media. The setup is left for curing. The sample blocks were then filed to remove the undesired epoxy around the actual sample. Thin sections of the shaped samples were obtained using a diamond edge knife. The sections were set up on the 400 nm thin bar mesh sample holder and stained with uranyl acetate in 50% methanol and lead citrate.

LIVE DEAD ASSAYS

A macroscopic alginate bead about 2mm in diameter is cut open or pressed against a coverslip to get a uniform section of encapsulated bioreporters and enable imaging in a Confocal microscope. To each bead about 1.5 microliters of 1:1 mixture of SYTO 9® and Propidium iodide (Probes Inc) is added for every 0.5 ml of bacterial suspension, assuming each bead would hold approximately hold 0.5 ml of bacterial cells. The samples are then incubated in dark for 15 minutes before it is imaged.

Chapter Three

HYDROGELS: EQUILIBRIUM SWELLING MEASUREMENTS

ABSTRACT

Hydrogel finds its use in large number of application such as micro actuators, filtration, tissue engineering, controlled drug delivery and it would only serve better to obtain a better understanding in such materials. Even though numerous applications are pursued using hydrogels very little is known about the mechanical behavior and theoretical models that describe the various processes in hydrogels. Typically the size of the gel increases or decreases in response to the bath/surrounding pH and salt concentration. Such dimensional changes significantly affect the mechanical characteristics and surface properties like porosity. A study on hydrogel swelling/de-swelling characteristics would help predict the behavior of these materials particularly when utilized to immobilize bioreporters for biosensor applications. This chapter uses thermodynamic models to explain the hydrogel swelling/de-swelling responses. The study also analyzes the competing solvent and ionic interactions, while making an effort to understand the swelling effects by providing a thermodynamic background. In addition, the degree and rate of swelling/de-swelling in basic polyelectrolyte hydrogels were obtained experimentally. 2-hydroxyethyl methacrylate (HEMA) - a neutral monomer and a strong basic monomer - 2-methacryloxy ethyltrimethyl ammonium chloride (MAETAC), and a weak basic monomer - N,N-dimethyl aminomethyl methacrylate (DMAEM) were used for the experimental section. These combinations of monomers yield a series of

biocompatible gels with different swelling states which were then used to immobilize live bacterial cells.

INTRODUCTION

Polyelectrolyte gels are special macromolecules; in these many of the attached acidic/basic groups are charged by gaining or loosing electron. By developing branches and intermolecular connections called cross-linking these macromolecules can form three dimensional networks.

Polyelectrolyte swelling equillibria have been described as a balance between solvent, elastic, electrostatic, and ion osmotic pressures [37-39]. The important contribution of electrostatic interactions to the swelling equilibrium has been considered in a number of reviews [40, 41]. In addition, solvent interactions that can lead to phenomenon such as microphase segregation and avalanche type condensation have also been described theoretically by Khokhlov and experimentally in recent studies [42-45].

This section of the study deals with the fabrication and analysis of polyelectrolyte hydrogels. The internal salt concentration of the hydrogels are varied logarithmically and allowed to equilibrate in a series of solutions such as DI water, 154 mM Nacl solution and 1X PBS. The equilibrium swelling responses are measured as a function of the change in the diameter of the hydrogels and expressed as a ratio of initial diameter.

THEORY

A. System definition

The universe is divided into two phases: a hydrogel phase and a bath phase. The volume, temperature, and total number of particles are constants. The solvent quality in this system will be assumed a function of temperature. Solvent and ions are free to distribute themselves between these two phases and, ultimately, the limiting case where the bath phase becomes very large will be used. Since the total volume, temperature, and particle numbers are assumed constant the Helmholtz Free energy will be an extremum in equilibrium. Hence, in equilibrium the hydrogel and bath ion chemical potentials are equal, dissociation equilibrium is satisfied for the acidic and basic monomers, and osmotic swelling equilibrium is obtained.

B. Free energy model

The total system free energy, ΔFT, can be decomposed into a sum of hydrogel and bath components such that

$$\Delta \boldsymbol{F}^{\boldsymbol{T}} = \Delta \boldsymbol{F}^{\boldsymbol{H}} + \Delta \boldsymbol{F}^{\boldsymbol{B}}$$

where ΔFH and ΔFB represent the hydrogel and bath contributions, respectively. The hydrogel free energy is defined as

$$\Delta F^{H} = \Delta F_{el} + \Delta F_{M} + \Delta F_{0} + \Delta F_{ex}$$

Where $\Delta \boldsymbol{F}_{\boldsymbol{el}}$, $\Delta \boldsymbol{F}_{\boldsymbol{M}}$, and $\Delta \boldsymbol{F}_{\boldsymbol{0}}$, represent the hydrogel elastic, solvent, and ionic contributions and $\Delta \boldsymbol{F}_{\boldsymbol{ex}}$ represent the excess free energy correction, respectively.

The Gaussian affine model for the elasticity and the solvent components of the free energy are given by the relations,

$$\Delta F_{el} = \Box F_{F_{el}} = \frac{3k_B T}{2}\frac{n_0 V_0}{N_x}\left[\left(\frac{n_0}{n}\right)^{\frac{2}{3}} - 1 - \frac{1}{3}\ln\left(\frac{n_0}{n}\right)\right]$$

$$\Delta F_M = k_B T n_0 V_0 (1 - n_0 V_0)\left[\ln(1 - nv) + \chi nv\right)\Big]$$

where, v is the lattice site volume, n the monomer density, n_0 is the reference state monomer density, V_0 the reference state polymer volume, K_B Boltzman constant, T temperature , N_x is the number of monomers between crosslink and 'χ' is the solvent interaction parameter. The third term in the hydrogel component of the Free energy, which represents the translational free energy of the ions in the uniform Donnan potential, is given by

$$\Delta F_0 = k_B T \sum_{i=1}^{\sigma} N_i \left\{\ln\left(\frac{N_i}{V^H}\right) - 1\right\} + \sum_{i=1}^{\sigma} z_i e N_i \varphi$$

where, is the iizth valance, N_i is the number of the ith particle in the hydrogel phase, V^H the hydrogel volume, e the unit electrostatic charge, 'σ' is the number of ion species, and 'φ' represents the uniform contribution to the internal potential arising from the electrostatic double layer at the hydrogel boundary.

The fourth term, which is the excess free, energy using the Debye-Huckel plus second virial coefficient, is given by

$$\left(\Delta F_{ex}\right) DHLL + B2 = -k_B TV\left[\frac{K^3}{12\pi} + \sum_{i=1}^{\sigma}\ \sum_{i=1}^{\sigma} c_i c_j B_{ij}\ (k)\right]$$

Where, is the inverse Debye length, are the concentrations of the ikjcic, th and j th ions and B_{ij} is the second virial coefficient in the Mayer ionic solution. The bath component includes the translational freedom of the bath ions and the electrostatic contribution from a uniform potential. The bath free energy for the polyampholyte system can be defined as

$$\mathbf{\Delta F^B = \Delta F_0 + \Delta F_{ex}}$$

where,

$$\Delta F^B = k_B T \sum_{i=1}^{\sigma} N_i^{\ B} \left\{\ln\left(\frac{N_i^{\ B}}{V^B}\right) - 1\right\} + \sum\nolimits_{i=1}^{\sigma} z_i e N_i \varphi$$

where the superscript indicates the corresponding bath volume, particle numbers, and uniform potential. Normally, the internal uniform contribution to the electrostatic potential of the hydrogel is referenced to that of the surrounding bath.

C. Hydrogel swelling/de-swelling mechanism

Hydrogels are liquid-swollen networks of hydrophilic homo-polymers or copolymers. A variety of techniques can be used to achieve this, the most common being the free radical polymerization of vinyl monomers with the active involvement of cross-linking agents. Synthetic hydrogels consist of monomers that are polymerized into linear chains and

cross-linked into a nonlinear three-dimensional mesh network. Polymer hydrogels are basically ion exchangers that are able to absorb solvents in which they are placed. Absorption of this solvent causes 'swelling' of the hydrogel network. This swelling, as such, occurs only up to a limited degree and stops after equilibrium is attained. Basic Polyelectrolyte hydrogels are made from basic monomeric units, which contain ionogenic groups, which tend to surround themselves with polar solvent molecules, thereby being soluble in the latter. Polymers containing linear links are soluble like polyacrylic acid. But basic (as well as acidic) polyelectrolyte hydrogels prepared as part of experiments contain cross-links. In this case, the affinity of the ions for the polar solvent drives the dissolution process, which causes the coiled matrix to unfold and accept solvent molecules, but the cross-links ensure that the polymer strands do not separate completely thereby preventing dissolution. The ability of the ionic constituents of the hydrogel network to surround themselves with the solvent, thereby stretching the matrix is met with strong opposition from the hydrogel itself due to its favoring a low energy state. There are a variety of forces, which can help characterize this. For one, the interior of the polyelectrolyte hydrogels, containing a highly concentrated solution of charged ion, has the tendency to dilute itself by absorbing additional solvent. This can be characterized as a difference in osmotic pressure between the interior of the hydrogel and the external solution. Another force that can be considered is that of the electrostatic repulsive force between the fixed charges on the hydrogel, which cause the strands of the matrix to expand. For hydrogels with acidic groups bound to its polymer chain, the H^+ ions comes off in basic solution and combines with OH^- ions to form water. Hydrogels with basic

groups show opposite pH sensitivity, exhibiting swelling in acidic conditions. The stepwise procedure for ionic hydrogel swelling in basic solution

1. Ionization of carboxyl groups releasing H^+ ions – At high ionic group density the carboxylate ions repel one another driving swelling, though this is not the main driving force for swelling.
2. H^+ ions recombine with OH^- ions to form water.
3. Charge electro-neutrality is maintained through diffusion of cations (Na^+) and OH^- ions into the gel.
4. Influx of new ions creates osmotic pressure that drives the swelling.

RESULTS

A. HEMA-DMAEM hydrogels

Table 3.1 and Table 3.2 illustrate the equilibrium swelling measurements of HEMA-DMAEM hydrogels in a series of solutions (DI water, 154 mM NaCl, 1X PBS).

Figures 3.1 – 3.4 represent the increase in diameter (normalized to internal diameter) against change in concentration of the internal salt concentration of the hydrogels. The hydrogels do not exhibit significant change in dimensions until a base charge of 100 mM. However there is a noted sharp increase for a small increase in the charge concentration.

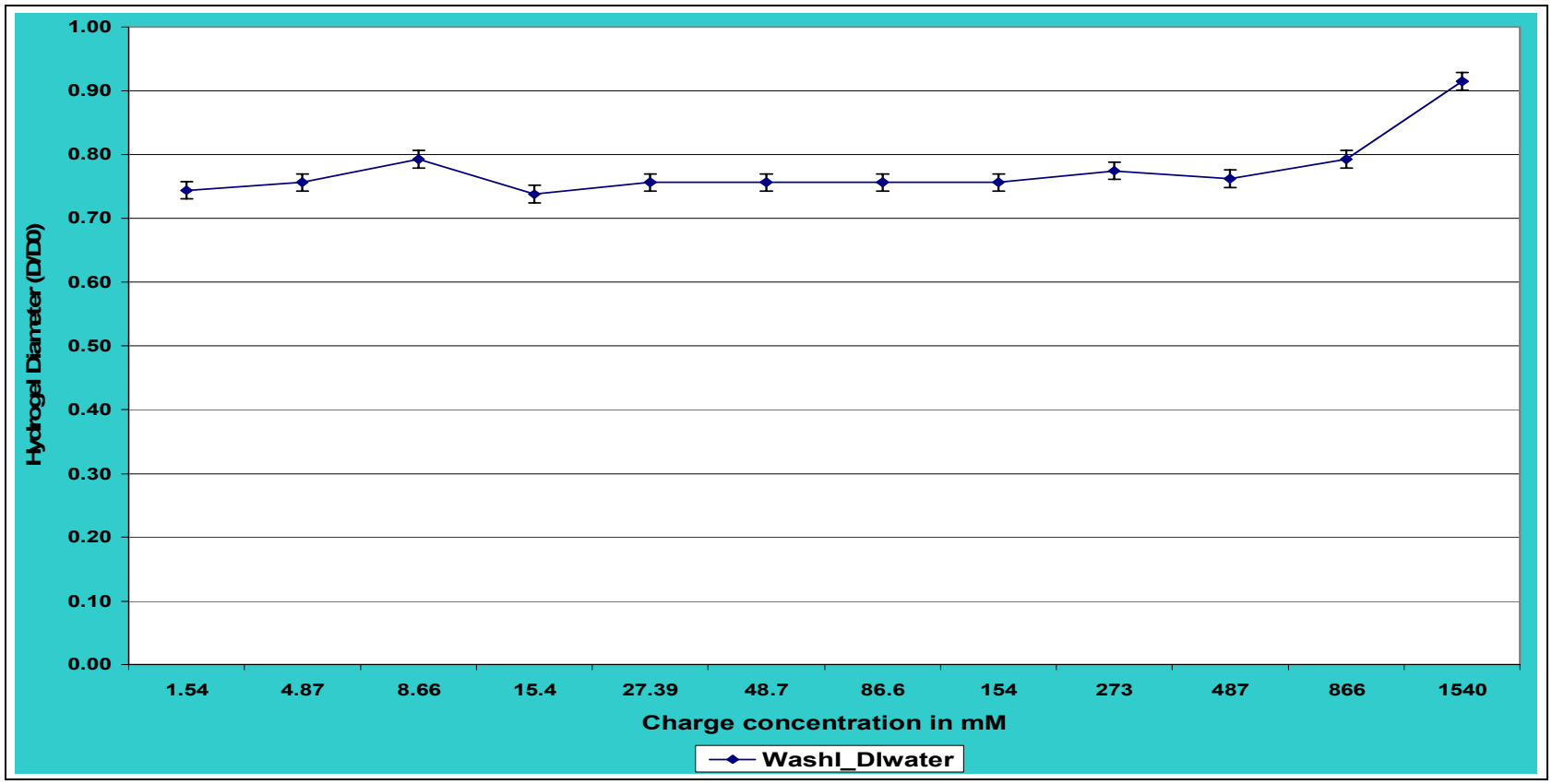

Figure 3.1 Equilibrium swelling of HEMA-DMAEM hydrogels in DI water.

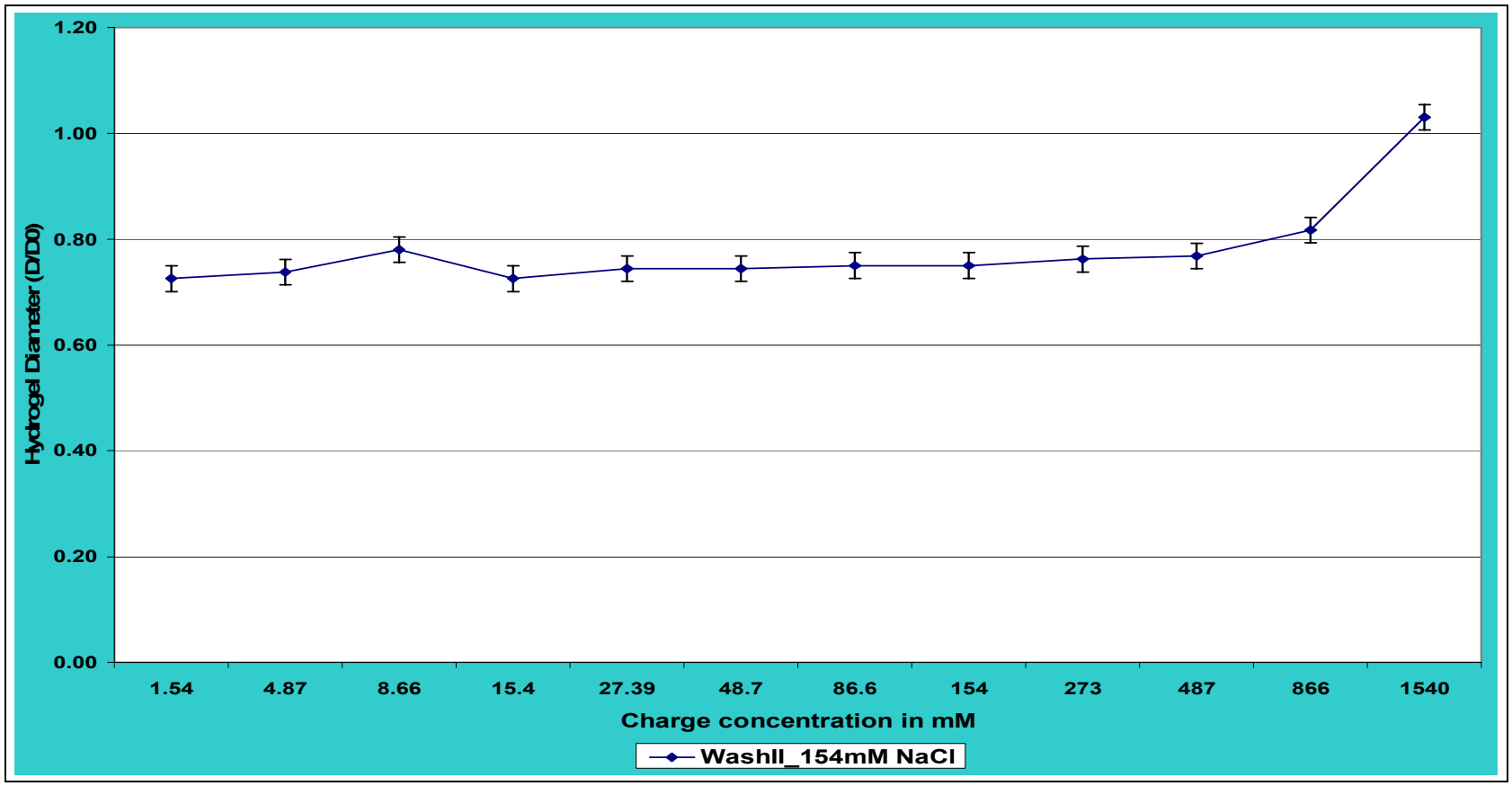

Figure 3.2 Equilibrium swelling of HEMA-DMAEM hydrogels in 154mM NaCl solution.

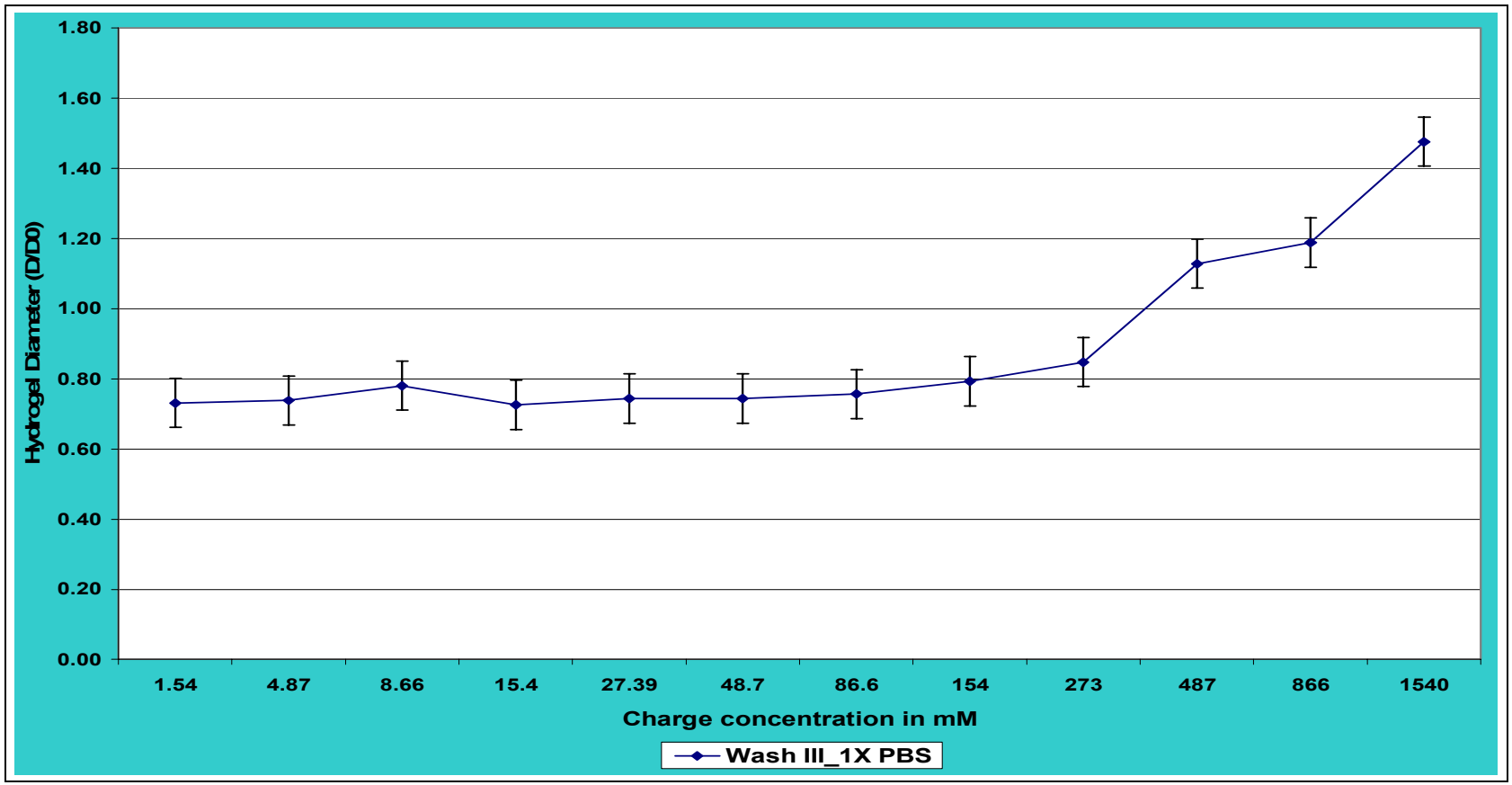

Figure 3.3 Equilibrium swelling of HEMA-DMAEM hydrogels in 1X PBS solution.

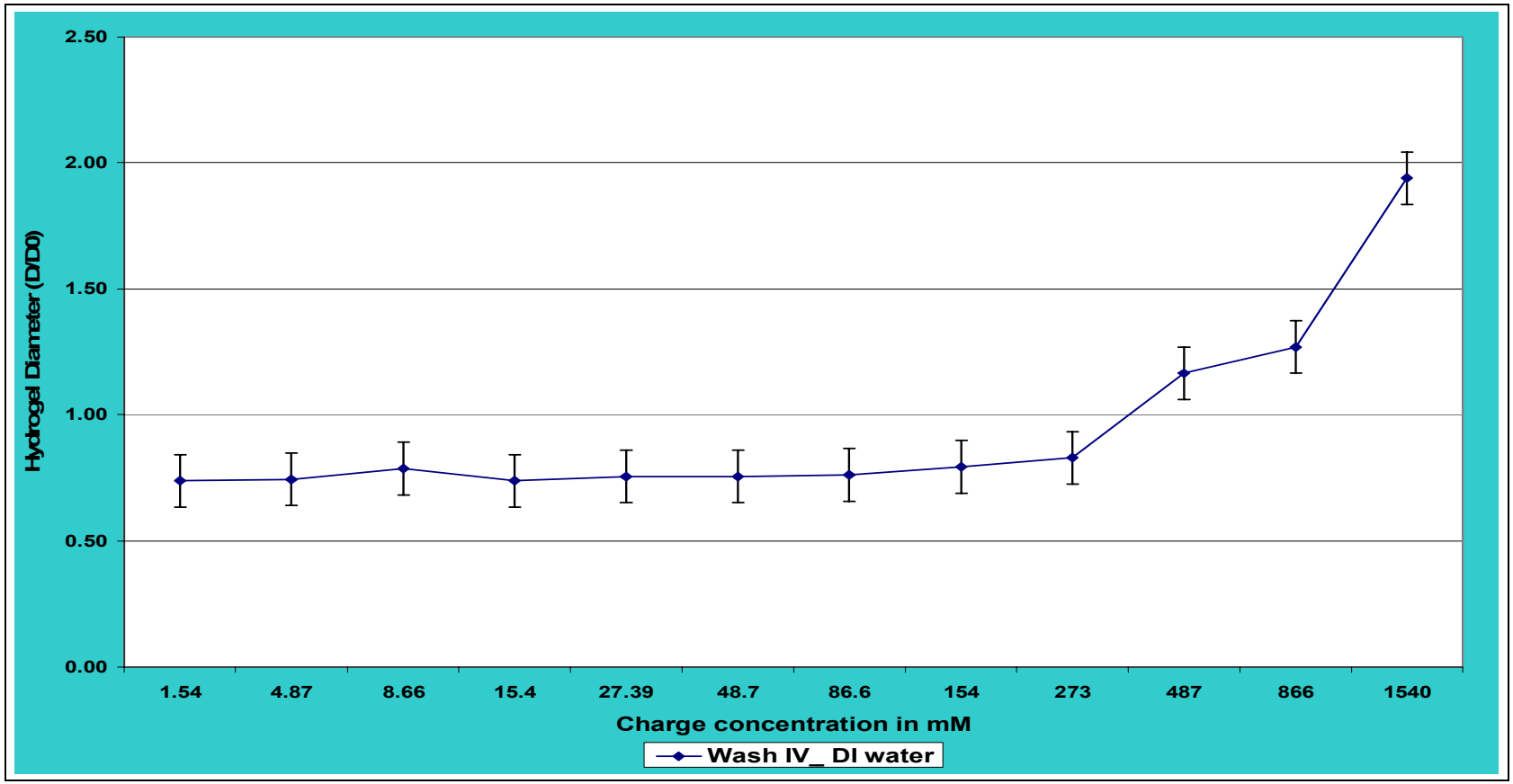

Figure 3.4 Equilibrium swelling of HEMA-DMAEM hydrogels in DI water.

B. HEMA-MEATAC hydrogels

Table 3.3 and Table 3.4 illustrate the equilibrium swelling measurements of HEMA-MAETAC hydrogels in a series of solutions (DI water, 154 mM NaCl, 1X PBS).

Figures 3.5 – 3.8 summarize the increase in diameter of hydrogel specimens corresponding to increase in salt concentration. Contrary to the HEMA-DMAEM hydrogels the HEMA-MAETAC hydrogels show a sharper increase curve for a much lower salt concentration.

DISCUSSION

Basic Polyelectrolyte hydrogels are made from basic monomeric units which contain ionogenic groups which tend to surround themselves with polar solvent molecules, thereby being soluble in the latter. Polymers containing linear links are soluble like polyacrylic acid. But the basic polyelectrolyte hydrogels prepared as part of this experiment contain cross-links. In this case, the affinity of the ions for the polar solvent drives the dissolution process which causes the coiled matrix to unfold and accept solvent molecules but the cross-links ensure that the polymer strands do not separate completely thereby preventing dissolution. The ability of the ionic constituents of the hydrogel network to surround themselves with the solvent, thereby stretching the matrix is met with strong opposition from the latter itself due to its favoring a low energy state. This can be characterized as a difference in osmotic pressure between the interior of the hydrogel and the external solution. Another force that can be considered is that of the

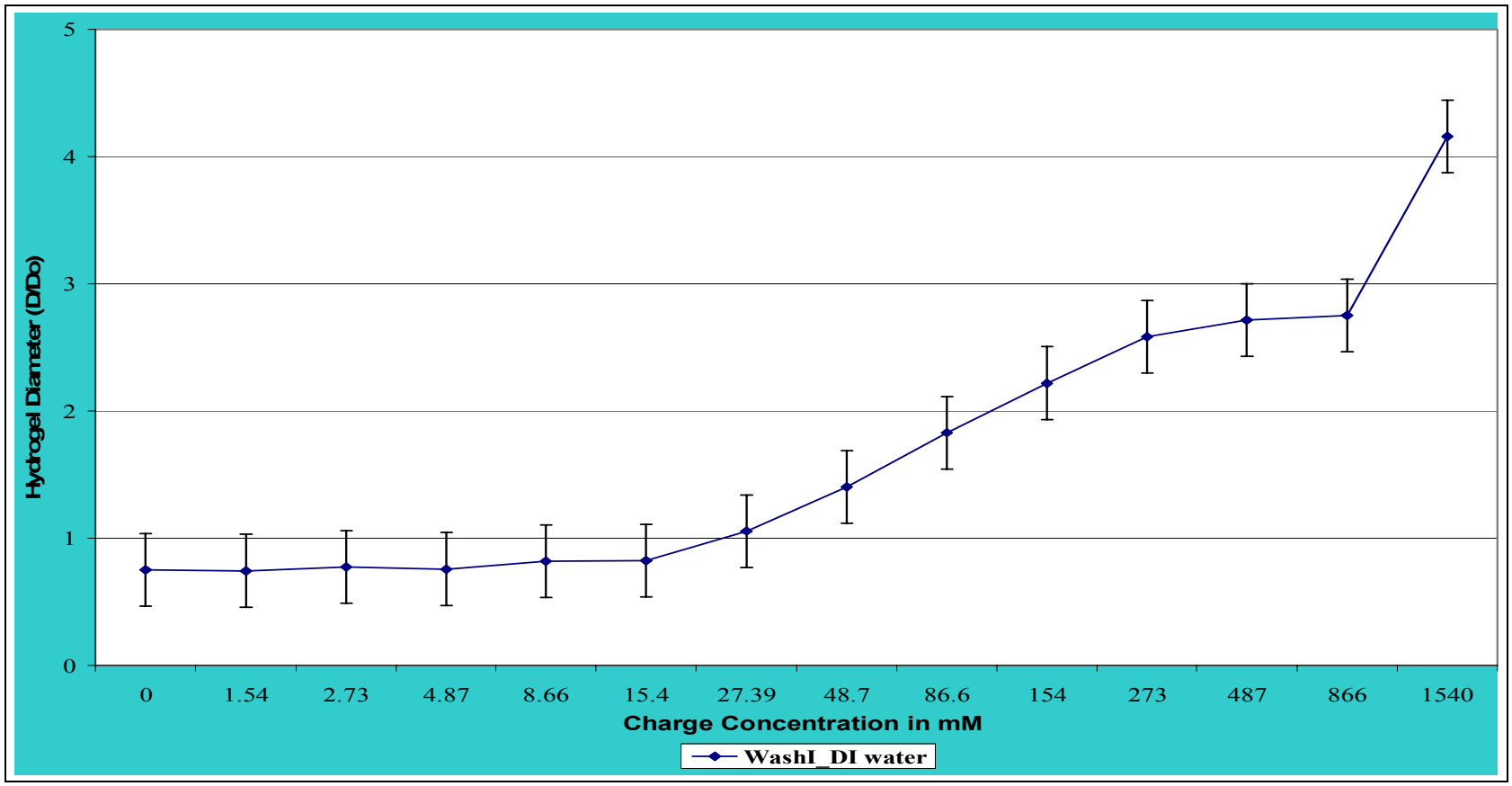

Figure 3.5 Equilibrium swelling of HEMA-MAETAC hydrogels in DI water.

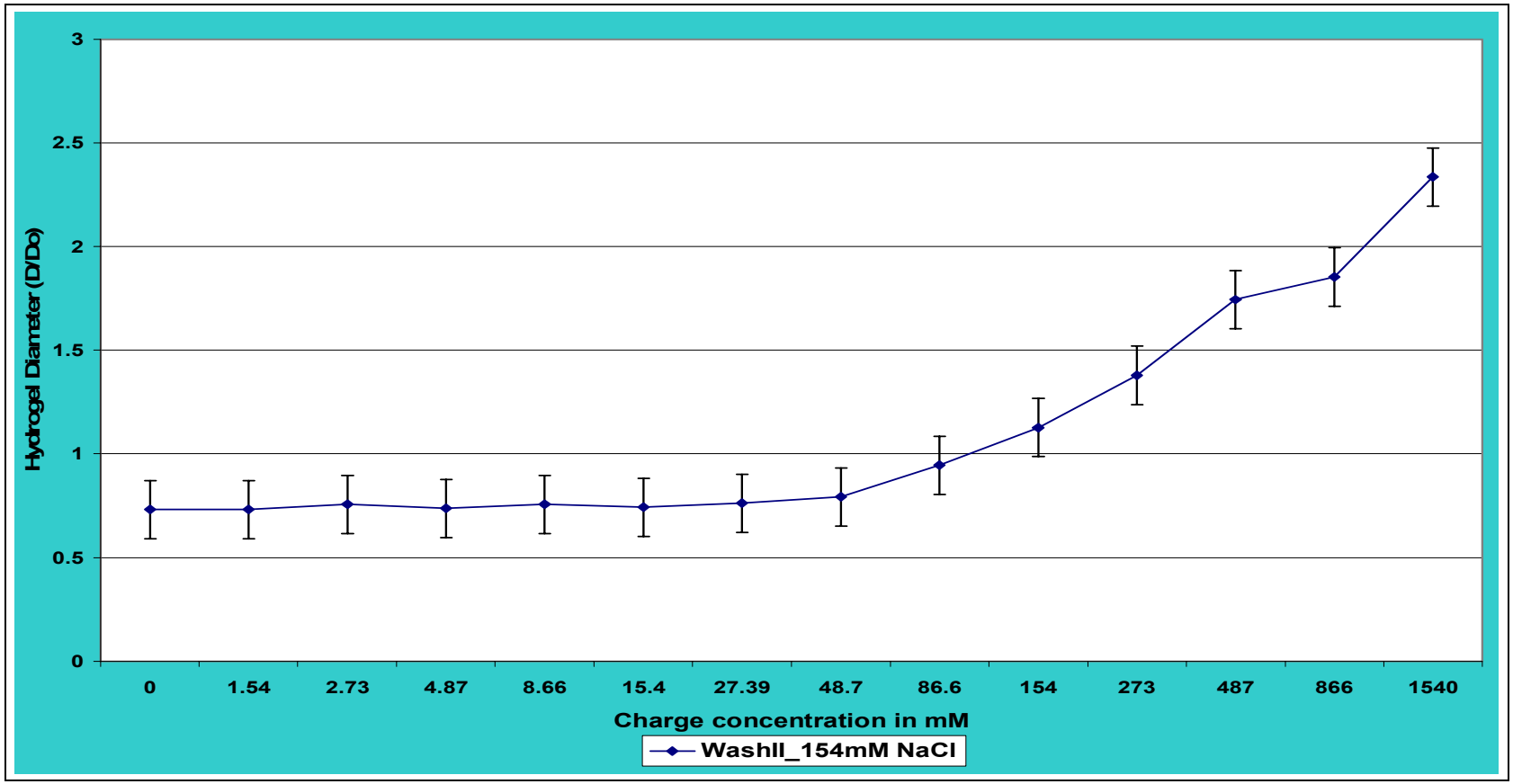

Figure 3.6 Equilibrium swelling of HEMA-MAETAC hydrogels in 154 mM NaCl solution.

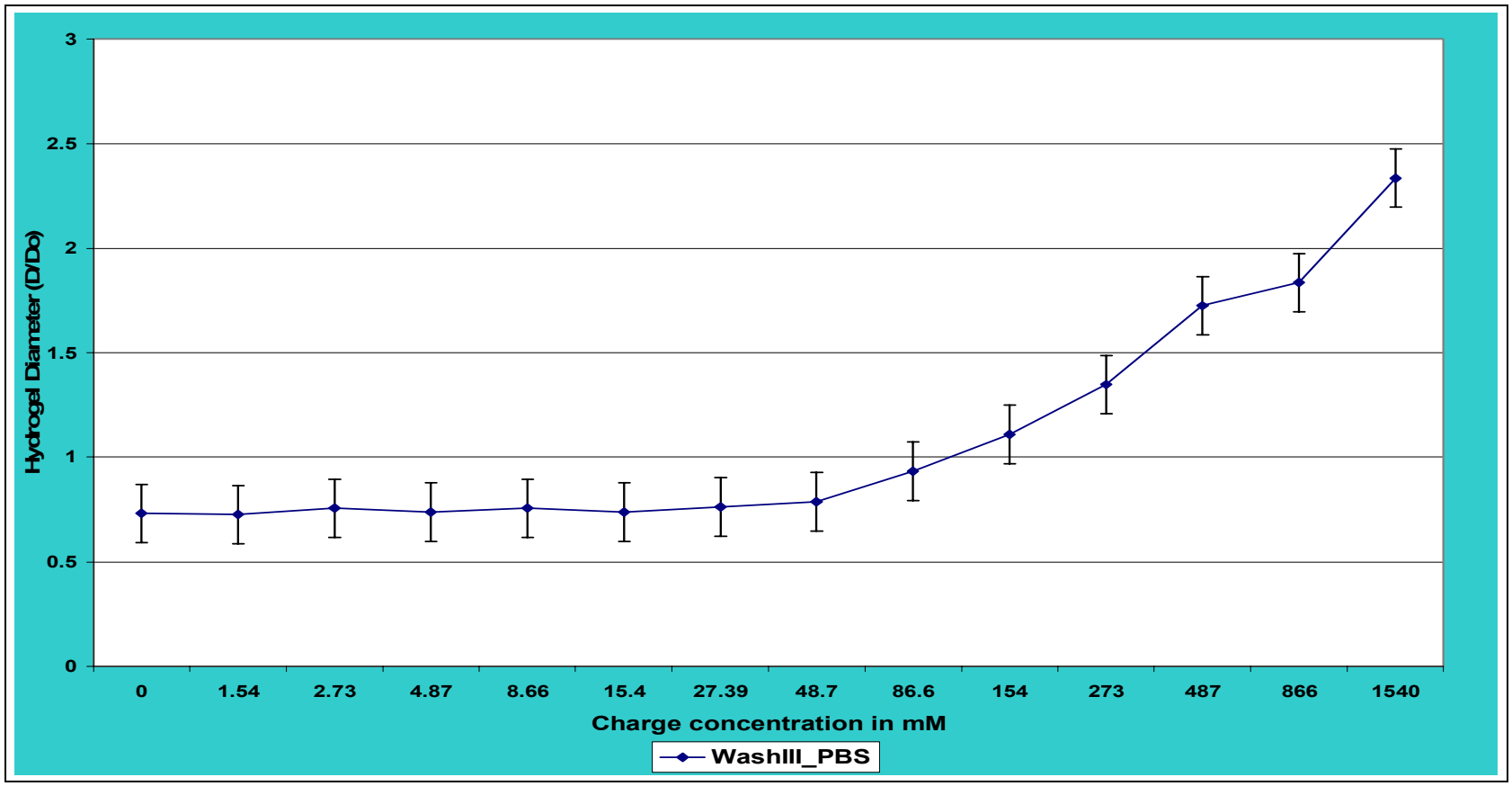

Figure 3.7 Equilibrium swelling of HEMA-MAETAC hydrogels in 1X PBS solution.

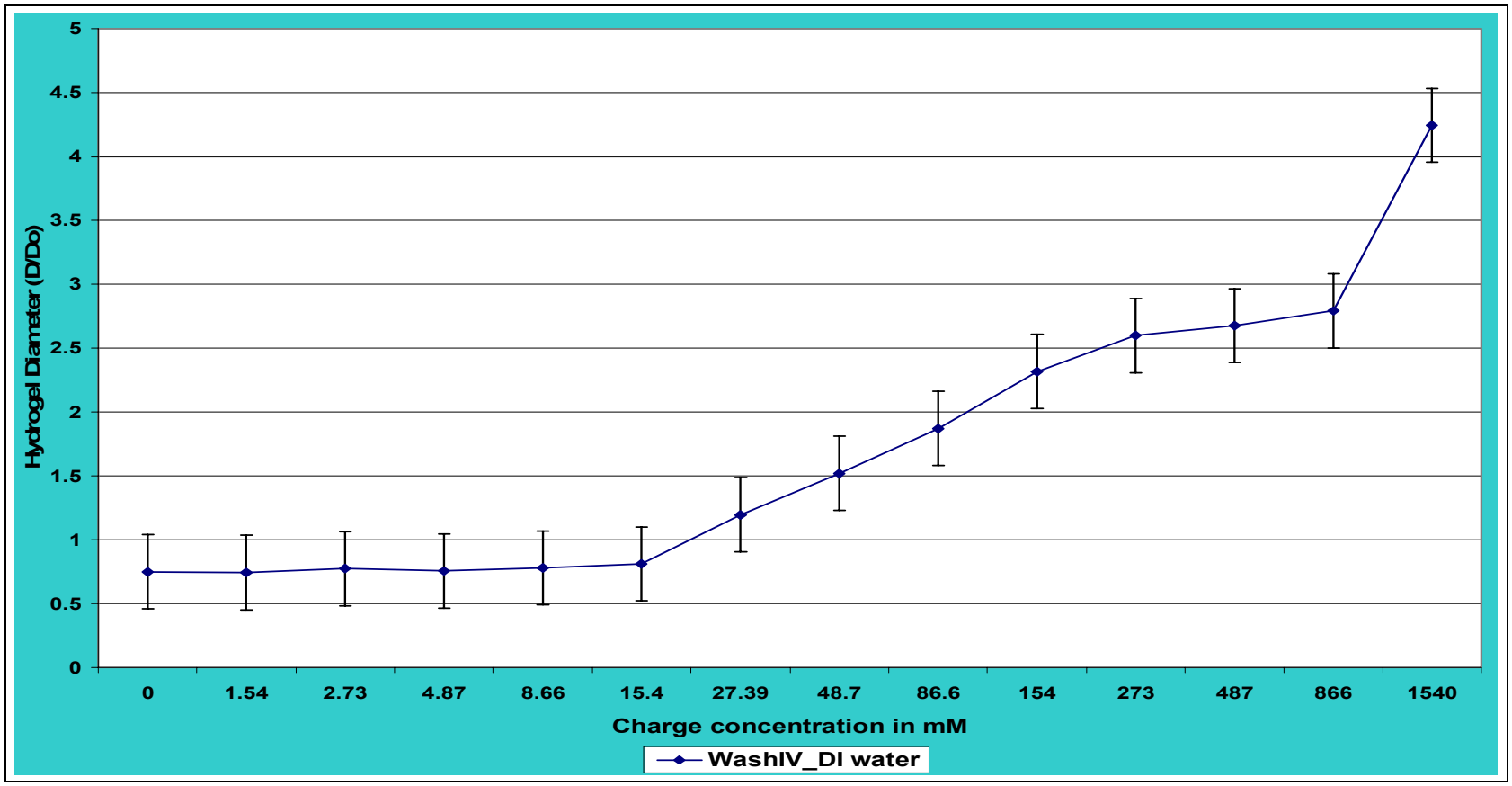

Figure 3.8 Equilibrium swelling of HEMA-MAETAC hydrogels in DI water.

electrostatic repulsive force between the fixed charges on the hydrogel which cause the strands of the matrix to expand. Recent experimental studies have shown that, depending on the magnitude of the net polymer charge and bath ionic strength, the swelling properties can be dominated by acid and base dissociation, electrostatic repulsion, and electrostatic attraction. The swelling response of polyelectrolyte hydrogels to changes in bath salt concentration illustrates the competing effects of ion dissociation and polyelectrolyte screening. The acid and base dissociation constants play an important role in determining the background of positive and negative charges at the iso-electric point. When the difference in the dissociation constants of the acidic and basic monomers is much higher, there exist a large background of positive and the negative charges at the iso-electric point. When a significant background of charges exists at the iso-electric point, attraction between oppositely charged side chains leads to a relatively tight coiling of the polyions at low bath ionic strengths due to the ion association. The subsequent loss in charge density and the osmotic pressure therefore produces a de-swelling transition at low ionic bath salt concentration. Increasing the bath salt concentration weakens the intra-chain attractions and leads to the exchange of sodium ions and chloride ions in the acidic and basic monomers and hence the acidic and basic monomers dissociate which creates the swelling transition in the hydrogels. Thus at the low ionic strengths, ion dissociation equilibrium effects dominate the swelling responses. At the intermediate bath ionic strengths, polyelectrolyte screening produces the de-swelling transition as a result of losing the osmotic pressure difference between the hydrogel and the surrounding bath. Upon a further increase in the bath salt concentration, there is a swelling transition again because of the screening and the excluded volume effects. The electrostatic

interactions between polymeric and mobile charges that determine the hydrogel swelling equilibrium at high ionic strengths are, yet to be comprehended completely. The swelling response of the polyelectrolyte basic gels were obtained and the results are represented as a graph of the charge concentration against change in diameter ratio (D/D_0).

CONCLUSION

This chapter has attempted to measure the swelling responses of polyelectrolyte hydrogels as function of their internal charge concentration, and their equilibrium swelling is explained by providing a thermodynamic background. The importance has been laid on the selection of the monomers for the preparation of hydrogel, the micro-structural arrangement of the monomeric groups during the polymerization reaction and the counter ions in the polyelectrolyte hydrogel phase. The internal charge concentration of the hydrogel was systematically increased and the corresponding swelling response was recorded through observed change in diameter of the gel. Swelling transitions were observed for charge variations between 200 to 1000 mM in the case of weakly basic hydrogels (HEMA-DMAEM), while significantly higher swelling ratio was recorded at lower charge variation between 30 to 1000 mM in the case of strongly basic hydrogels (HEMA-MAETAC). The change in the solvent quality with increasing ionization and the similar changes in solvent interactions in response to bath pH have not been considered for this analysis. Thus the hydrogel internal charge concentration was indirectly measured with reasonable precision and an understanding of the swelling responses as a measure of the internal charge concentration was obtained. The experimental results provided

considerable insight into hydrogel surface characteristics particularly in the event of designing hydrogel based immobilization matrices for bioreporter biosensors.

Chapter Four

HYDROGELS: STEADY STATE DIFFUSION POTENTIAL

ABSTRACT

The primary reason for the origin of the membrane charge of the hydrogel networks in contact with aqueous electrolyte solution could be attributed to dissociation of functional groups, adsorption of ions from solution or adsorption of charged macromolecules. The acquired membrane charge could be on the exterior surface or on the interior pore surface. Recently there is a particular emphasis in cartilage research has been the determination of the fluid and ion flows and electric potentials within the extra cellular matrix, which would be used to immobilize living cells eventually. The aim of this study will be to determine the nature of the electric fields governing the electro-chemical and other related phenomena in hydrogel membranes, thereby providing an insight into how these forces would be at play in the case of an articular cartilage, while accounting for both the streaming potential and the diffusion potential. Much of the purpose behind this study is to evaluate the nature of electric fields inside a basic polyelectrolyte hydrogel membrane while accounting for the effects of both the Interfacial Donnan potential and the Diffusion potential. The membrane potential across the gel membranes was measured for both HEMA-MAETAC and HEMA-DMAEM hydrogels. The experimental data were analyzed on the basis of the Donnan equilibrium and the Nernst Planck equations. Results obtained using simulation and the code for the same are also attached.

INTRODUCTION

The hydrogel networks are three dimensional meshes with distributed fixed positive charge, in the case of cationic gels. This is analogous to the case of articular cartilage wherein the fixed negative charges are in the form of sulphide and other ions distributed along the chondroitin, keratan sulfates and other molecules comprising the aggrecan inside the tissue. Thus better understanding of the electrical characteristics of hydrogel networks could develop better insight into cartilage and tissue engineering concepts. The flow of water across a semi permeable membrane, in the absence of a hydraulic pressure difference can result from chemical potential, electric potential and thermal potential, which in turn, results in a flow of solutes, electricity and/or heat. This flow is called osmosis. A neutral membrane is known to separate solutes based on the differences in their size and/or in their interaction with the membrane, whereas a charged membrane separates solutes according to the charge of the membrane. When there is a charge separation between two regions, arising from a predominantly positive charge due to the accumulation of cations at one end and a predominantly negative charge due to the accumulation of anions at the other, it gives rise to an electric potential. In a simple solution of electrolytes where in the ions are free to move, equilibrium is eventually attained resulting in zero potential difference between different regions of that electrolyte. Evaluation of the membrane potential is a good indicator for characterizing the transport phenomena across a charged membrane. Theoretically the membrane potential in a polyelectrolyte hydrogel membrane can be analyzed using the Donnan equilibrium theory and the Nernst-Planck equation, if it is assumed that the fixed charge groups are homogeneously distributed in the membrane and provided, the effect of mean activity

coefficient of the electrolytes in the external solution is negligible. In this experiment, salt solutions of different concentrations are used with a reference salt concentration in order to estimate the potential. When a semi-permeable membrane is used to separate the chambers containing two different concentrations of solutions, it gives rise to a potential (Nernst) due to the concentration difference in the two chambers and a potential (Donnan) due to the charges in the boundary. In this chapter an attempt is made to measure membrane potential of Polyelectrolyte hydrogel due to the diffusion of charges between two different concentration of NACL solution separated by the membrane and the measurement is continued with different salt concentration and also with ionic hydrogel of varying charge densities. The boundary potential - the potential obtained due to the charges in the surface of the hydrogel is also considered along with diffusion potential obtained due to the concentration of charges. The charge of a membrane can be also reflected in the boundary potential as the charges at the pore walls play a significant role on the ions flow in the membrane. It would be interesting to see if the experimental observations agree with the theoretical computations, taking Donnan and Nernst equations into account [46].

THEORY

The potential across a membrane separating two compartments containing different concentrations of salt solutions can be evaluated as the sum of *(i)* the Donnan potential between the hydrogel membrane surface and the electrolyte solution and *(ii)* a diffusion potential in the hydrogel membrane itself.

A. Donnan potential

The electrochemical potentials of the i^{th} ion in the salt solution and in the polyelectrolyte hydrogel are given by μ_i and, $\mu_i{}^0$ respectively:

$$\mu_i = \mu_i^{\,0} + RT \ln \gamma_i C_i + z_i F \phi, i = +, -$$
$$\overline{\mu_i} = \overline{\mu_i^{\,0}} + RT \ln \overline{\gamma_i}\,\overline{C_i} + z_i F \overline{\phi}, i = +, -$$

where μ_i and $\mu_i{}^0$ (with superscripts) are the standard electrochemical potentials, z_i is the valence of the ion, R is the gas constant, T is the absolute temperature, γ_i and $\overline{\gamma}_i$ are the ion activity coefficients, C_i and $\overline{C}_i$ are the ion concentrations, F is the Faraday constant while Φ and $\overline{\Phi}$ are the electrical potentials; the bar denotes the values in the charged membrane.

At the interface between the membrane and the external electrolyte solution, the electrochemical potentials in the two phases are equilibrated:

$$\mu_i = \overline{\mu_i}, i = +, -$$

The Donnan potential, between the membrane surface and the electrolyte solution is given as

$$\Delta\phi_{Don} = \overline{\phi} - \phi = -\frac{RT}{z_i F} \ln \frac{\overline{\gamma_i}\,\overline{C}_I}{k_i \gamma_i C_i}, i = + -$$

where k_i is the distribution coefficient of the ion i, defined as

$$\overline{\mu_i^0} - \mu_i^0 = -RT \ln k_i, i = +, -$$

Under the condition, $z_+ = -z_-$, the relationship between the concentrations of ions in the membrane and in the external solution can be obtained:

$$\overline{C}_+ \overline{C}_- = \frac{\gamma^2_{+/-} C_s^2}{Q^2}$$

where Cs is the electrolyte concentration in the external solution equated as $(C_+C_-)^{1/2}$, $\gamma\pm$ is the mean activity coefficient of the electrolyte equated as $(\gamma_+\gamma_-)^{1/2}$,

Q can be expressed as

$$Q = \left(\frac{\overline{\gamma_+ \gamma_-}}{k_+ k_-} \right)^{\frac{1}{2}}$$

On the other hand, the condition of electro neutrality in the membrane is given by

$$\sum_{i=+,-} z_i \overline{C_i} + z_x c_x = 0$$

where z_x is the valence of fixed charge groups, and Cx is the fixed charge density.

$$\overline{C_+} = \sqrt{\left(\frac{z_x C_x}{2z_+}\right)^2 + \left(\frac{\gamma_{+/-} C_s}{Q}\right)^2} - \frac{z_x C_x}{2z_+}$$

$$\overline{C_-} = \sqrt{\left(\frac{z_x C_x}{2z_+}\right)^2 + \left(\frac{\gamma_{+/-} C_s}{Q}\right)^2} + \frac{z_x C_x}{2z_+}$$

Note that by substituting this value of concentrations inside the hydrogel in the earlier equation for Donnan potential, the Donnan potential at the left- and right-hand sides of the interface between the membrane and the surrounding solution are obtained.

Further, if the activity coefficients of ions are not the function of the ion concentrations in the membrane, the total Donnan potential through the membrane can be expressed by the sum of the Donnan potentials at the left- and right-hand sides for an electrolyte solution system.

B. Membrane diffusion potential

The ionic flux across the membrane is given by the Nernst-Planck equation which can be applied to the phase of the membrane:

$$J_i = -\overline{\omega_i} RT \frac{d\overline{C_i}}{dx} - z_i F \overline{\omega_i}\,\overline{C_i} \frac{d\overline{\phi}}{dx}, i = +, -$$

where $\overline{\omega_i}$ is the ionic mobility of the ion i in the membrane.

The electro-neutrality condition in a membrane requires that

$$J_+(x) = J_-(x)$$

Differentiating hydrogel concentration terms used earlier,

$$\frac{d\overline{C_+}}{dx} = \frac{d\overline{C_-}}{dx}$$

Now after substitutions the diffusion potential can be expressed as

$$\Delta\phi_{diff} = \overline{\phi}'' - \overline{\phi}' = -\frac{RT}{z_+F}\frac{r-1}{r+1} * \ln\left[\frac{(r+1)\overline{C_+}'' + (Z_x/Z_+)C_x}{(r+1)\overline{C_+}' + (Z_x/Z_+)C_x}\right]$$

where r is the cation-to-anion mobility ratio in the membrane defined as

$$r = \frac{\overline{\omega}_+}{\overline{\omega}_-}$$

where $\overline{\omega}_+$ and $\overline{\omega}_-$ are the cation and anion mobilities in the membrane, respectively.

RESULTS

Tables 4.1 – 4.5 represent the steady state potential data for HEMA-DMAEM hydrogels. Tables 4.6 – 4.10 represent the steady state potential for HEMA-MAETAC hydrogels. An Ussing chamber was used to measure the steady state potential values for the hydrogels. The right compartment of the chamber contained the 154 mM NaCl (Physiologic ion strength) and concentration of the NaCl was varied logarithmically in the left chamber. Figures 4.1 & 4.2 illustrates graphical plot of the steady state values of HEMA-DMAEM and HEMA-MAETAC against the charge concentration of the hydrogels.

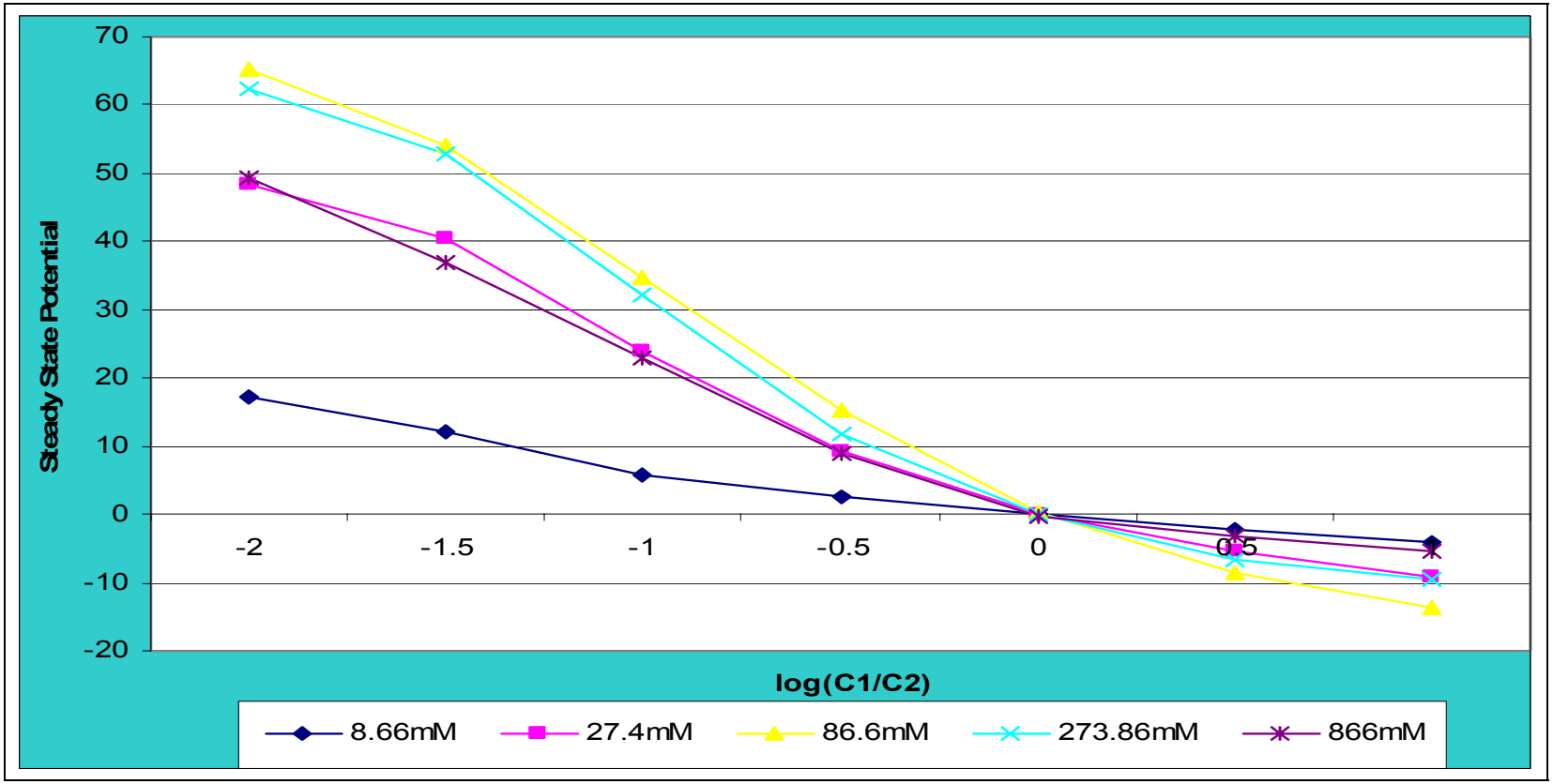

Figure 4.1: Steady state potential of HEMA-DMAEM hydrogels

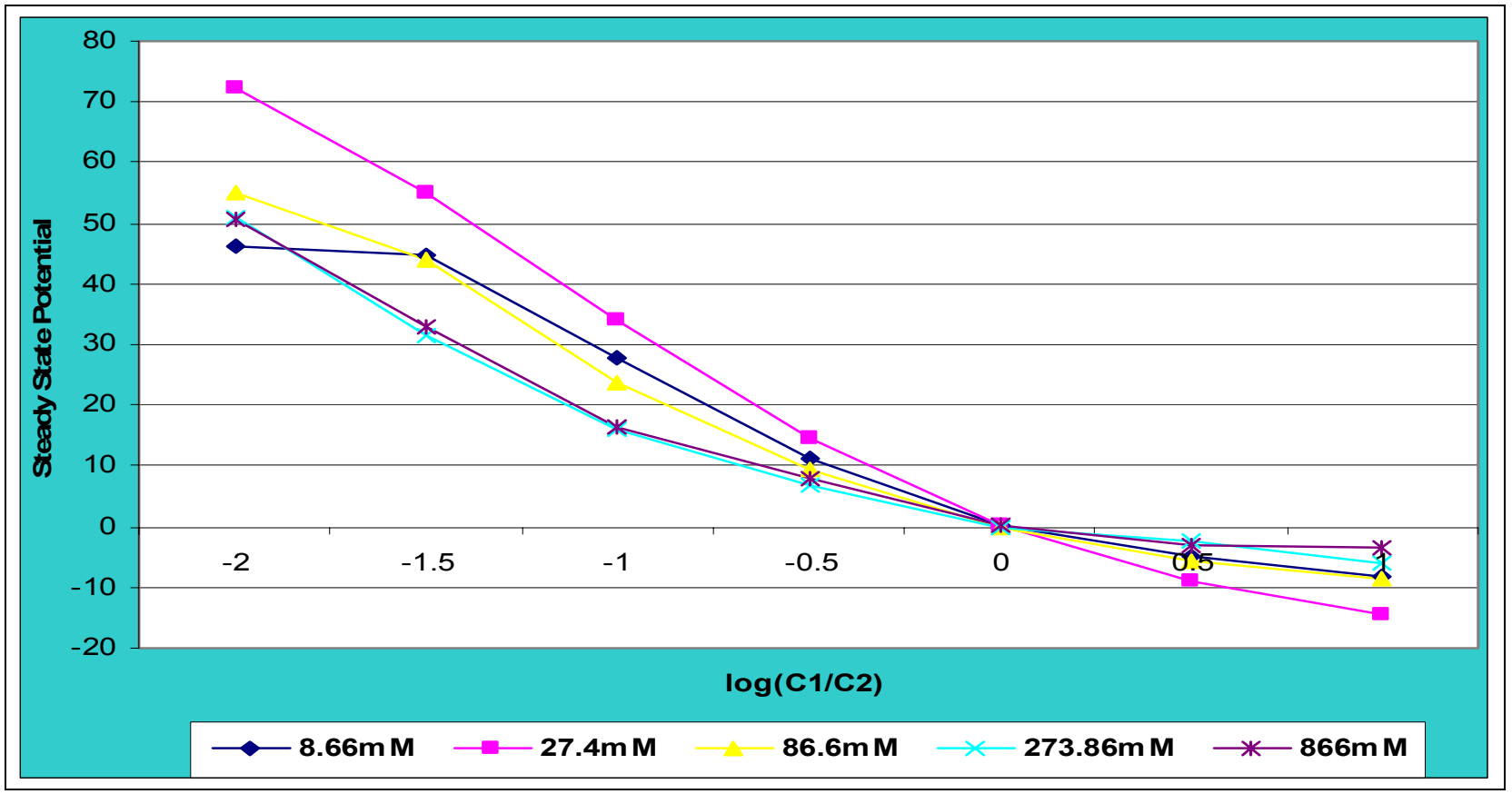

Figure 4.2: Steady state potential of HEMA-MAETAC hydrogels

DISCUSSION

The main assumptions used in this experimental evaluation is that the fixed charge groups are homogeneously distributed in the membrane and the effect of mean activity coefficient of the electrolytes in the external solution is negligible. These assumptions help us conveniently analyze the total membrane potential using the Donnan equilibrium theory and the Nernst-Planck equation. In the event that the hydrogel membrane has an inhomogeneous Fixed Charge Density (FCD) distribution that could be natural or induced due to deformation, its FCD gradient will lead to gradients of ion concentrations, with cations and anions having opposite directions for the gradients. Consequently, there would be a gradient of electric potential inside the hydrogel membrane, i.e., the diffusion potential, caused by the tendency of the ions to diffuse from a region of higher concentration to a region of lower concentration, resulting in a slight separation of the positive and the negative charges. The establishment of this diffusion potential opposes the diffusion tendency of the ions. Therefore even at equilibrium, it gives rise to an electric potential difference between two locations within the membrane having non uniform FCD. The in-homogenous distribution of FCD may be natural as is the case in articular cartilage that may be due to flow-induced compaction or compression. During the non-equilibrium condition in the case of this basic polyelectrolyte hydrogel, it remains true that the anion concentrations increase with the FCD (which in this case is positive), whereas the anion concentrations decrease with the FCD at every point inside the hydrogel. In these non-equilibrium problems, there exists another source of electric potential inside the membrane, the streaming potential, due to movements of ions being convected by interstitial fluid flow. Also due to complexities involved in the distribution

of ions, boundary and initial conditions have to be taken into account. In the simplified case of uniform FCD, the two Donnan interfacial potentials can be evaluated using the general formulae. The Diffusion potential analysis can then be done, using the model of coupled ion diffusion in a binary electrolyte in which the binary electrolyte diffuses as a whole relative to the convective fluid with an effective diffusion co-efficient. The separation distance of the ions (sodium and chloride) is of the order of few Debye lengths, owing to their dissimilar diffusivity rates. Thus the potential due to that is not deemed significant in this context. If the diameter of the pore in itself were of the order of Debye lengths, then this would need to be considered. In most cases, when the drift dominates diffusion effect, which happens in most macro cases, the electric field and the associated space charge, which arise due to ions with unequal diffusivities, can be neglected. But in this case that the diffusion term is comparable to the drift term, this Electric field becomes appreciable. The effect of electrode potentials is insignificant and thus neglected. The experimental results for HEAM-DMAEM and HEAM-MATEAC series of gels with charges from 8.6mM to 866mM are tabulated in Tables (4.1 – 4.10). A graph was plotted between steady state potential and log (C1/C2), in each case. In the case of HEMA-DMAEM gels the plots indicate that slope is initially negative, but gradually becomes positive for gels with a charge of 86.6mM and from there on till 866mM. In contrast all the slopes for HEMA-MAETAC gels have a positive slope, and it increases with increasing charge of the gel. The twin potentials of Donnan (at the two interfaces of the gel and the electrolyte) and diffusion (arrived at using Nernst-Planck equation) contribute to the total membrane potential. It could be that either of the potentials which dominated when the charge on the hydrogel is low is swamped by the

other effect as the charge on the gel increases. The diffusion potential arises from the slight separation of the bulk of positive charges from that of the negative charges due to diffusion caused by the gradients of mobile ions. It might also be necessary to investigate the effect of the streaming potential that arises from the slight separation of the bulk of the positive charges from that of the negative charges due to the flow convection effects caused by a pressure gradient that could be hydraulic or osmotic. Unequal Pressure heads in the experiment were observed at times, which implies that streaming potential could be an important variable to account for. Finally, we would also need to take into account the ion dissociation constants for the bases under consideration. For the weak basic monomer (DMAEM), the dissociation constant is low but it is high for the strong base MAETAC. As a result, the PEG-MAETAC membrane might contain undissociated ions even at low ionic strengths. Given that MAETAC is a stronger base than DMAEM and also taking the dissociation of these at low ionic strengths, it could be that the charges inside the membrane could have been replaced in significant numbers by new charges, which in the case of the MAETAC gel happened at low charge of hydrogel itself, but the same required more positive charge in the case of DMAEM gel to achieve.

CONCLUSION

An experimental study into the electric fields and forces characterizing charged hydrogel membranes has been analyzed in detail. The results are interesting for their sheer pattern and the consistency associated with it. The results of the steady state diffusion potential measurements of the HEMA-DMAEM and HEMA-MAETAC gels indicate an interesting pattern and shift in slopes. The measured membrane potential is a result of

two potential – Donnan and Diffusion. There is a clear evidence of change in the dominating effect of one of the potential through the change in the charge of gels from 8.66mM to 866mM for HEMA- DMAEM. In the case of HEAM-MAETAC there is total swamping effect of one of the potentials through the chosen range of charge of the gels. A neutral membrane, as is known, separates solutes according to the differences in their size and/or in their interaction with the membrane. A charged membrane separates charged solutes according to the charge of the membrane. The numerous counts of applications pursued using hydrogels particularly from the bacterial immobilization purposes; it has absolutely critical to analyze the ion transport phenomena in electrolyte solution systems across a charged membrane. Experimental evaluation of the membrane potential of the polyelectrolyte hydrogels proves to be a fair index to characterize the transport phenomena across a charged membrane. This study combined with the swelling measurements yields crucial insight into the choice of hydrogel for bacterial immobilization wherein the ion transport through the membrane and swelling phenomenon are important criteria.

Chapter Five

IMMOBILIZATION OF A BIOLUMINESCENT BIOREPORTER

ABSTRACT

This section of the study attempts to devise techniques to successfully immobilize bioreporter using hydrogels. The data from the study of the properties of the hydrogels plays an important role in the choice of hydrogel for immobilization. The main objective is to achieve long term viability of the bioreporters without the loss of its functionality. The surface immobilization and the cellular encapsulation were the two techniques employed. The bioreporters used for the experiments were a genetically modified strain called *Pseudomonas fluorescens 5RL*. It was hypothesized that the gram negative bioreporters should preferentially adhere to the surface of the hydrogels with a net positive charge. Series of experiments involving inoculation on hydrogel with varying surface charges were carried out to verify the hypothesis. The surface inoculation method could only be employed in stationary biosensors wherein the bioreporters had no chances of being displaced. Thus another technique was tested, which encapsulated the cells in three dimensional hydrogel networks. It was ensured that the membrane was porous to allow for the interaction while, isolating it from the harsh environmental conditions. DMAEM and Alginate hydrogels were used for the encapsulation process.

INTRODUCTION

Bacterial cells tend to attach and associate with most surfaces they come in contact. The initial adhesion process is usually followed by the formation of a complex and heterogenous biofilm [1]. Bioluminescent Bioreporter sensors developed by sayler et.al are an inexpensive, sensitive and rugged device to measure physical and chemical changes in the environment. One of the major challenges in such sensors is the need for an immobilization matrix that can hold the bioreporters metabolically active without loss of bioluminescence.

Biofilms are generally foul smelling and have a damaging effect to food equipment, heat exchangers, ship hulls and biomaterial implants, but they are also beneficial for degradation of environmentally hazardous substances in a bioreactor [2-8]. Akihiko Terada et. al has demonstrated the promotional effect of radiation induced graft polymerization on adhesion of bacterial cells to polymer surfaces. Bacterial adhesion to silicone lenses was extensively studied by Henriques et. al [9]. Sug-joo Ahn et. al developed quantitative analysis techniques for studying adhesion to orthodontic implants and metal brackets [10].

The main objective of this section of the thesis was to attain better understanding of the bacterial adhesion to polymer and biomaterial surfaces and develop cell immobilization techniques. The design of experiments was structured to analyze the surface inoculation and the cellular encapsulation protocols.

A. Mechanism of bacterial adhesion

The study of the underlying principles behind the bacterial adhesion and its significance is an extensive field encompassing numerous aspects of nature and human life, such as marine science, soil and plant ecology, food industry, and most importantly, the biomedical field [2, 3, 4, 5]. Adhesion of bacterial cells to human tissue and other biomedical implants surfaces is an important step in the pathogenesis of infection [2, 6]. Bacterial adhesion leading to the biofilm formation is a two step process. The first step is the reversible process involving the physicochemical forces and the second is the irreversible chemical process followed by the formation of the extra-cellular substances, which cements the cells to the contact surface. Similar to the tissue cells growing in in-vitro culture, bacteria prefer to grow on available surfaces rather than in the surrounding aqueous phase [7].

Physicochemical interactions - phase I. The long range Van der Waals forces and the electrical double layer forces typically determine the deposition rate of a charged colloidal particle to a surface. These forces collectively form the basis of the DLVO theory, which summarizes the electrostatic and the Van der Waals interactions and yields the overall interaction energy between the surfaces as a function of separation distance. The Van der Waals arising as a result of the induced dipole interactions between the molecules in the colloidal particle and the molecules in the substrate are generally attractive. Electrical double layer forces as a result of the overlap of counter ion clouds near charged surfaces and the change in free energy as the surfaces move closer or farther apart. The result is an attractive force for like charged surfaces and a repulsive force for

oppositely charged surfaces. The DLVO theory however assumes homogeneity, molecularly flat surfaces, uniformly charged surfaces which may be strongly violated for real bacteria. Nonetheless the DLVO theory is discussed to provide a conceptual framework for understanding the relationship between the long range forces and the adhesion of bacteria to the surface.

Molecular and cellular interactions – phase II. In this phase the molecular reactions between the surfaces are predominant. It implies a firmer and non reversible kind of adhesion of bacteria to a surface by the bridging function of bacterial surface polymeric structures, which include capsules, fimbriae, pilli and slime. A number of studies indicate that the cell capsules made of polysaccharides and proteins act as adhesions. This kind of adhesion occurs both in Gram positive and Gram negative bacteria.

B. Miscellaneous factors

Environment – The medium. The bacterial adhesion depends on the adhering bacteria, substrate and the suspended medium. The adhesion is known to be dependant on the medium's shear stress, pH, bacterial concentration, temperature and time of exposure. The flow patterns are an important factor in attachment of bacteria to solid surfaces and under these conditions a shear stress is applied. Adhesion is optimal for a shear stress value of 6-8 N/m^2.

Bacterial surface charge. The surface charge is another significant physical factor for bacterial adhesion. It is the involved in the initial step of bacterial colonization and is

governed by long range Van der Waals. Most particles acquire an electric charge in aqueous suspension due to the ionization of their surface groups. The surface charge attracts ions of opposite charge in the medium and results in the formation of electric double layer. The surface charge is usually characterized by the isoelectric point or the electro kinetic potential (Zeta potential), electrophoretic mobility, colloid titration, electrostatic interaction chromatography.

C. Encapsulation of whole cells

Sol-gel has been one of the successful methods adopted for whole cell encapsulation for well over a decade now. The main concern in the sol gel process is the formation of alcohol during the condensation reaction [47, 48]. The effect of the alcohol by products on the cells was studied by Premkumar.et.al [49, 50]. This resulted in a number of other encapsulation techniques are being explored. Investigators have also tried the aqueous routes that do not produce alcohol as by-product and yield mesoporous hydrogels. Several studies reveal that the encapsulation does not introduce additional mass transfer issues [51]. It also showed no significant differences in the response of the cells in the case of thick or thin films. Inama et.al observed similar Line-weaver plots and Km values for encapsulated cells and cells in solution suggesting the absence of a mass transfer issue [52]. The other important consideration for encapsulated cells is the possibility of cellular division in the polymer matrix. Studies conducted by Premkumar et.al shows that the tensile strength of gels are high enough to prevent cellular division. The confocal studies following the encapsulated cells also did not indicate any division. The final issue for

encapsulated cells is the escape from the matrix. The percentage of escaped cells was low and there was no significant loss in the response due to the escaped cells.

D. Live dead assay

Live dead assays are easy to use, simple and direct verification of the cell viability as a function of the cell membrane integrity. The test essentially employs two nucleic acids stains – the SYTO® 9 stain and the red-fluorescent propidium iodide stain. These stains differ in their ability to penetrate healthy bacterial cells. When used alone, SYTO 9 stain labels both live and dead bacteria. In contrast, propidium iodide penetrates only bacteria with damaged membranes, reducing SYTO 9 fluorescence when both dyes are present. Thus, live bacteria with intact membranes fluoresce green, while dead bacteria with damaged membranes fluoresce red. Live and dead bacterial cells can be imaged separately or simultaneously by fluorescence microscopy with suitable optical filter sets. Moreover the excitation/emission maxima for these dyes are about 480/500 nm for SYTO 9 stain and 490/635 nm for propidium iodide. Thus the background remains virtually nonfluorescent making it easier during the process of imaging.

RESULTS

A. Surface inoculation - Polyelectrolyte Hydrogels

Figures (5.1 – 5.4) illustrate the results from the bioluminescence tests conducted on anionic polyelectrolyte hydrogels surfaces, inoculated with a bioluminescent bioreporter (*Pseudomonas fluorescens 5RL*).

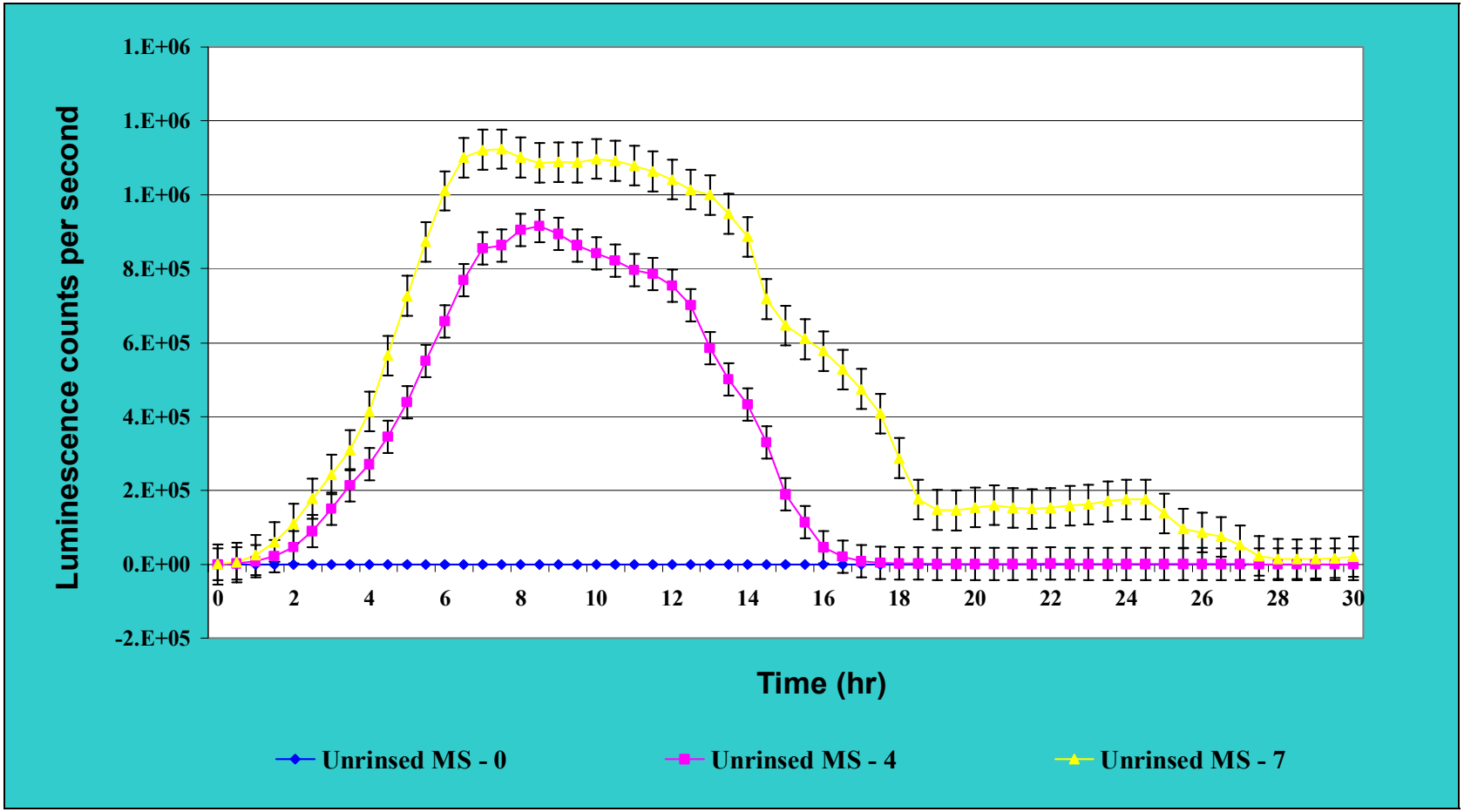

Figure 5.1 Bioluminescence curve for bioreporter on Unrinsed anionic HEMA hydrogels (Trial 1).
Each data curve is the mean of triplicates with the error bars representing the standard error at that data value. "Unrinsed MS # "refers to the unrinsed (not rinsed) surface inoculated membrane samples numbered according to the charge concentration.

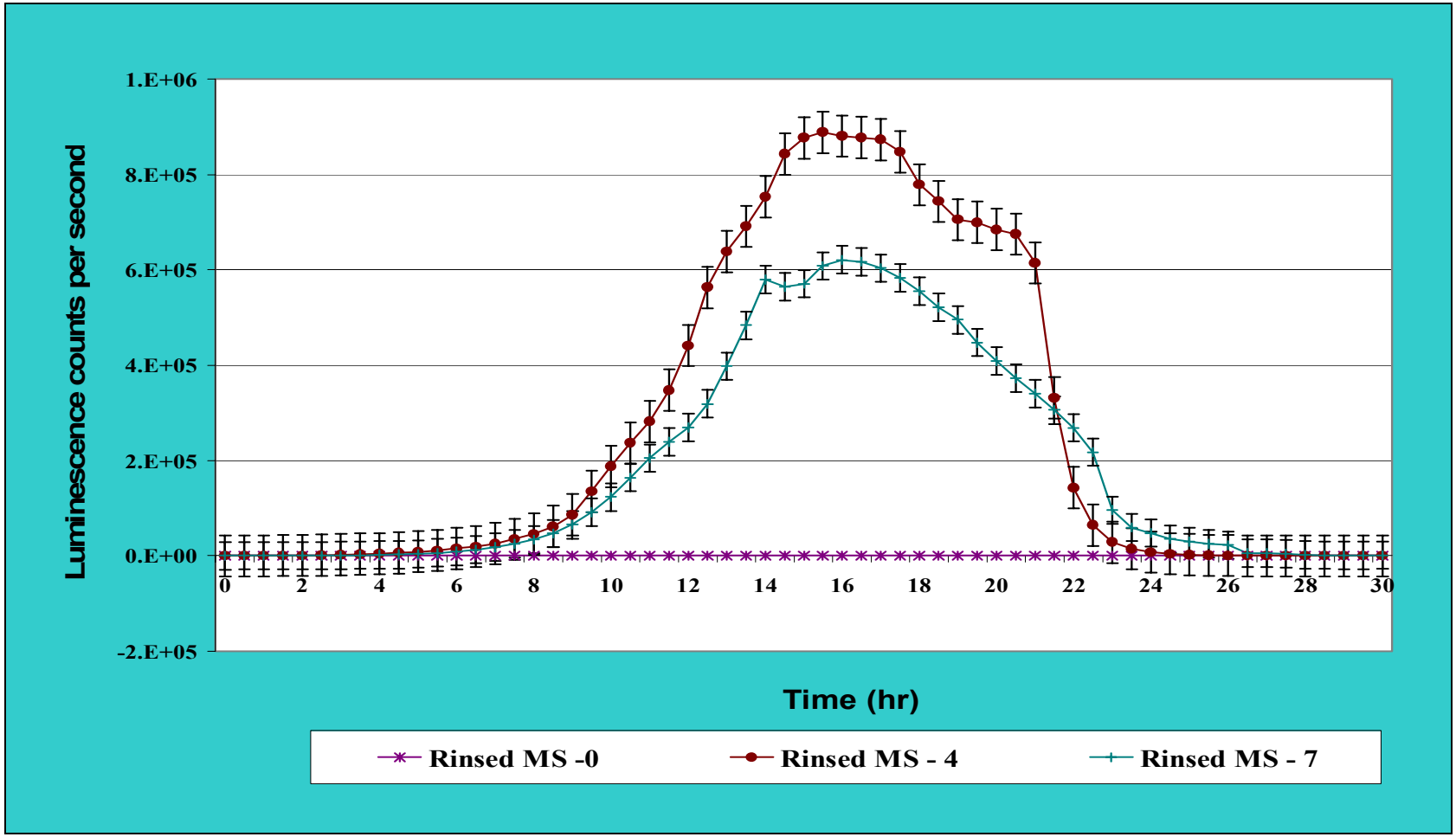

Figure 5.2 Bioluminescence curve for bioreporter on rinsed anionic HEMA hydrogels (Trial 2).
Each data curve is the mean of triplicates with the error bars representing the standard error at that data value. "Rinsed MS # "refers to the rinsed surface inoculated membrane samples numbered according to the charge concentration.

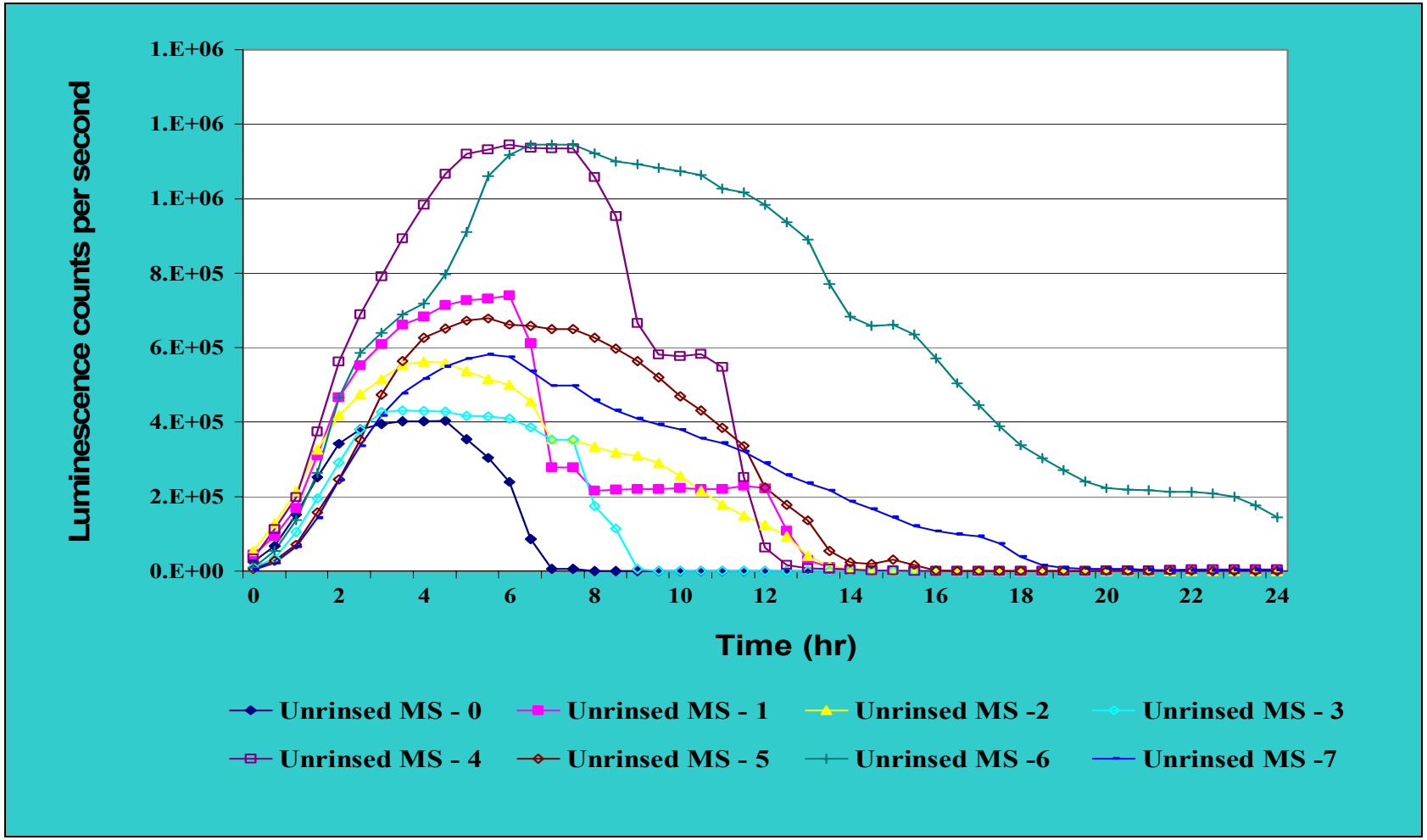

Figure 5.3 Bioluminescence curve for bioreporter on Unrinsed anionic HEMA hydrogels (Trial 3).
Each data curve is the mean of triplicates. "Unrinsed MS # "refers to the unrinsed (not rinsed) surface inoculated membrane samples numbered according to the charge concentration.

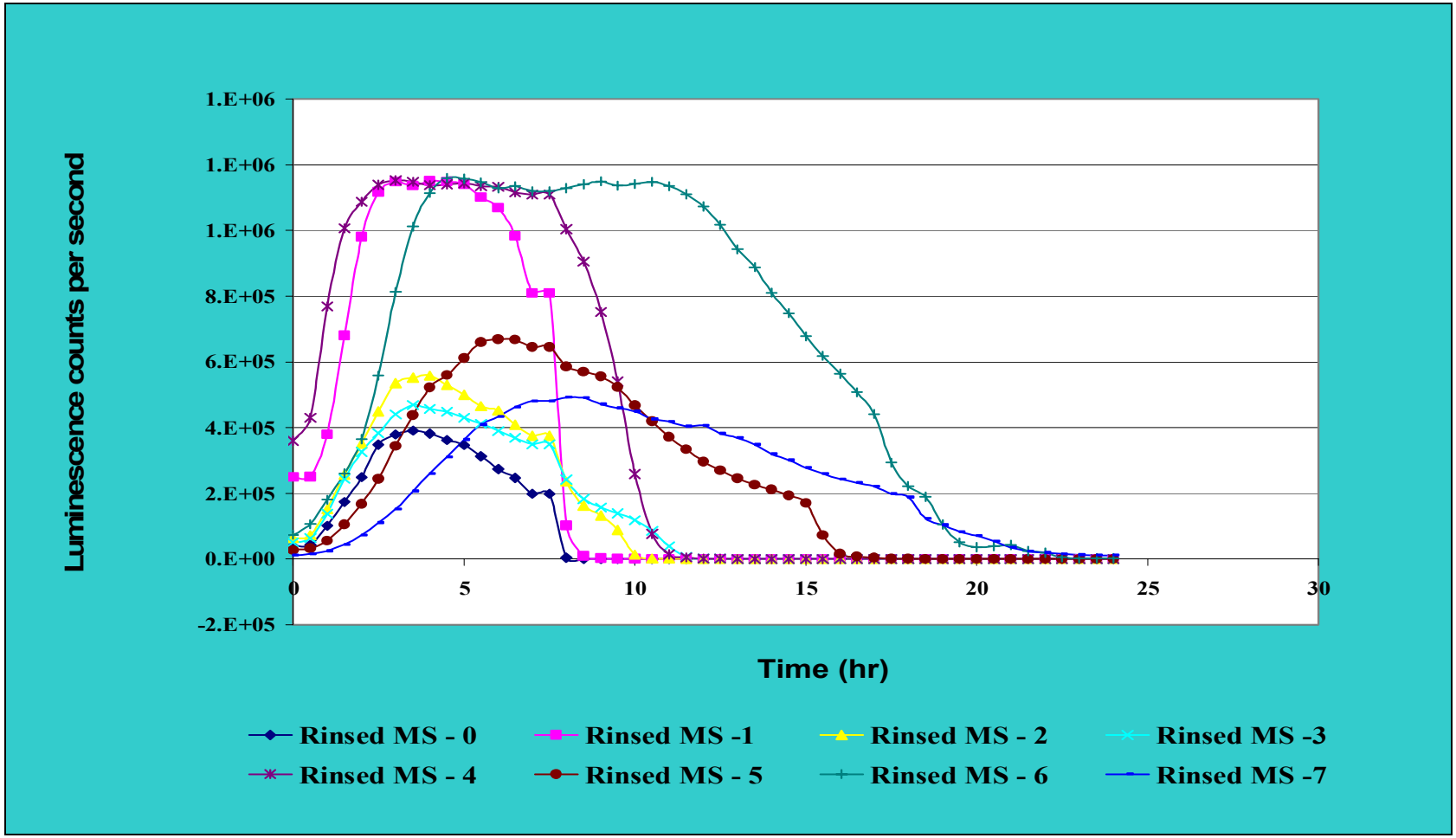

Figure 5.4 Bioluminescence curve for bioreporter on rinsed anionic HEMA hydrogels (Trial 4).
Each data curve is the mean of triplicates. "Rinsed MS # "refers to the rinsed surface inoculated membrane samples numbered according to the charge concentration.

The results of the graphical plot indicate an interesting pattern depicting a charge specific adhesion phenomenon. The cells adhered better to membrane samples with higher charges. The membrane sample -0 corresponds to pure HEMA hydrogel shows insignificant bioluminescence indicated a fewer number of adhered cells. The membrane samples -7 with the maximum charge of 1540 mM recorded a higher and longer bioluminescence response, corresponding to a greater number of adhered cells. The membrane samples with an intermediate charge between 0mM – 1540 mM recorded a comparatively lower response in most of the cases with a few exceptions. Some of the samples were rinsed with fresh MSM to wash away the loosely attached cells and analyze the degree of adhesion. The response pattern was similar with a nominal reduction of the peak bioluminescence value as expected. The experiment was repeated with more samples and the results conformed significantly to the previous observations in most of the cases with a few unexplained anomalies. The charge of the hydrogel samples was logarithmically varied from 0mM – 1540mM, giving rise to seven different specimens.

B. Surface inoculation – Polyampholyte hydrogels

Figure 5.5 summarizes the results from the bioluminescence tests conducted on polyampholyte hydrogels surfaces inoculated with *Pseudomonas fluorescens 5RL* (Bioluminescent bioreporter).

The bioluminescence experiment with similar protocol was conducted with polyampholyte hydrogels surfaces to verify the pattern observed in the previous cases. The polyampholyte hydrogels with positive and negative charges recorded a higher peak

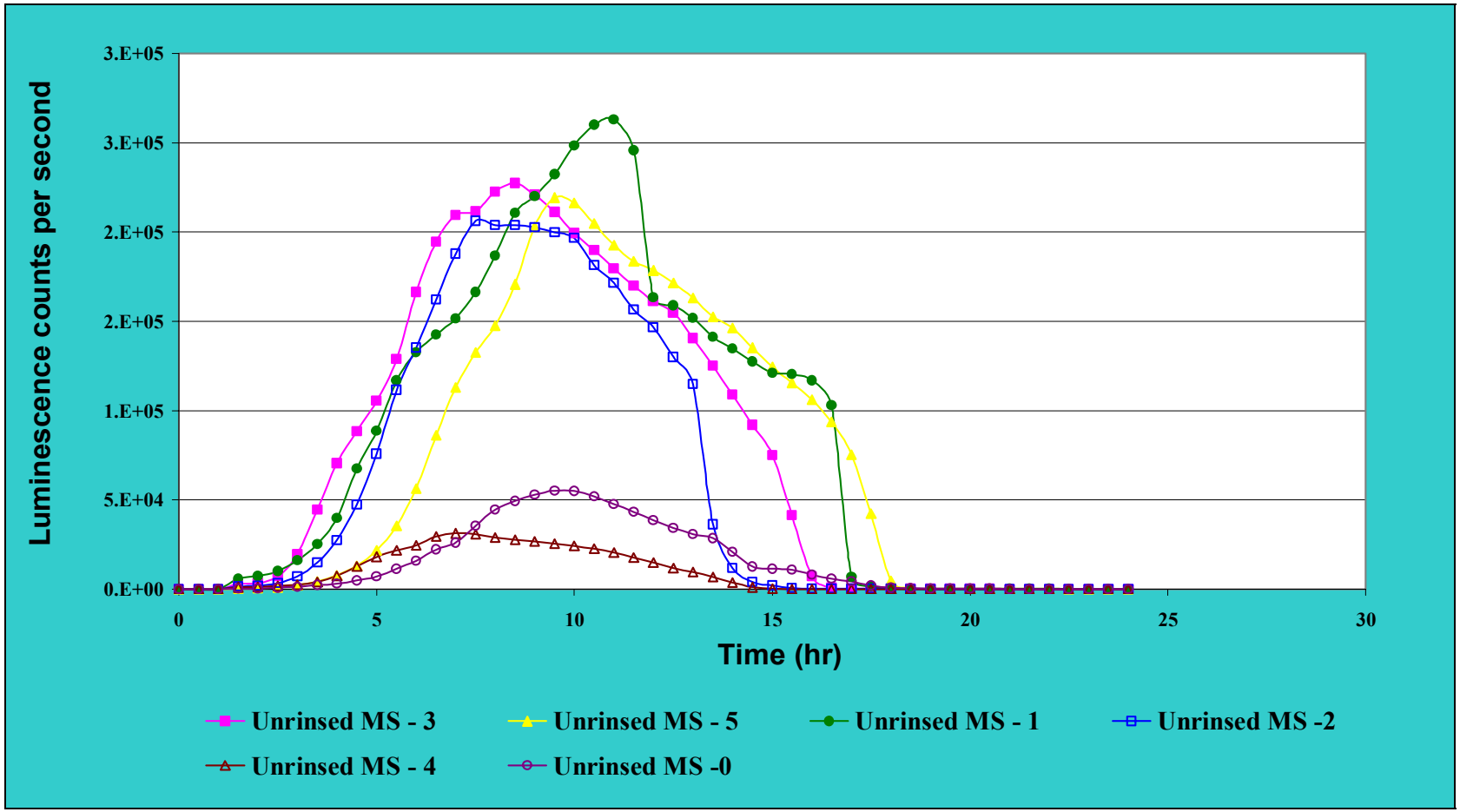

Figure 5.5 Bioluminescence curve for bioreporter on unrinsed Polyampholyte hydrogels.
Each data curve is the mean of triplicates. "Unrinsed MS # "refers to the unrinsed (not rinsed) surface inoculated membrane samples numbered according to the charge concentration.

bioluminescence response to the anionic polyelectrolyte gels. In contrast the cells adhered to the polyampholyte gels needed a longer time period to reach the peak value and the total response time was also interestingly shorter. In contrast to the anionic polyelectrolyte hydrogels the adhesion of cells to polyampholyte hydrogels does not exhibit a particular pattern. Polyampholyte membrane samples with the exception of those with charges - 0mM and 48.7 mM recorded a similar bioluminescence response. The charge specific adhesion pattern, wherein the degree of adhesion increased with increasing charge, as observed in the anionic polyelectrolyte hydrogels was not observed in the case of polyampholyte gels. The gram negative bacterial cells with access to abundant positive charge in the case of polyampholyte gel surfaces, was expected to exhibit increased adhesion owing to double layer formation. The results however did not support this hypothesis.

C. Cellular encapsulation - DMAEM hydrogels

Figures (5.6 - 5.8) illustrate the results of the bioluminescence response of the bioreporter cells encapsulated in DMEAM hydrogels.

The results from Fig 5.6 suggest the lack of any significant activity of the cells after the DMAEM polymerization process. The membranes were monitored for a period of 24 hours with no peak values above the background, indicating an instantaneous death of the cells or a mass transport issue. To eliminate one of the possibilities, the experiment was repeated with a modified protocol wherein the encapsulated cells were pretreated with the inducer (30ppm Sodium salycylate) before the encapsulation. The results of this repeat experiment are illustrated in Fig 5.7. The plot does not indicate any response from the

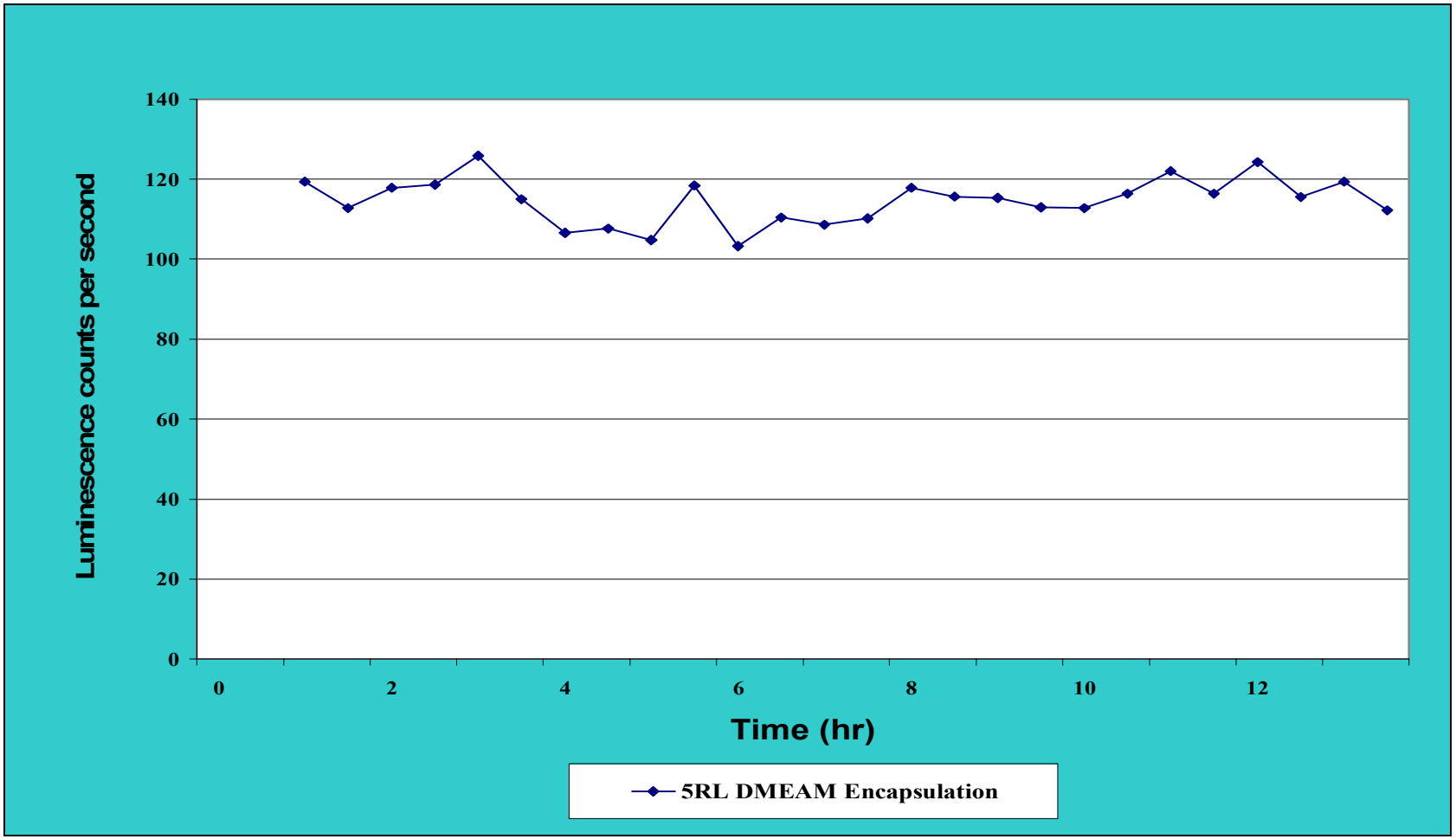

Figure 5.6 Bioluminescence curve for bioreporter encapsulated in PEG-DMAEM hydrogels (Trial 1).
The data curve is the mean of four identical samples.

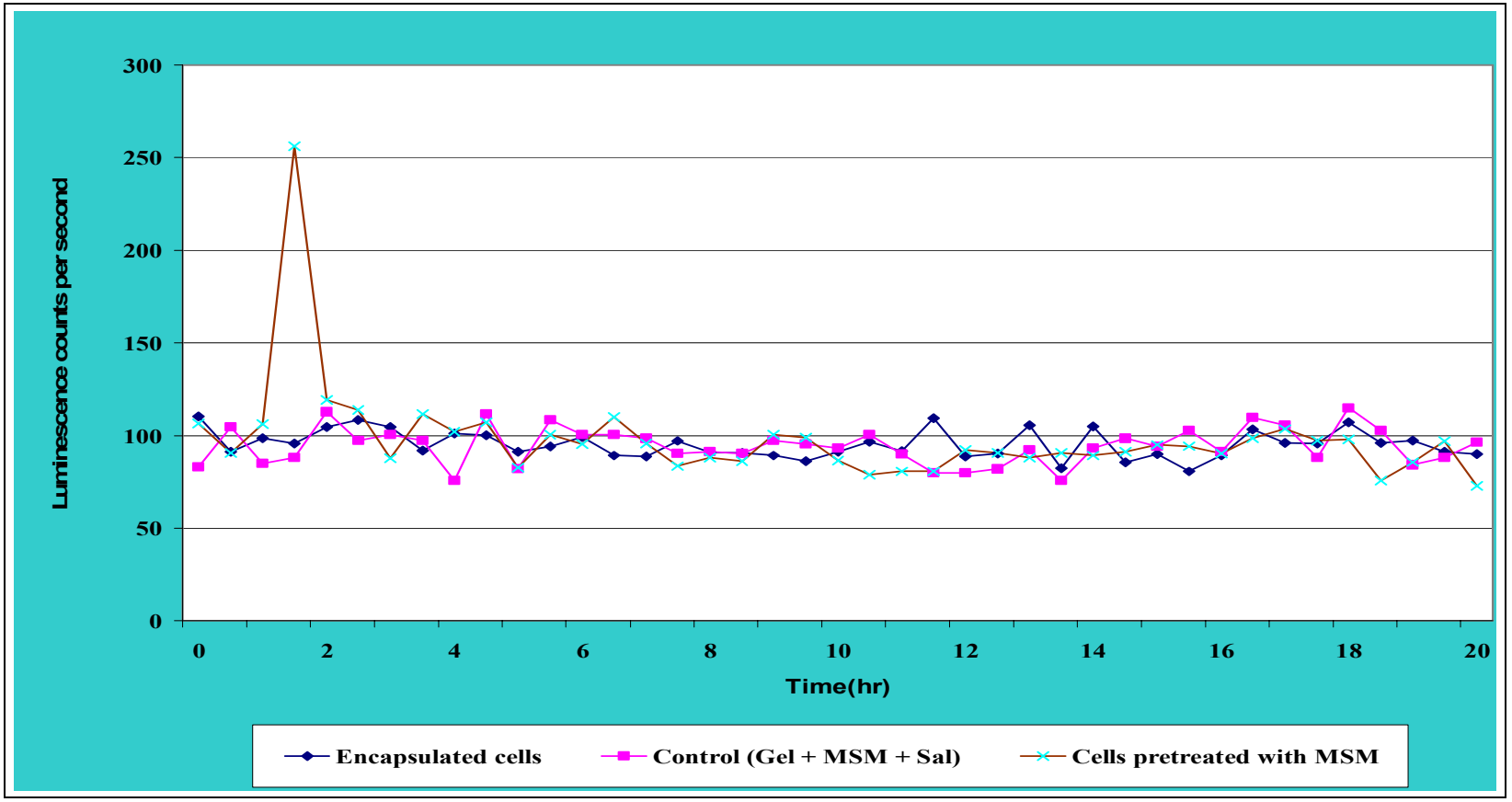

Figure 5.7 Bioluminescence curve for bioreporter encapsulated in PEG-DMAEM hydrogels (Trial 2).
The data curve is the mean of triplicates. The samples included pre-induced cells as negative control.

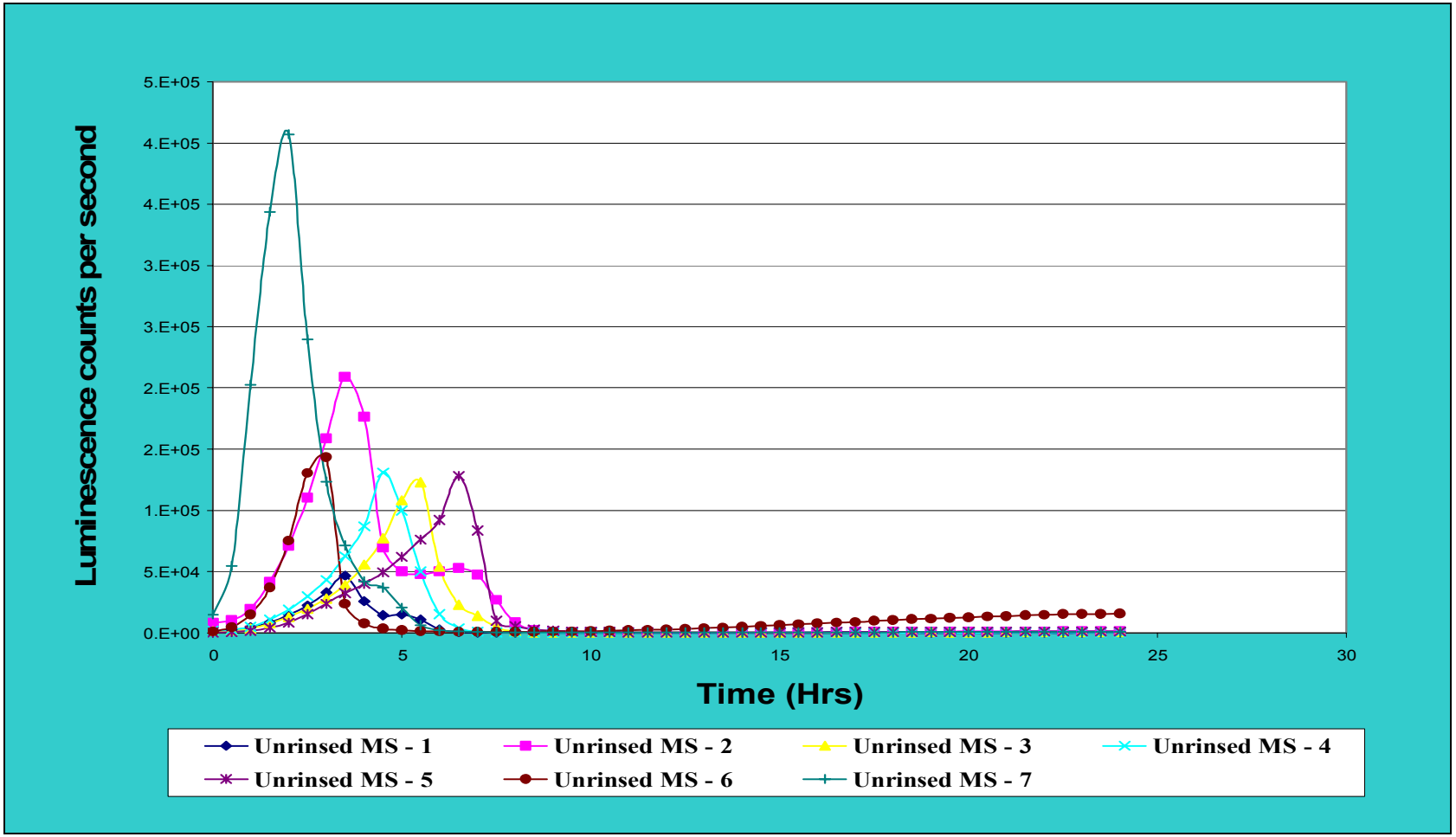

Figure 5.8 Bioluminescence curve for surface inoculated bioreporter on unrinsed PEG-DMAEM.
Each data curve is the mean of triplicates. "Unrinsed MS # "refers to the unrinsed (not rinsed) surface inoculated membrane samples numbered according to the charge concentration.

pretreated cells. To finalize the unfavorable nature of the polymerization process the cells were inoculated on the surface of these gels. Figure 5.8 reports the bioluminescence response of the cells inoculated on the surface of the PEG DMAEM gels. The bioluminescence response recorded in plot Fig 5.8 is significantly lower in terms of the registered peak value and total response time, when compared to the surface inoculation of anionic polyelectrolyte hydrogels. The DMAEM being a negatively charged monomer should have promoted adhesion similar to the case of anionic polyelectrolyte gels. On the contrary there was no considerable adhesion pattern observed and the bioluminescence response was short lived and insignificant. The results clearly indicate the cytotoxic nature of the polymer leading to the death of the cells. The pretreated cells experiment clearly proved the absence of a mass transport issue.

D. Cellular encapsulation – Alginate gels

Figures (5.9 – 5.11) illustrate the results of the bioluminescence response of the bioreporter cells encapsulated in alginate gels and beads. The failures of DMEAM as an encapsulation matrix lead to an alternative encapsulation strategy –Alginate encapsulation. The alginate gels were prepared according to the protocol as mentioned in the materials and methods section earlier. The cells were encapsulated in the gels and then tested for the bioluminescent response by artificially inducing it with a 30 ppm solution of sodium salycylate solution.

The bioluminescence plot in Fig (5.8) indicates comparison of the bioluminescence response of the encapsulated cells in DMAEM and alginate gels. The results were encouraging suggesting the possibility of the alginate as a far superior method to

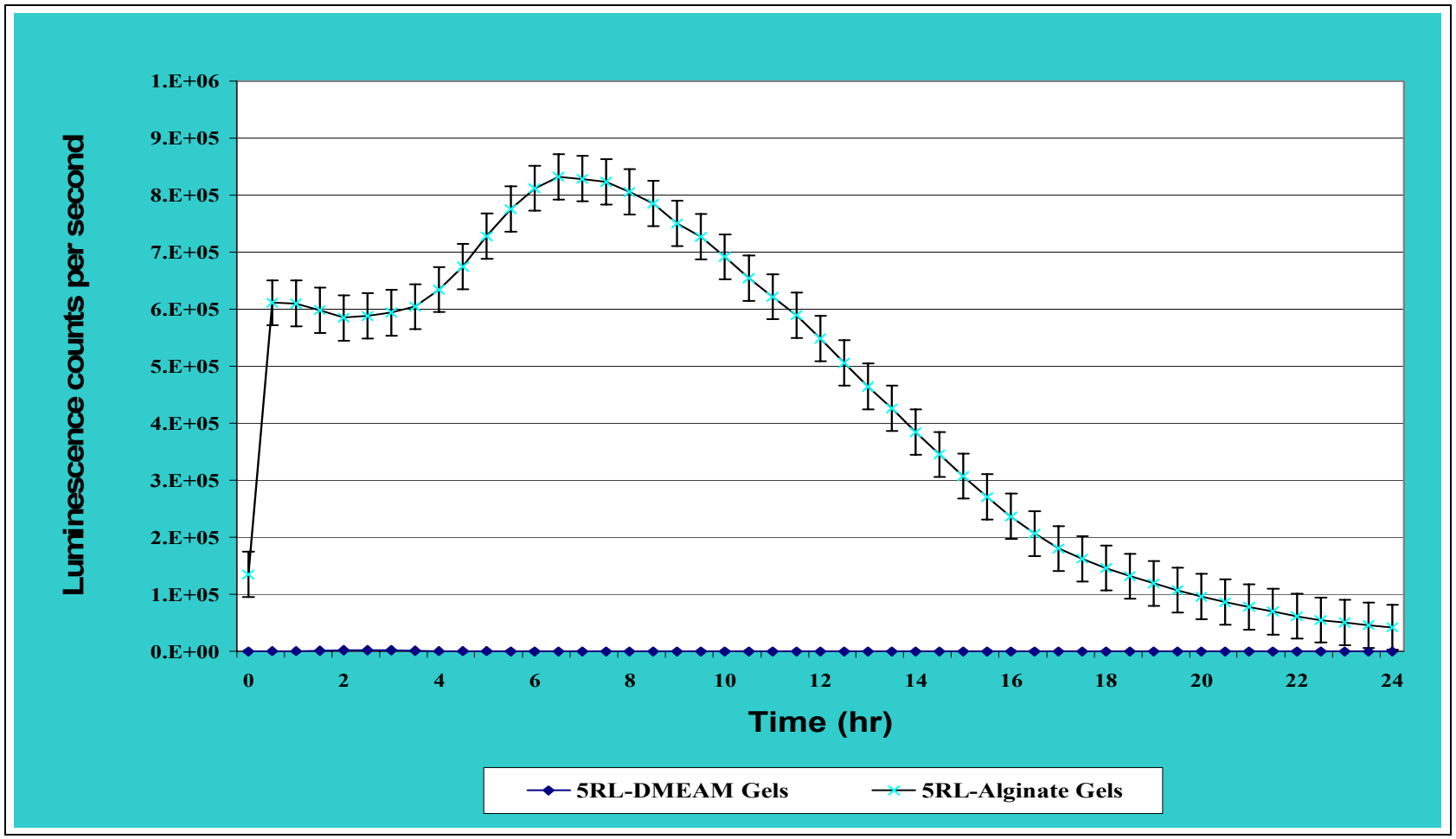

Figure 5.9 Bioluminescence curve for bioreporter encapsulated in PEG-DMAEM and alginate gels.
The data curve is the mean of triplicates and error bars represent the standard error of each data point.

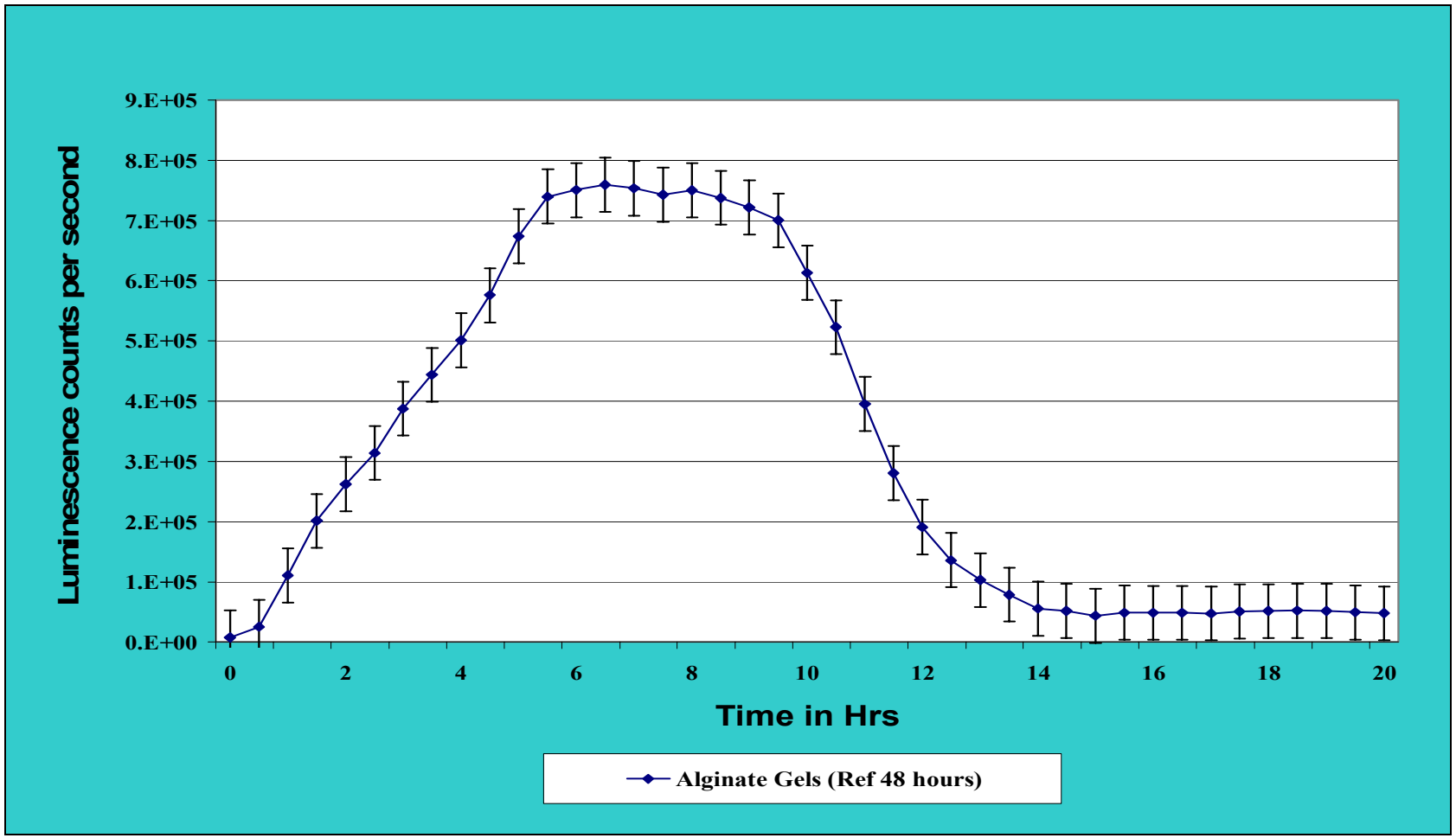

Figure 5.10 Bioluminescence curve for bioreporters encapsulated in alginate films.
The data curve is the mean of triplicates and error bars represent the standard error of each data point.

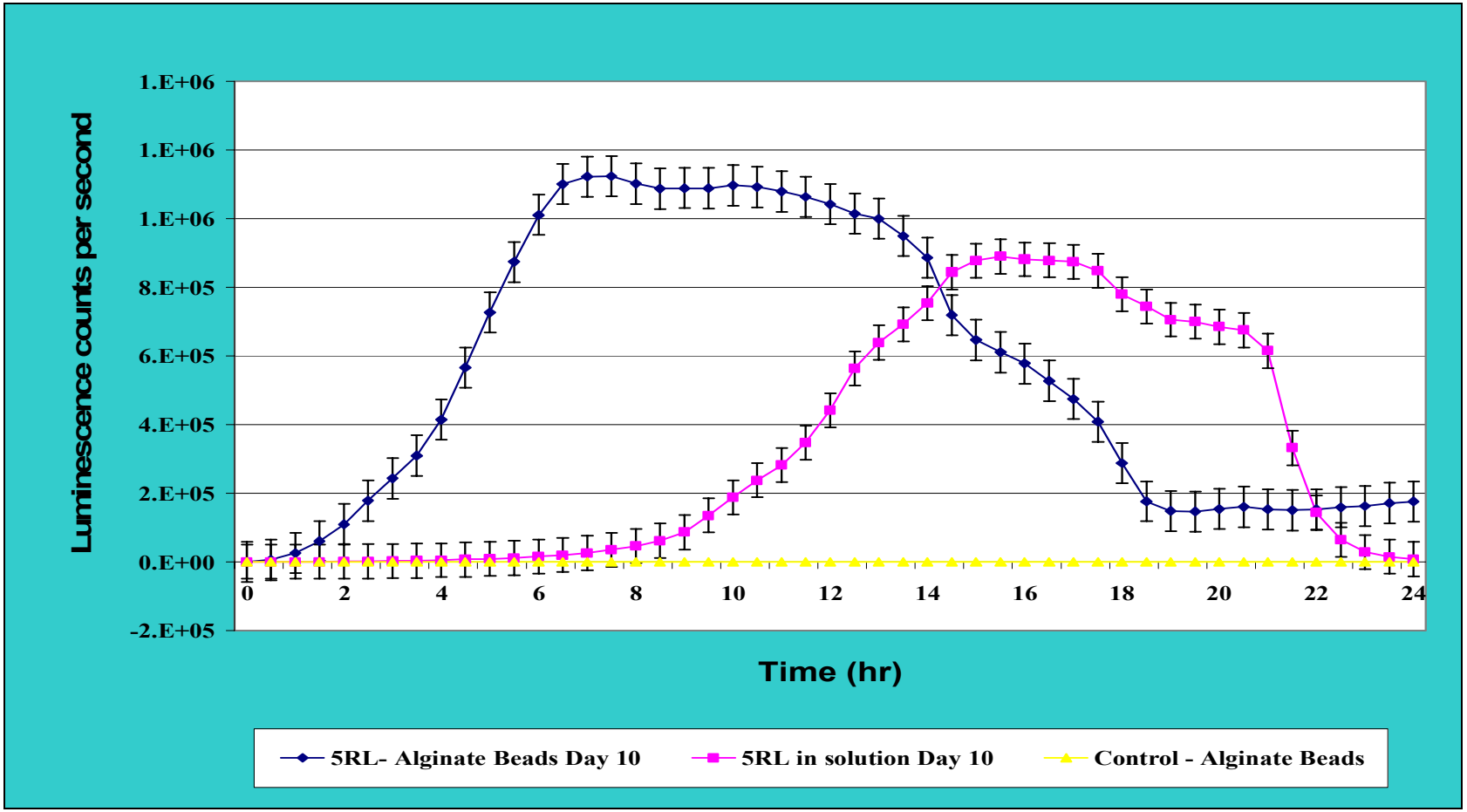

Figure 5.11 Bioluminescence curve for bioreporters encapsulated in alginate beads.
The data curve is the mean of triplicates and error bars represent the standard error of each data point. The bioluminescence was tested after a period of 10 days to observe the long term storage effects.

encapsulate bioreporter cells than DMAEM. The cells encapsulated in the alginate gels responded well to the inducer (sodium salycylate) with high peak value and longer response time periods compared to DMAEM and also surface inoculated gels. The alginate gels used from here on were prepared to a slightly modified protocol and made in the form of beads to facilitate easier and longer storage. Fig (5.10) and Fig (5.11) reports the response of the encapsulated cells (in alginate beads) after 48 hours and 10 days respectively. The long term response also confirmed the cell activity within the membrane, reaffirming the alginate gels as a good encapsulation membrane for the specific bioreporter in question (*Pseudomonas fluorescens 5RL*). The plain alginate beads used as a negative control did not record any bioluminescence activity higher than the background.

E. Live dead assay

Figures 5.12 – 5.14 illustrates an account of the live and dead bioreporter cells distributed inside an alginate bead. *Pseudomonas fluorescens 5RL* cells were used for the encapsulation experiment. A Olympus Confocal microscope was used to image the fluorescence after staining. The images include both the red and green channel inputs. The SYTO 9™ dye (green) and Propidium dye (red) are excited using the same laser (480nm). The viable cells indicated by green fluorescence and the dead cells indicated by red fluorescence provides a good measure of the amount of the viable cells.

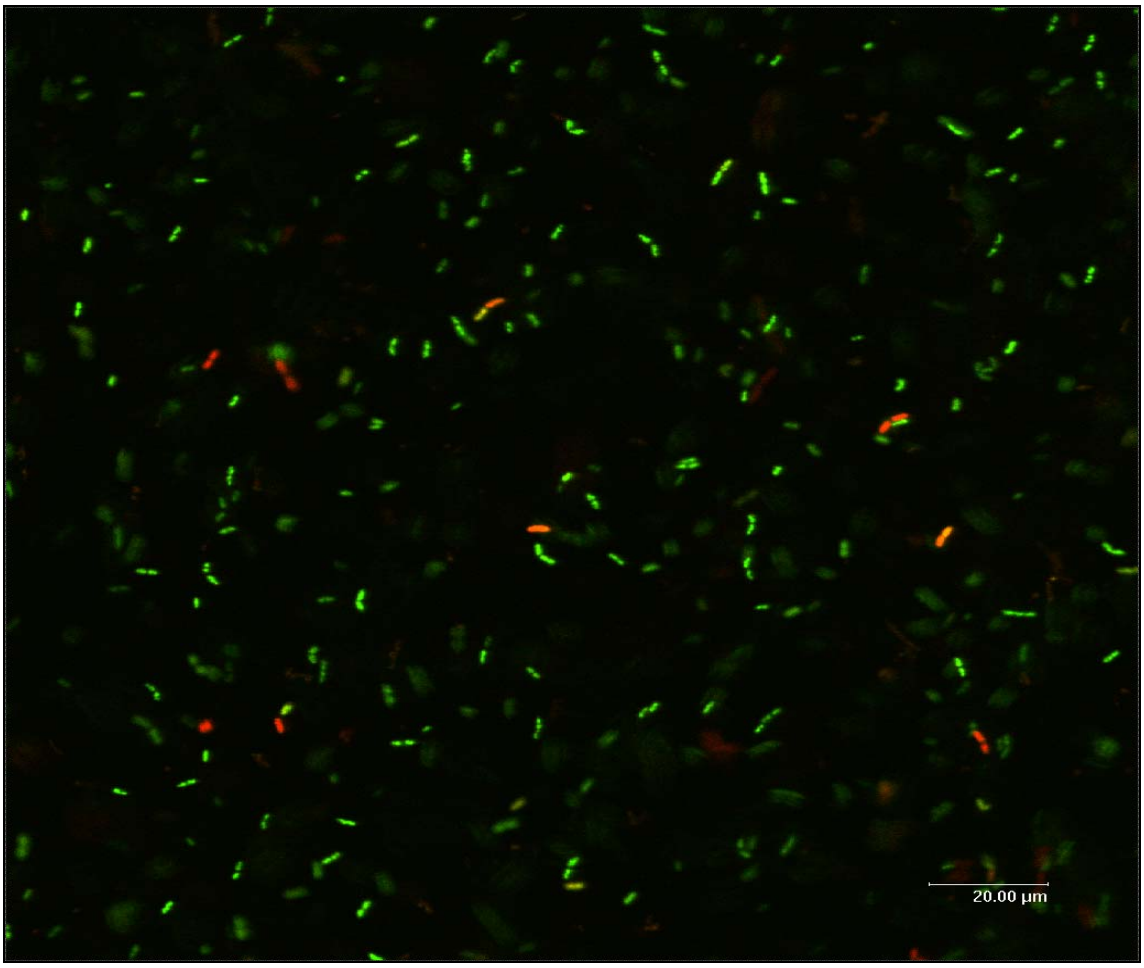

Figure 5.12 Confocal micrograph of 5RL cells encapsulated in alginate beads (Trial 1).

The live cells are stained green and the dead cells are stained red using the live dead assay. The image was captured using a 63X objective.

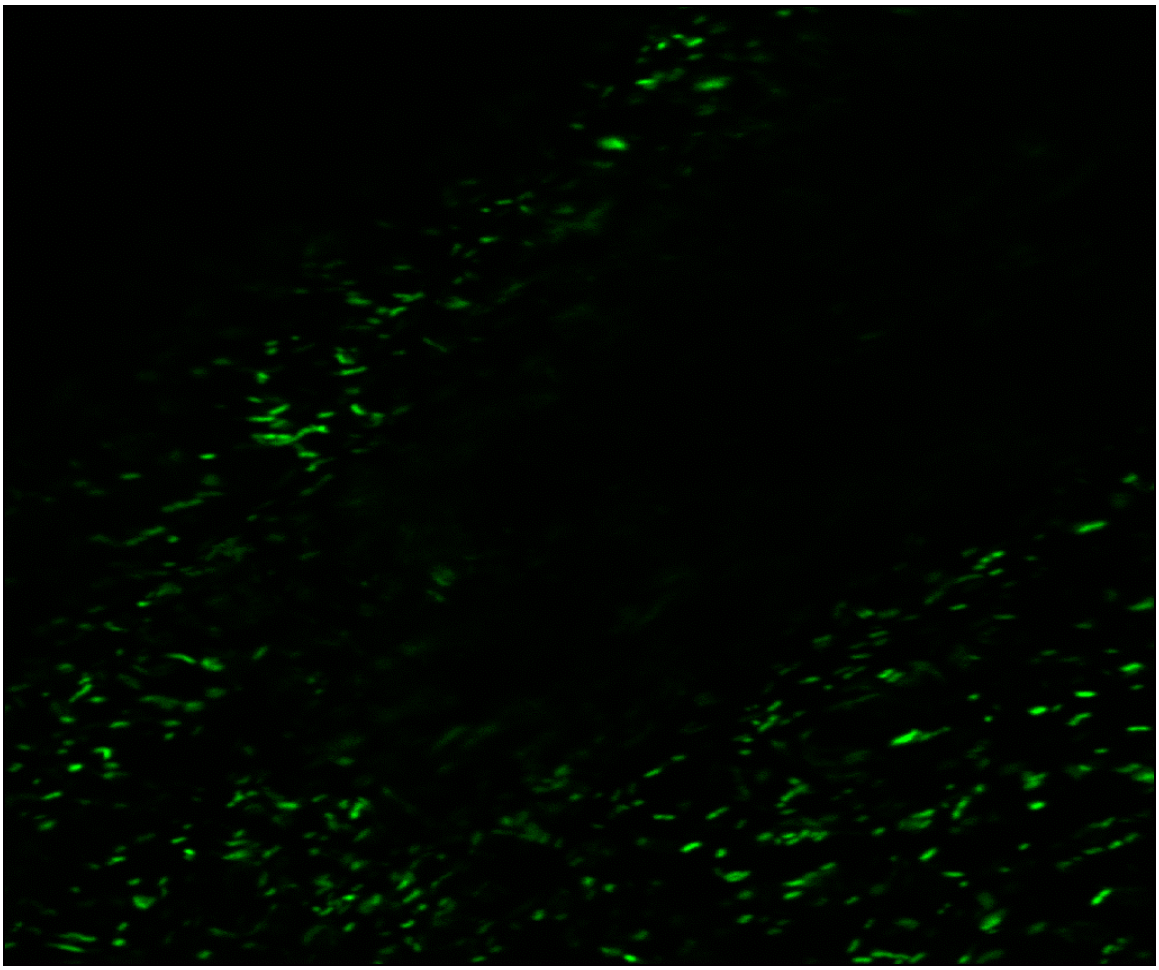

Figure 5.13 Confocal micrograph of 5RL cells encapsulated in alginate beads (Trial 2).

The live cells are stained green and the dead cells are stained red using the live dead assay. The image was captured using a 10X objective.

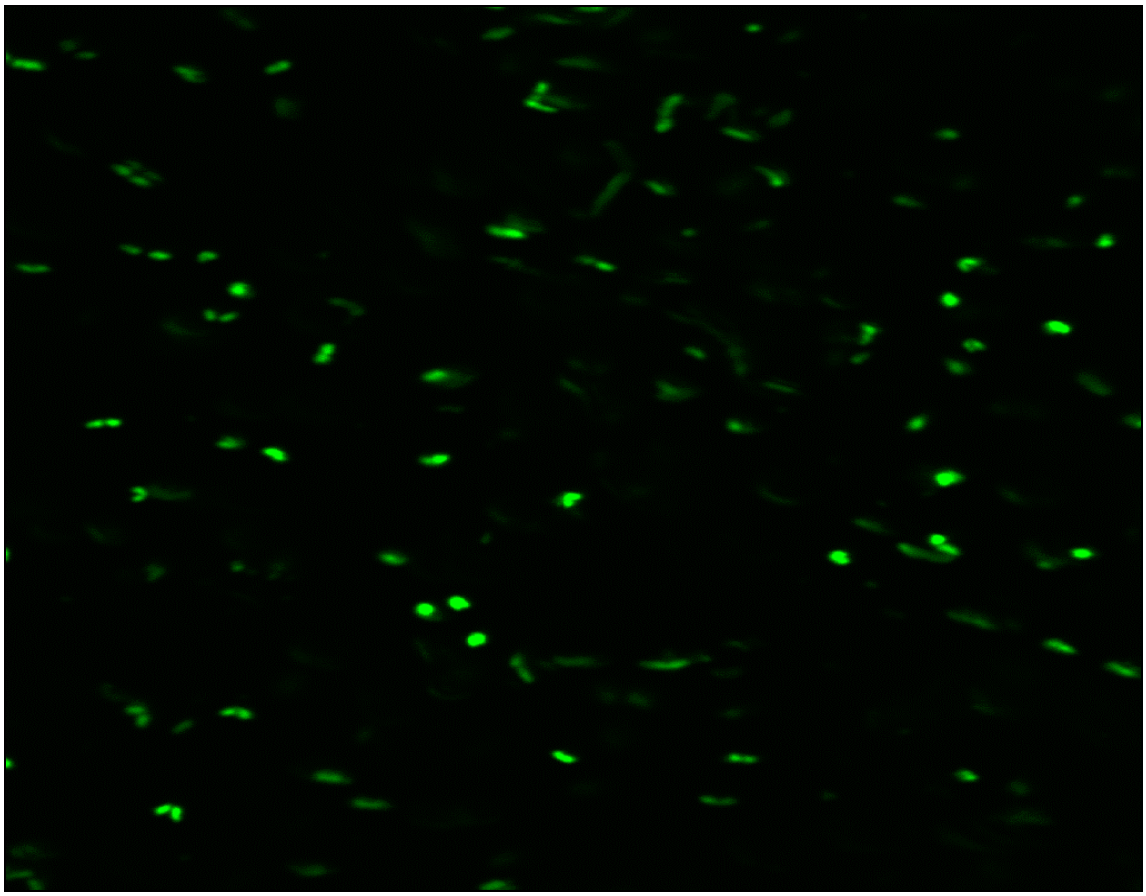

Figure 5.14 Confocal micrograph of 5RL cells encapsulated in alginate beads (Trial 3).

The live cells are stained green and the dead cells are stained red using the live dead assay. The image was captured using a 20X objective.

F. Electron microscopy

Figures 5.15 – 5.18 represent the images of the alginate beads with encapsulated bioreporter cells. The encapsulated cells are *Pseudomonas fluorescens 5RL* bacterial strain. A Hitachi H800 was used to obtain images the thin sections of the alginate encapsulated bioreporter cells. All the TEM micrographs indicate intact cell walls of the encapsulated bioreporter cells. The possible cell division evident on the micrographs could have been at the time of encapsulation, as the cells enmeshed in the alginate matrix cannot divide due to the constrained space.

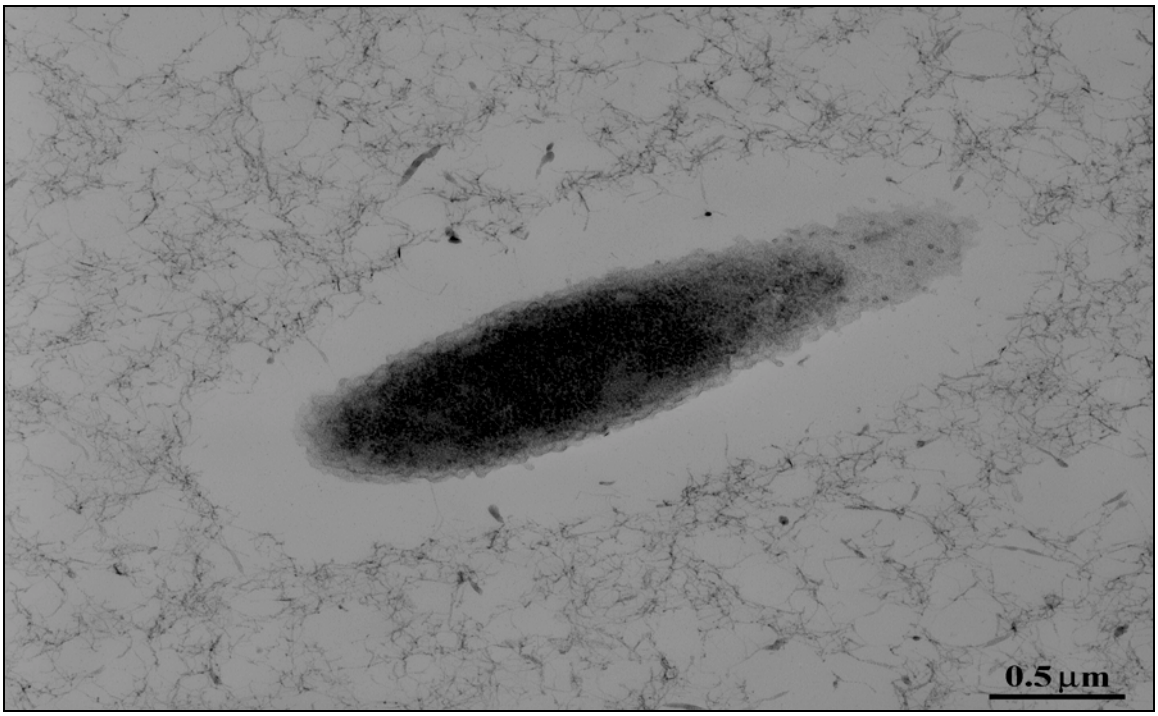

Figure 5.15 TEM micrograph of a 5RL cell in alginate bead (Trial 1).

The rest of the area of the image is the alginate gel.

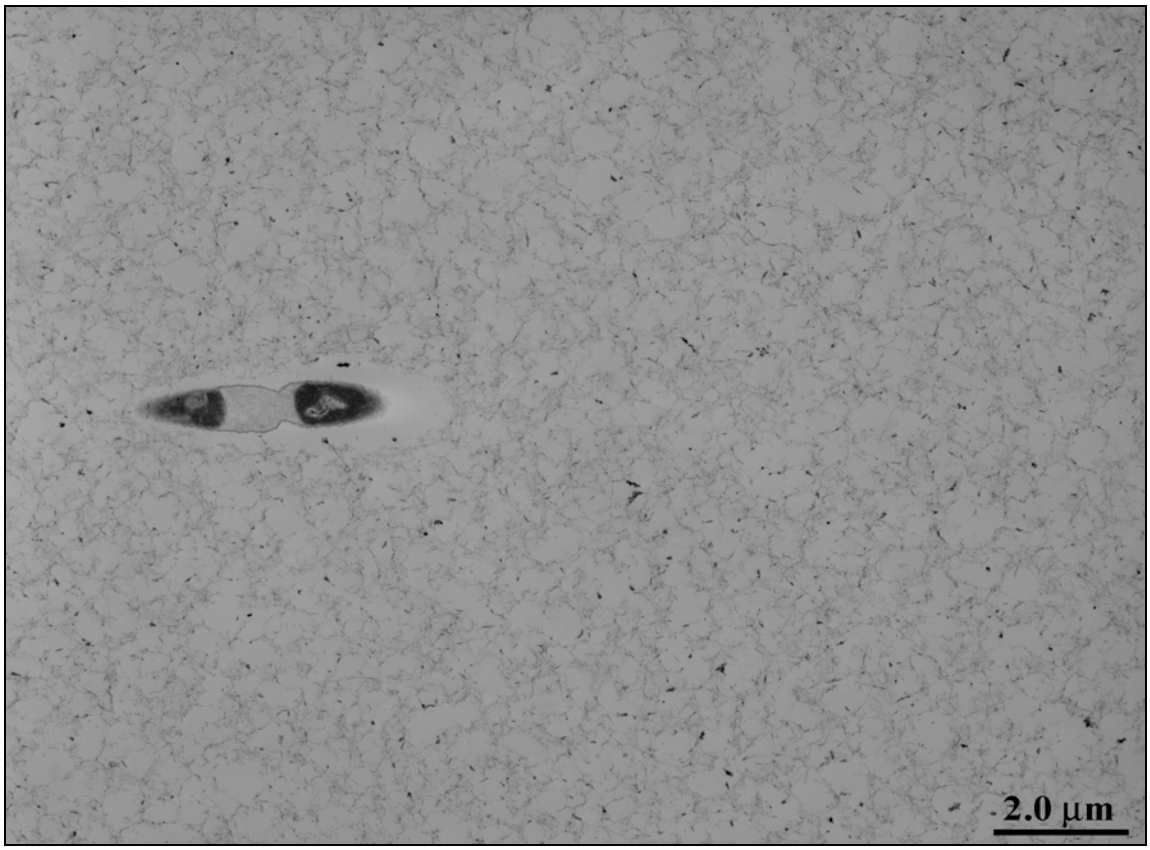

Figure 5.16 TEM micrograph of a 5RL cell in alginate bead (Trial 2).

The figure shows a possibly dividing cell. The rest of the area of the image is the alginate gel.

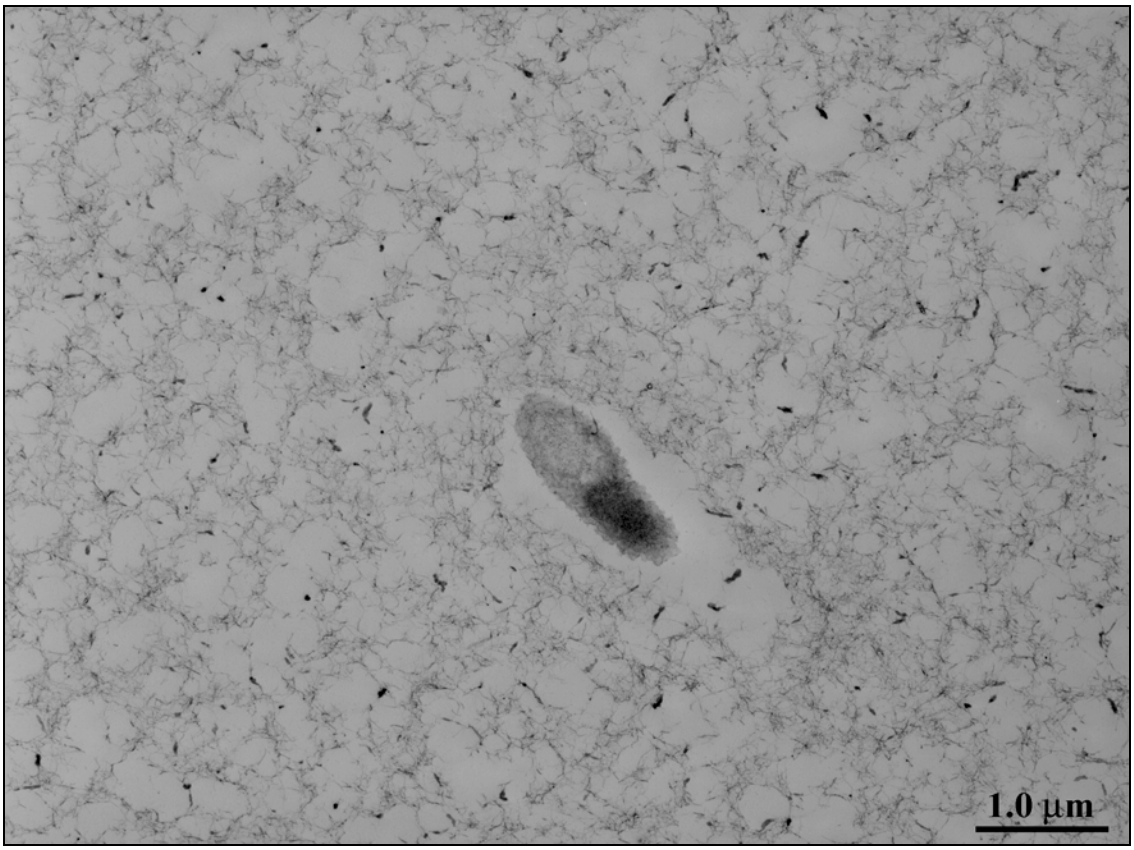

Figure 5.17 TEM micrograph of a 5RL cell in alginate bead (Trial 3).

The rest of the area of the image is the alginate gel.

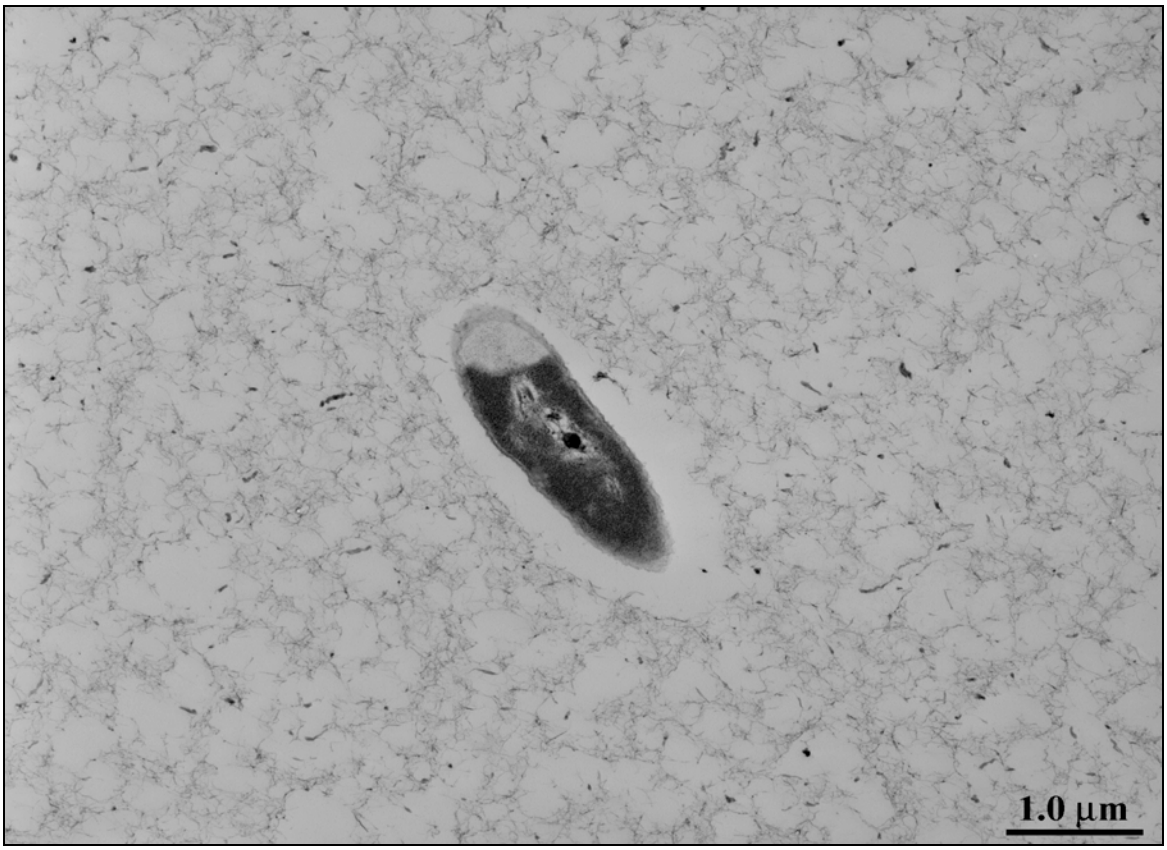

Figure 5.18 TEM micrograph of a 5RL cell in alginate bead (Trial 4).

The rest of the area of the image is the alginate gel.

DISCUSSION

A. Surface inoculation studies

The section of the thesis involved an extensive study on the adhesion pattern of *Pseudomonas fluorescens 5RL* to anionic polyelectrolyte and polyampholyte hydrogel samples with fixed charges varying from 0mM to 1540 mM. The bioreporters responded positively with an enhanced adhesion and registered higher counts of luminescence to hydrogel samples with higher fixed charges particularly in the case of anionic polyelectrolyte hydrogels. The adhesion study results indicate a significant pattern and a marked dependence on the fixed charge of the gel. The dependence on charge was prominent in the case of Neutral hydrogel with no net charge and in the case of Hydrogel with maximum charge. The results of the gel samples with intermediate charges recorded a lower bioluminescence counts than the samples with the maximum charge in most of the cases. The knowledge of hydrogel equilibrium swelling suggests that the gels with higher charge concentration tend to swell to a greater extent. The enhanced swelling could have resulted in the increased porosity and roughness of the gels surfaces. It is evident from several studies that the adhesion is particularly greater on rougher surfaces which have higher number of binding sites to promote adhesion and biofilm formation. The other supporting line of thought for the observed adhesion pattern is the effect of cations like Na^+, Ca^+ and Fe^+ that could have influenced the adhesion. However no conclusive evidence could be drawn regarding the role of cations in the adhesion process as these ions could not produce the same effect in a later experiment surface inoculation experiment with PEG DMAEM gels. The adhesion mechanism is found to be dependant on the species of bacteria, biomaterial surface characteristics and inherent charge content

of the surface to some extent. The effect of the nature of surface is found to be particularly dominating in this case.

B. DMEAM encapsulation

The cellular encapsulation in DMAEM was an attempt to achieve higher and longer response characteristics from the encapsulated cells, compared to the conventional sol-gel encapsulation technique. The polymerization of DMAEM was stable, quick, and could be conducted at room temperature in laboratory conditions. The technique however did not prove to be a viable option for cellular encapsulation, owing to the lack of any noticeable activity from the enmeshed cells. A series of control experiments were conducted to eliminate the possibility of any mass transport issue that was leading to the absence of any bioluminescence activity by the cells. The continued lack of response in the case of cells induced with salycylate prior to the encapsulation, confirmed the cytotoxic nature of the DMAEM polymerization process. Cellular encapsulation has been employed with success especially with different kind of gels, but the choice of the DMAEM hydrogels and the gelation mechanism was found to be inappropriate for *Pseudomonas fluorescens 5RL*. Thus it was concluded that the gelation process does not provide the bioreporter with the required chemical condition for the viability of the same and alternative methods were tried to encapsulate the bioreporters.

C. Alginate encapsulation

The failure of DMAEM as a viable encapsulation matrix is the motivation for bioreporter encapsulation experiments in alginate gels. The protocol for producing alginate

membranes or beads is specified in the earlier part of this chapter in the methods and materials section. The encapsulated cells survived the polymerization process and registered a higher and longer bioluminescent response compared to those from the surface inoculation experiments and far greater than those obtained from the DMAEM encapsulation. The bioluminescence response of the cells to the salycylate inducer could be considered as an indirect evidence of the number of viable or culturable cells. The long term response of the encapsulated cells was found to be significantly higher in comparison to the cells allowed to grown in a rich culture medium (solution). Also the Confocal micrograph of the live dead assay clearly shows a significantly larger proportion of green fluorescence spots, indicating a large number of viable cells inside the alginate matrix. Thus the bioluminescence test results and live dead assay micrographs exhibits considerable potential in the use of alginate gels for long term storage of cells without significant loss of functionality. The alginate beads also give an edge over other hydrogels in terms of the control of the number of cells. The accuracy with which the number of bacterial cells/colonies is employed in the biosensors is crucial and determines the sensitivity of the sensor. Thus alginate gels and beads in particular were found to be an excellent entrapment matrix for bioreporters for use in biosensors.

D. Confocal microscopy

The TEM images revealed good cell wall integrity in case of encapsulated bioreporters, but the evidence of the metabolic functions remained to be explained. The live dead assay is a simple, inexpensive methodology to confirm cell viability. The fluorescence images of the encapsulated cells captured using a Confocal microscope, illustrates a significant

number of green fluorescent spots corresponding to the viable cells. The images also showed a few red fluorescent spots corresponding to the dead cells. However the ratio of viable to dead cells was positively in favor of the viable cells.

E. Electron microscopy

The transmission electron micrograph shows the encapsulated bioreporter cells surrounded by the alginate gel matrix. All of the micrograph shows a clear image of the bioreporter without loss of integrity of cell wall. This clearly indicates that the alginate encapsulation has not resulted in any cell apoptosis in contrast to those in DMAEM hydrogels. The TEM samples were imaged at different spots to verify the consistency of the viability of the cells throughout the volume of the immobilized matrix. The dark black shade seen in some of the TEM sections is due to minor discrepancies during the fixation procedure.

CONCLUSION

The test results indicate that surface inoculation of anionic polyelectrolyte hydrogels and encapsulation within alginate gels are alternative cell immobilization techniques with potential. The surface inoculation results are encouraging and the degree of adhesion can be favorably controlled through the addition of the charged monomers. The cellular activity of the immobilized cells monitored through the bioluminescence response to sodium salycylate indicated no significant loss of functionality. The long term response of the encapsulated cells was also noticeably higher than those registered by bioreporter cells in solution, suggesting the success of the encapsulation process. The quick response

time of the encapsulated cells shows the absence of mass transport issues too. Moreover the bioreporter cells encapsulated in alginate gels provide an easy, efficient method of cellular encapsulation with higher and longer response characteristics presenting an edge over other hydrogels. The beads are easy to make with complete control over its size, shape and hardness. The beads can also be conveniently stored until 2 to 4 months. The control and measure of the number of bioreporter cells in the case of beads is higher. Thus two viable techniques for bioreporter immobilization namely the surface inoculation and cellular encapsulation were tried and tested with reasonable success for its application to a new class of sensors known as bioreporter biosensors. In addition the electron microscopy and Confocal microscopy studies positively reinforces the previous findings, that the alginate gel have tremendous potential in being used as a bioreporter immobilization matrices. Both the live dead assay images and TEM micrographs demonstrate a good environment for the encapsulated cells. No evidence accounting for significant loss in cell wall integrity of the encapsulated bioreporter cells was observed. Thus using simple microscopic techniques the viability of the cells within the alginate gel was established beyond reasonable qualms.

Chapter Six

CONCLUSION

SECTION CONCLUSIONS

A. Equilibrium swelling

The equilibrium swelling test results for polyelectrolyte hydrogels are in qualitative agreement with the continuum thermodynamic theory. The increase in the bath solution (NaCl) concentration causes exchange of hydrogen ions for sodium ions resulting in the rise of pH. This causes the dissociation of hydrogen ion and increase in the internal osmotic pressure. With further increasing salt concentration the poly-ion shielding and a reduction in the osmotic pressure differences between the hydrogel and surrounding bath causes a collapse transition. Thus the polyelectrolyte hydrogel collapses at high salt concentration and exhibit swelling behavior at low ionic strengths. At the intermediate bath ionic strengths, polyelectrolyte screening produces the de-swelling transition. The swelling analysis was conducted by increasing the salt concentration within the hydrogels, having a constant bath salt concentration. The equilibrium swelling response of HEMA-MAETAC and HEMA-DMAEM hydrogels to DI water and Phosphate Buffer Solution was recorded and found to be in agreement with the theoretical predictions. The graphs of the results indicate a gradual increase of the hydrogel diameter with increasing salt concentration.

B. Steady state diffusion potential

The results of the membrane potential measurements of the polyelectrolyte hydrogels were interesting. The final measured potential across the membrane represents the collective contributions from both the Diffusion and Donnan potential. There was a clear masking of the one of the potential for low charges and domination of the other potential for higher charges giving rise to the change in slope from negative to positive. In the case above the streaming potential was not considered, especially in the cases wherein inequalities in the pressure heads and osmotic pressure differences could be observed. The shift in the slope from negative to positive could also be attributed to streaming potentials.

C. Surface inoculation

The experimental results of the surface inoculation on hydrogel surfaces indicate that the cells preferentially adhere to hydrogels surfaces with a positive charge than those with a negative or no charge. The bioreporter cells formed a bacterial lawn and resisted a mild rinsing action. The bioluminescence response recorded from hydrogel samples with positive charges were higher and longer, suggesting that the gram negative bioreporter were loosely attached to the negatively charged hydrogels and were washed off with rinsing action.

D. Encapsulation

The encapsulation was attempted with two different kinds of hydrogel matrices. The polymerization conditions in DMAEM encapsulation proved to be unfavorable for the

survival of bacterial cells. The alginate encapsulation on the other hand was mild and suitable for the 5RL immobilization. The viability of the cells was tested by inducing the cells with sodium salycylate. The resulting bioluminescence indicated the viability of cells without loss of functionality. Also there was no significant difference between encapsulated cells and bacterial cells in solution. This indicates that the encapsulation has not reduced the response time and has not introduced any mass transfer issues either.

D. Microscopic analysis

The microscopic analysis using the confocal microscope and a transmission electron microscope reaffirms the viability of the bioreporter cells within the hydrogel matrices. Certain images even show the cell division, indicating a very cordial environment for bacterial growth. The cell division could have been at the moment of the encapsulation too. However the images of the stained encapsulated bioreporters proves beyond doubt the existence of all metabolic functions of the cells. Confocal images were obtained at different sections of the entire volume of the hydrogel matrix to ensure a complete uniform distribution of the bioreporter cells. The predominant number green colored stained cells clearly demonstrates the success of the alginate gel matrix as a effective immobilization membrane for the bioluminescent bioreporters.

THESIS CONCLUSION

The thesis project provided an opportunity to study the equilibrium swelling properties and steady state diffusion potential of polyelectrolyte hydrogels. The results developed greater insights into the response of the hydrogels in physiological conditions. The study of equilibrium swelling transitions and membrane potential measurements of hydrogel scaffolds proved to be a valuable tool in the choice of hydrogels for bioreporter immobilization. The test results of the equilibrium swelling phenomenon of the hydrogels led to surface inoculated negative bacterial cells could be immobilized on hydrogel surfaces with a net positive surface charge by forming bacterial lawn. Encapsulation of whole cells also proved useful in the immobilization process. The procedure was simple and inexpensive, which could keep the cells viable for a long time without any loss of metabolic functions. The encapsulation did not introduce any mass transfer issues and reduction in response time. Also the encapsulated cells could respond well higher to salycylate above the background and un-induced cells. The bioreporters could be enmeshed in hydrogels and stored at 4^0 c for a period of few months until they are needed for use. Thus the thesis gives a brief account of the properties of the polyelectrolyte hydrogels and discusses an important application in the field of whole cell immobilization for Bioreporter biosensors.

FUTURE WORK

One of the major issues in the gas phase testing and simulation protocols of hydrogel immobilized bioreporters are the "dry out" owing to evaporation of moisture. It would be beneficial to explore the possibility of using Polydimethylsiloxane (PDMS) based enclosures with fluid circulation to prevent desiccation issues during tests. PDMS is inexpensive, optically transparent and easy to fabricate. There is also a need to design elaborate test protocols involving harsher environments resembling real life conditions, to better test the response characteristics of bioreporter sensors. Finally the immobilization techniques could be extended to hold multiple strains of bacteria each designed to detect a particular analyte, to better tap the potential of such sensors.

Reference

1. Bolton EK, S. G., Nivens DE, Rochelle JM, Ripp S, Simpson ML (2002). "Integrated CMOS Photodetectors and Signal Processing for very Low-Level Chemical Sensing with the Bioluminescent Bioreporter Integrated Circuit." Sensors and Actuators **85**: 179-185.

2. Belkin, S. (2003). "Microbial Whole-Cell Sensing Systems of Environmental Pollutants." Current Opinion in Microbiology **6**: 206-212.

3. Bergstorm.E, G. D. M., Norton.I.T (1990). "Kinetics of ion binding and structural changes in alginates." Philips.G.O, Williams.P.A, Wedlock.D.J. (ed.). Gums and Stabilisers for the food industry.IRL press, Oxford.

4. Christenson. L, D. K., Lysaught.M (1993). "Biomedical Application of Immobilized Cells." In Goosen(ed.), Fundamentals of Animal Cell Encapsulation, CRC Press, Boca Raton, M.F.A.

5. Daunert S, B. G., Feliciano JS, Shetty RS, Strestha S, Smith-Spencer W (2000). "Genetically Engineered Whole-Cell Sensing Systems : Coupling Biological Recognition with Reporter Genes." Chemical Revolution **100**: 2705-2738.

6. David E. Nivens, T. E. M., Scott A. Moser, Stephanie J. Osbourn, Michael L. Simpson and Gary S. Sayler (2004). "Bioluminescent Bioreporter Integrated Circuits: Potentially Small, Rugged and Inexpensive Whole-Cell Biosensors for Remote Environmental Monitoring." Journal of Applied Microbiology **96**(1): 33-46.

7. Dictionary, O.-l. M. (1997-98). Academic Medical Publishing & CancerWEB.

8. E.A, M. (1991). "Molecular-Biology of Bacterial Bioluminescence." Microbiological Reviews **55**: 123-142.

9. EA, M. (1994). "Genetics of Bacterial Bioluminescence." Annual Review of Genetics **28**: 117-139.

10. Gary S. Sayler, S. R., David Nivens and Michael Simpson (2001). "Bioluminescent Bioreporter Integrated Circuits: Sensing Analytes and Organisms with Living Microorganisms." Journal of Environmental Biotechnology **1**(1): 33-39.

11. Grant.G.T, M. E. R., Rees.D.A., Smith.P.J.C, Thom.D (1973). "Biological Interactions Between Polysaccharides and Divalent Cations : the egg -box model." FEBS Letters **32**: 195-200.

12. Grasdalen.H, L. H., Smidsrod.O (1981). "^{13}C-NMR Studies of Monomeric Composition and Sequence in Alginate." Carbohydrates Res. **89**: 179-184.

13. Hang.A (1959). "Fractioning of Alginic Acid." Acta Chem.Scand. **13**(601-603).

14. Hansen LH, S. S. (2001). "The Use of Whole-Cell Biosensors to Detect and Quantify Compounds or Conditions Affecting Biological Systems." Microbiological Ecology **42**: 483-494.

15. Heitzer A, e. a. (1994). "Optical Biosensor for Environmental Online Monitoring of Napthalene and Salicylate Bioavailabilty with an Immobilized Bioluminscent Catabolic Reporter Bacterium." Applied and Environmental Microbiology **60**: 1487-1494.

16. Jen.A.C, W. M. C., Mikos.A.G (1995). "Review : Hydrogels for Cell Immobilization." Biotechnology Bioengineering **50**: 357-364.

17. Keane A, P. P., Ghoshal S, Lau PCK (2002). "Exposing Culprit Organic Pollutants : A review." Journal of Microbiological Methods **39**: 103-119.

18. King J.M.H, e. a. (1990). "Rapid, Sensitive Bioluminscent Reporter Technology for Napthalene Exposure and Biodegradation." Science **249**: 778-781.

19. Kohler S, B. S., Schmid RD (2000). "Reporter Gene Bioassays in Environmental Analysis." Fresenius Journal of Analytical Chemistry **366**: 769-779.

20. L. Flemming, D. (2004). Evaluating Bacterial Cell Immobilization Matrices for use in a Biosensor. Materials Science and Engineering. Blacksburg, Virginia Polytechnic Institute and State University**:** 76.

21. Leaveau JHJ, L. W. (2002). "Bioreporters in Microbial Ecology." Current Opinion in Microbiology **5**: 259-265.

22. Meighen (1991). "Molecular-Biology of Bacterial Bioluminescence." Microbiological Reveiws **55**(1): 123-142.

23. Meighen EA, D. P. (1993). "Physiological, Biochemial and Genetic-Control of Bacterial Bioluminescence." Adances in Microbial Physiology **34**: 1-67.

24. Michael L. Simpson, G. S. S., Bruce M. Applegate, Steven Ripp, David E. Nivens, Michael J. Paulus and Gerald E. Jellison, Jr (1998). "Bioluminescent-Bioreporter Integrated Circuits for Novel Whole-Cell Biosensors." TIBTECH **16**: 332-338.

25. Mitchell, E. F. (2004). Sol-gel Encapsulation of a Bioluminescent Bioreporter. Center for Environmental Biotechnology. Knoxville, University of Tennessee**:** 110.

26. Nigam S.C, T., Sakoda A, Wang H.Y (1988). "Techniques for Preparing Hydrogel Membrane Capsules." Biotechnology Techniques **2**(4): 271-276.

27. Rakesh K.Gupta, S. S., Patterson, Steven Ripp, Michael L.Simpson, Gary Sayler (2003). "Expression of the Photorhabdus Luminescens Lux Genes (luxA, B, C, D, and E) in *Saccharomyces cerevisiae*." FEMS Yeast Research **4**: 305-313.

28. S.S, P. (2003). Optimization of Bacterial Luciferase for Expression in Mammalian Cells. Department of Microbiology. Knoxville, University of Tennessee**:** 219.

29. SF, D. S. (2001). "Microbial Biosensors." Biosensor and Bioelectronics **16**: 337-353.

30. Skjak-Braek.G, G. H., Smidsrod.O (1989). "Inhomogenous Polysaccharide Ionic Gels." Carbohydrate Polymers **10**: 31-54.

31. Alvarez-Lorenzo C, K. T., Kimani Stancil, Alexander YU. Grosberg and Toyoichi Tanaka. (2001). "Simulataneous Multiple Point Adsorption of Aluminium ions and Charged Molecules in a Polyampholyte Thermosensitive Gel: Controlling Frustrations in a Heteropolymer Gel." Langmuir **17**(12): 3616-3622.

32. Kantor Y, K. M. (1995). "Instabilities of Charged Polyampholytes." Physical Review E **51**(2): 1299-1312.

33. Wittmer J, J. A., Joanny JF (1993). "Random and Alternating Polyampholytes." Europhysics Letters **24**(4): 263-268.

34. Anthony E English, T. T., Elazer R Edelman (1998). "Polyampholytic Hydrogel Swelling Transitions: Limitations of the Debye-Hucker Law." Macromolecules **31**.

35. Anthony E. English, E. R. E., Toyoichi Tanaka (2000). "Polymer Hydrogel Phase Transitions." Macromolecules.

36. Osada.Y (1987). "Conversion of Chemical into Mechanical Energy by Synthetic-Polymers (Chemomechanical systems)." Advances in Polymer Science **82**: 1-46.

37. Katchalsky.A, L. S., and Eisenberg.H (1951). "Polymer Sciences." .

38. P. Flory (1953). Principles of Polymer Chemistry, Cornell University Press,

Ithaca. **Chapter XIII**.

39. I. Michaeli, A. K. a. (1955). Journal of Polymer Sciences **9**(69).

40. J. Joanny, J. B. a. (1996).Advances in Chemical Physics. New York, Wiley**:** p 1.

41. Oosawa.F (1971). Polyelectrolytes, Dekker, New York.

42. R. Skouri, F. S., J.P. Munchan and S.J.Candau (1995). Macromolecules **28**: 197.

43. A. Moussaid, F. S., J.P. Munch and S.J. Candau (1993). Journal of Physics II **3**: 573.

44. I.A. Nyrkova, A. R. K. a. M. D. (1994). Macromolecules **27**: 4220.

45. K.A. Khachaturian, A. R. K. a. (1982). Polymer **23**: 1743.

46. A. Szymczyk P.F, J. C. R., J. Pagetti (1998). "Characterization of Surface Properties of Ceramic Membranes by Streaming and Membrane Potentials." Journal of Membrane Science **146**: 277-284.

47. Livage J, R. C., DaCosta J.M, Desportes I & Quinson J.F (1996). "Immunoassays in Sol-Gel Matrices." Journal of Sol-Gel Science and Technology **7**: 45-51.

48. Wright J.D, S. N. A. (2001). Sol-Gel Mateials: Chemistry and Applications. London, Taylor & Francis Inc.

49. Premkumar J.R, R. R., Belkin S & Lev.O (2002). "Sol-Gel Luminescence Biosensors: Encapsulation of Recombinant E.Coli Reporters in Thick Silicate Films." Analytica Chimica Acta. **462**: 11-23.

50. Premkumar J.R, L. O., Rosen R, Belkin S. (2001). "Encapsulation of Luminous Recombinant E.Coli in Sol-Gel Silicate Films." Adavanced Materials **12**: 1773-1775.

51. J.R, P. (2002). "Fluorescent Bacteria Encapsulated in Sol-Gel Derived Silicate Films." Chemistry of Materials. **14**: 2676-2686.

52. Inama L, D. S., Carturan.G & Cavazza.A. (1993). "Entrapment of Viable Microorganisms by Sio2 Sol-Gel Layers on Glass Surfaces - Trapping, Catalytic Performance and Immobilization Durability of *Saccharomyces cerevisiae*." Journal of Biotechnology **30**: 197-210.

53. J.M.H. King, P. M. D., B. Applegate, R. Burlage, J. Sanseverino, P. Dunbar, F. Larimer, G.S. Sayler "Rapid, Sensitive Bioluminescent Reporter Technology for

Napthalene Exposure and Biodegradation." Science **249**: 778-780.

54. S. Ripp, K. A. D., T. McKnight, L.H. Levine, J.L. Garland,M.L. Simpson, G.S. Sayler (2003). "Bioluminescent Bioreporter Integrated-Circuit Sensing of Microbial Volatile Organic Compunds." Journal of Industrial Microbiology Biotechnology **30**(30): 636-642.

55. Gary S.Sayler, S. R., David Nivens and Michael Simpson (2001). "Bioluminescent Bioreporter Integrated Circuits: Sensing Analytes and Organisms with Living Microorganisms." Journal of Environmental Biotechnology **1**(1): 33-39.

56. David E. Nivens, T. E. M., Scott A. Moser, Stephanie J. Osbourn, Michael L.Simpson and Gary S.Sayler "Bioluminescent Bioreporter Integrated Circuits: Potentially Small, Rugged and Inexpensive Whole-Cell Biosensors for Remote Environmental Monitoring." Journal of Applied Microbiology.

57. Eric K. Bolton, G. S. S., David E. Nivens, James M. Rochelle, Steven Ripp, Michael L. Simpson (2002). "Integrated CMOS Photodetectors and Signal Processing for very Low Level Chemical Sensing with the Bioluminescent Bioreporter Integrated Circuit." Sensors and Actuators B **85**: 179-185.

58. Rakesh k. Gupta, S. S. P., Steven Ripp, Michael L. Simpson, Gary S. Sayler (2003). "Expression of the Photorhabdus Luminescens Lux Genes (luxA, B, C, D and E) in *Saccharomyces cerevisiae*." FEMS Yeast Research **4**: 305-313.

59. Michael L. Simpson, G. S. S., Bruce M. Applegate, Steven Ripp, David E. Nivens, Michael J. Paulus and Gerald E. Jellison, Jr (1998). "Bioluminescent-Bioreporter Integrated Circuits for Novel Whole-Cell Biosensors." TIBTECH 16: 332-338.

60. Nadine Nassif, C. R., Thibaud Coradin, Marie-Noelle Rager, Odie M.M.Bouvet and Jacques Livage (2003). "A Sol-Gel Matrix to Preserve the Viability of Encapsulated Bacteria." Journal of Materials chemistry 13: 203-208.

61. K. Sharma, P. (2001). "Surface Studies Relevant to Microbial Adhesion and Bioflotation of Sulphide Minerals."

62. P.K. Sharma, A. D., K. Hanumantha Rao, K.A. Natarajan, K.S.E. Forssberg (2001). "Surface Characterization of Thiobacillus Ferrooxidans Cells Grown under Different Conditions." International Journal of Mineral processing September, 2001.

63. P.K. Sharma, K. H. R. (2001). "Surface Characterization of Bacterial Cells Relevant to Mineral Industry." International Journal of Mineral processing.

64. P.K. Sharma, K. H. R., K.S.E. Forssberg, K.A. Natarajan (2000). "Surface Chemical Characterisation of *Paenibacillus polymyxa* before and after Adaptation to Sulphide Minerals." International Journal of Mineral processing **62**.

65. AJ, B. (2003). "Biosensors for Environmental Pollutants and Food Contaminants." Analytical and Bioanalytical CHemistry **377**: 434-445.

66. S, B. (2003). "Microbial Whole-Cell Sensing Systems of Environment." Current Opinion in Microbiology **6**: 206-212.

67. Bott C.B, L. N. G. (2001). "The Immunochemical Detection of Stress Proteins in Activated Sludge Exposed to Toxic Chemicals." Water Research **35**: 91-100.

68. Bousse.L (1996). "Whole Cell Biosensors." Sensors and Actuators B: Chemical **34**: 270-275.

69. Chee G.J, N. Y., Ikebukuro.K, Karube.I (2000). "Optical Fiber Biosensor for the Determination of Low Biochemical Oxygen Demand." Biosensors and Bioelectronics **15**: 371.

70. Collings A.F., C. F. (1997). "Biosensors : Recent Advances." Reports on Progress in Physics **60**: 1397-1445.

71. Coradin T., N. N., Livage J (2003). "Silica-Alginate Composites for Microencapsulation." Applied Microbiology and Biotechnology **61**: 429-434.

72. Dennison M.J., T. A. P. F. (1995). "Biosensors for Environmental Monitoring." Biotechnology Advances 13: 1-12.

73. S.F., D. S. (2001). "Microbial Biosensors." Biosensors and Bioelectronics 16: 337-353.

74. Gehrke .S.H, C. E. L. (1989). "Mass Transfer in pH-sensitive Hydrogels." Chemical Engineering Science 44: 559.

75. (Heo.J, Thomas .K.J, Seong G.H). "2003." A Microfluidic Bioreactor Based on Hydrogel Entrapped *E.Coli*: Cell Viability, Lysis, and Intracellular Enzyme Reactions. Analytical Chemistry(75).

76. Horsburg A.M, M. D. P., Turner N.L, Henkler R, Stachan N, G. Lover L.A, Paton G.I, Killham K (2002). "On-Line Microbial Biosensing and Fingerprinting of Water Pollutants." Biosensors and Bioelectronics 17: 495-501.

77. Ivaska A, V. M., Kahrua A (2002). "Construction and use of Specific

Luminescent Recombinant Bacterial Sensors for the Assessment of Bioavailable Fraction of Cadmium, Zinc, Mercury and Chromium in the Soil." Soil Biology and Biochemistry **34**: 1439-1447.

78. Koh W.G, R. A., Pishko M.V (2002). "Poly(ethylene glycol) Hydrogel Microstructures Encapsulating Living Cells." Langmuir **18**: 195-201.

79. Kuncova G, T. J., Vrchotova N, Podrasky O (2002). "The Influence of Immobilization of *Pseudomonas*sp.2 on optical Detection of Polychlorinated biphenyls." Materials Science and Engineering C **21**: 195-201.

Appendix

Table 1.1 Biosensors used for detecting common pollutants

Analyte	Environment	Biological Agent	Transducer	Reference
pesticides and estrone	river water	antibodies	optical	Rodriguez-Mozaz *et al.,* (2004), Mallat *et al.,(*2001), Mallat *et al.,* (1999)
phenols	wastewater	enzymes	electrochemical	Nistor *et al.,* (2002)
linear alkyl benzene sulphonate (LAS)	river water	bacteria	electrochemical	Nomura *et al.,* (1998)
toxicity	wastewater	bacteria	electrochemical	Farre *et al.,* (2001), Philp *et al.,* (2003)
alkanes	groundwater	bacteria	optical	Sticher *et al.,* (1997)
estrogens and xenoestrogens	lake water and wastewater	estrogen receptor (EC)	optical	Seifert *et al.,* (1999)
biological oxygen demand (BOD)	river water	bacteria	optical	Chee *et al.,* (2000)
zinc dichromate chromate	soil	bacteria	optical	Ivaska *et al.,* (2002)
mercury and arsenite	soil	bacteria	optical	Petanen and Romantschuk (2002)

Table 1.2 Merits and demerits of the different reporter systems

Reporter Systems	Merits	Demerits
Chloramphenicol acetyltransferase(CAT)	No Endogenous activity Automated detection with ELISA's	Requires addition of substrate, separation of product from substrate and often uses radioisotopes.
B-galactosidase (β-gal)	Simple assays (colrimetric and chemiluminescent) Applicable in anaerobic environments	Requires addition of substrate Endogenous activity
Firefly Luciferase (LUC)	Sensitive, No endogenous activity in mammalian cells	Requires addition of substrate (luciferin), O_2, and ATP
Bacterial Luciferase (lux)	Sensitive, No endogenous activity in mammalian cells. Does not require addition of substrate	Requires O_2, Heat labile above 45 ^{o} C
Aqueorin	Sensitive,No endogenous activity in mammalian cells.	Requires the addition of substrate and Ca^{++}
Green Fluorescent Protein (gfp)	Autofluorescent, Mutants available with different colors, Stable at biological pH	Requires exogenous excitation, Moderate sensitivity, Long induction period, Background fluorescence may interfere.
Uroporphyrinogen III Methyltransferase (UMT)	Auto fluorescent, may have a better noise to signal ration than gfp	Endogenous Activity

Table 2.1 250 ml 1.54M HEMA stock solution

CHEMICAL	MASS OF VOLUME
HEMA	49.45 mL
EG	100 mL
EGDMA	971 uL
APS	2.5 mL (4 wt%)
Water	Fill to 250mL

Table 2.2 50 ml 1.54 M DMAEM stock solution

CHEMICAL	MASS OF VOLUME
DMAEM	13.14 ml
EG	20ml
EGDMA	194 uL
Water	16.65 ml

Table 2.3 250 ml 1.54M MEATAC stock solution

CHEMICAL	MASS OF VOLUME
MAETAC	20.77 ml
EG	20 ml
EGDMA	194 uL
APS	500 uL (4 wt%)
Water	8.5 ml

Table 2.4 Concentration of charged monomer in HEMA membrane samples

Membrane samples	Charged monomer concentration (ml)	HEMA (ml)	Net charge (ml)
0	0.000	10.000	0
1	0.010	9.990	1.54
2	0.032	9.968	4.87
3	0.100	9.900	15.4
4	0.316	9.684	48.7
5	1.000	9.000	154
6	3.162	6.838	487
7	10.000	0.000	1540

Table 2.5 DMAEM hydrogels preparation

Chemical	Volume
DMAEM	3.4 ml
Ethylene Glycol (Solvent)	4.0 ml
EGDMA (Cross linker)	40 uL
Water / Bacterial Cell solution	2.5 ml

Table 3.1 Equilibrium swelling of HEMA-

DMAEM hydrogels in DI water, NaCl, PBS, measured in pixels.

Sample	Charge (mM)	DI water	154mM NaCl	1X PBS	DI water	DI water
1	1.54	122	119	120	121	121
2	4.87	124	121	121	122	121
3	8.66	130	128	128	129	129
4	15.4	121	119	119	121	121
5	27.39	124	122	122	124	123
6	48.7	124	122	122	124	123
7	86.6	124	123	124	125	123
8	154	124	123	130	130	123
9	273	127	125	139	136	125
10	487	125	126	185	191	151
11	866	130	134	195	208	134
12	1540	150	169	242	318	179

Table 3.2 Equilibrium swelling of HEMA-DMAEM hydrogels in DI water, NaCl, and PBS expressed as D/D0 (ratio)

Sample	Charge (mM)	Feb 8/04 DI water	Feb 10/04 154mM NaCl	Feb12/04 1X PBS	Feb 14/04 DI water	Feb 23/04 DI water
1	1.54	0.7439	0.7256	0.7317	0.7378	0.7378
2	4.87	0.7561	0.7378	0.7378	0.7439	0.7378
3	8.66	0.7927	0.7805	0.7805	0.7866	0.7866
4	15.4	0.7378	0.7256	0.7256	0.7378	0.7378
5	27.39	0.7561	0.7439	0.7439	0.7561	0.7500
6	48.7	0.7561	0.7439	0.7439	0.7561	0.7500
7	86.6	0.7561	0.7500	0.7561	0.7622	0.7500
8	154	0.7561	0.7500	0.7927	0.7927	0.7500
9	273	0.7744	0.7622	0.8476	0.8293	0.7622
10	487	0.7622	0.7683	1.1280	1.1646	0.9207
11	866	0.7927	0.8171	1.1890	1.2683	0.8171
12	1540	0.9146	1.0305	1.4756	1.9390	1.0915

Table 3.3 Equilibrium swelling of HEMA- MAETAC hydrogels in DI water, NaCl, and PBS expressed as D/D_0 (ratio)

Sample	Charge (mM)	Feb 9/04 DI water	Feb 10/04 154mM NaCl	Feb12/04 1X PBS	Feb 23/04 DI water
0	0	123	120	123	123
1	1.54	122	120	119	122
2	2.73	127	124	124	127
3	4.87	124	121	121	124
4	8.66	134	124	124	128
5	15.4	135	122	121	133
6	27.39	173	125	125	196
7	48.7	230	130	129	249
8	86.6	300	155	153	307
9	154	364	185	182	380
10	273	424	226	221	426
11	487	445	286	283	439
12	866	451	304	301	458
13	1540	682	383	383	696

Table 3.4 Equilibrium swelling of HEMA-MAETAC hydrogels in DI water, NaCl, and PBS expressed as D/D_0 (ratio).

Sample	Charge (mM)	Feb 9/04 DI water	Feb 10/04 154mM NaCl	Feb12/04 1X PBS	Feb 23/04 DI water
0	0	0.75	0.731707317	0.731707317	0.75
1	1.54	0.743902439	0.731707317	0.725609756	0.743902439
2	2.73	0.774390244	0.756097561	0.756097561	0.774390244
3	4.87	0.756097561	0.737804878	0.737804878	0.756097561
4	8.66	0.817073171	0.756097561	0.756097561	0.780487805
5	15.4	0.823170732	0.743902439	0.737804878	0.81097561
6	27.39	1.054878049	0.762195122	0.762195122	1.195121951
7	48.7	1.402439024	0.792682927	0.786585366	1.518292683
8	86.6	1.829268293	0.945121951	0.932926829	1.87195122
9	154	2.219512195	1.12804878	1.109756098	2.317073171
10	273	2.585365854	1.37804878	1.347560976	2.597560976
11	487	2.713414634	1.743902439	1.725609756	2.676829268
12	866	2.75	1.853658537	1.835365854	2.792682927
13	1540	4.158536585	2.335365854	2.335365854	4.243902439

Table 3.5: Bioluminescence measurement data for artificially induced bioreporters inoculated on the surface of negatively charged hydrogels. The hydrogels were rinsed before the bioluminescence measurement

Time	0R	1R	2R	3R	4R	5R	6R	7R
0.0	39114.80	249829.35	63648.25	50234.40	359634.15	27388.85	74511.15	11890.85
0.5	42325.30	251185.90	73095.45	64118.20	429889.30	31857.80	105892.25	15755.95
1.0	101360.90	379170.95	151572.15	137916.15	768827.55	55773.45	180411.25	24440.10
1.5	173856.80	680692.80	257331.80	244280.40	1006161.7	105351.30	261082.75	44218.55
2.0	248727.30	980918.65	350557.10	325802.65	1086848.0	167250.70	364431.60	72503.40
2.5	348456.15	1116939.6	449888.10	383747.10	1139444.3	243768.25	558578.95	110428.55
3.0	379768.30	1147665.9	534534.85	440272.05	1151803.6	344769.40	813465.90	151667.30
3.5	391266.50	1136938.8	551580.15	468978.85	1147500.4	437742.60	1011784.2	205932.95
4.0	381335.05	1150203.8	558071.70	456713.40	1137495.1	522296.40	1113716.8	260316.95
4.5	362911.45	1147769.9	529324.85	447470.80	1140031.1	560120.50	1159946.4	310883.65
5.0	347388.90	1140489.3	499723.85	429902.45	1144340.7	611250.85	1156514.9	363298.75
5.5	312550.95	1101483.1	464325.75	411847.20	1134757.8	660022.80	1146585.9	409121.40

Table 3.5 continued

Time	0R	1R	2R	3R	4R	5R	6R	7R
6.0	274605.25	1068324.3	452194.80	389143.60	1131985.2	669323.95	1128249.4	434148.55
6.5	247338.40	982693.90	408824.50	368788.20	1116182.9	666918.60	1134920.1	462320.15
7.0	198434.00	809121.80	375836.40	349473.20	1109012.5	645376.00	1119517.6	480900.50
7.5	198434.00	809121.80	375836.40	349473.20	1109012.5	645376.00	1119517.6	480900.50
8.0	3670.45	102965.25	236376.25	241627.45	1003309.4	586226.15	1128962.0	492538.95
8.5	426.20	9574.10	161971.60	183060.15	905007.80	570280.10	1140796.2	491532.70
9.0	152.30	2442.45	132067.85	156715.15	752551.50	555883.15	1149877.3	471997.70
9.5	87.15	1278.70	88744.10	139256.90	540541.55	522957.30	1136303.6	459483.85
10.0	97.40	651.20	12525.75	117676.90	258636.10	467393.90	1142119.0	449534.65
10.5	81.55	231.15	1635.30	85268.05	76915.05	420080.80	1147994.5	426589.45
11.0	70.70	205.00	1076.75	39252.10	13844.55	371331.65	1135596.2	417676.65
11.5	91.20	190.65	384.95	5979.40	4583.10	334386.00	1111020.0	404310.35
12.0	73.30	164.40	128.10	1439.00	1172.70	295817.10	1072630.5	406611.60
12.5	73.80	163.45	116.75	1226.95	661.55	269899.20	1016942.7	382278.20

Table 3.5 continued

Time	0R	1R	2R	3R	4R	5R	6R	7R
13.0	68.70	169.10	97.80	249.40	491.30	245894.05	942509.20	368265.40
13.5	70.75	147.55	89.65	147.20	413.60	225573.65	888381.90	348215.40
14.0	75.85	175.75	95.25	133.90	397.55	212252.70	810250.20	320116.05
14.5	83.05	173.70	76.80	102.55	423.25	193595.45	748633.50	300787.40
15.0	78.40	186.55	89.60	108.70	429.10	170102.60	677723.80	278433.65
15.5	79.50	206.50	104.45	107.15	429.40	72849.70	618535.95	260298.45
16.0	70.75	183.95	90.15	121.00	438.10	15820.35	563905.25	243381.65
16.5	72.25	148.05	102.90	124.60	456.50	7316.85	508192.20	232524.65
17.0	80.50	130.10	94.25	116.40	450.75	3719.35	440985.05	221308.15
17.5	72.80	118.85	97.85	135.85	459.70	1838.00	293471.50	199145.95
18.0	74.35	113.20	80.90	113.30	491.90	904.55	222494.80	187933.15
18.5	82.50	106.55	88.60	125.10	455.55	524.45	189628.05	122927.45
19.0	77.95	123.95	103.45	113.85	492.45	462.80	105517.30	103993.90
19.5	92.80	103.95	100.40	114.85	484.90	497.25	50767.90	83758.40

Table 3.5 continued

Time	0R	1R	2R	3R	4R	5R	6R	7R
20.0	69.75	111.15	91.15	118.40	512.00	523.20	36176.30	72004.00
20.5	83.60	101.90	103.95	134.90	464.25	526.95	39013.20	54626.20
21.0	69.20	103.95	92.20	126.10	466.90	506.15	42819.40	35116.30
21.5	76.90	107.55	94.25	127.70	498.10	488.35	24811.15	23390.45
22.0	83.55	88.60	81.45	128.70	488.95	482.55	19415.75	19458.45
22.5	61.00	110.15	82.95	144.15	498.70	474.20	4821.50	16188.00
23.0	73.80	103.45	79.35	111.25	502.75	466.15	2483.55	13425.95
23.5	70.75	90.15	83.50	116.40	530.55	456.25	2529.95	12062.10
24.0	71.75	111.65	80.40	121.55	550.05	445.00	3098.35	11166.15

Table 3.6 Bioluminescence measurement data for artificially induced bioreporters inoculated on the surface of negatively charged hydrogels. The hydrogels were not rinsed before the bioluminescence measurement

Time	0u	1u	2u	3u	4u	5u	6u	7u
0.0	25088.95	44201.40	53533.15	9983.30	34283.15	5831.10	9399.20	3638.40
0.5	68235.15	93875.95	128413.70	34054.40	112495.20	28925.30	54864.45	21240.80
1.0	151083.95	169649.55	214307.15	105379.75	198393.60	70602.95	137306.10	65980.55
1.5	252280.90	311492.70	326556.70	195392.80	374270.05	158878.85	263463.05	143946.85
2.0	342163.30	466504.25	418937.65	291615.30	562473.10	247253.90	467045.45	244616.35
2.5	380837.30	551441.70	474790.25	379638.40	689494.95	351835.50	585992.80	336551.80
3.0	394562.75	609838.85	515630.75	426472.95	790690.30	473531.40	640061.30	417380.10
3.5	402924.35	661030.20	552554.40	430946.70	892860.45	563965.00	688303.45	476989.90
4.0	403257.75	684054.85	562712.35	430021.10	984001.00	626133.95	718533.50	515953.55
4.5	404055.35	713312.80	558839.90	428317.40	1066634.2	652263.55	796422.95	549240.25
5.0	354437.05	726183.45	536452.45	416739.05	1120399.8	672468.55	910108.15	570224.80
5.5	303904.65	730936.40	516940.85	415076.00	1131715.9	677928.90	1060039.6	582168.10

Table 3.6 continued

Time	0u	1u	2u	3u	4u	5u	6u	7u
6.0	240275.65	740520.60	499769.35	409965.40	1144689.5	661670.20	1117956.5	574556.05
6.5	85809.85	611983.25	455420.70	386612.35	1136401.6	658550.25	1144433.2	536823.75
7.0	7397.45	278501.10	353185.85	353268.00	1135466.3	649932.60	1144720.7	498352.10
7.5	7397.45	278501.10	353185.85	353268.00	1135466.3	649932.60	1144720.7	498352.10
8.0	557.40	216210.65	334483.00	175224.15	1057195.2	626059.70	1121221.0	458848.25
8.5	314.00	219129.60	318219.60	114260.65	952078.85	598058.45	1099392.6	431965.90
9.0	219.95	220632.85	309296.75	6631.70	666023.90	563537.05	1092703.7	410101.60
9.5	139.45	219764.30	289803.30	1426.55	582044.70	519772.20	1082530.4	393985.80
10.0	131.20	223470.05	256011.75	898.00	576859.00	469560.65	1073439.3	379375.30
10.5	121.95	220371.10	215900.20	751.85	582554.20	430914.65	1063314.1	356610.45
11.0	128.70	220539.30	179537.15	987.75	547860.75	384867.65	1026986.5	344693.55
11.5	130.20	229618.50	149550.20	1070.25	252014.40	336344.85	1016935.2	320862.00
12.0	135.80	222760.15	124431.10	236.15	62652.70	225021.10	983663.15	290822.60
12.5	125.60	108749.90	94447.65	137.40	17009.05	178072.30	935902.25	258575.10

Table 3.6 continued

Time	0u	1u	2u	3u	4u	5u	6u	7u
13.0	99.50	29600.45	41608.15	135.95	8155.95	136751.10	888961.85	236606.65
13.5	103.05	10110.20	14113.70	125.10	7198.05	53697.30	769448.45	217429.45
14.0	117.90	3923.85	7544.50	108.20	4929.70	23921.05	683713.70	188695.60
14.5	107.65	1862.85	3677.00	110.75	2743.75	19542.50	658234.10	167802.95
15.0	107.65	1292.40	1808.55	104.60	1854.80	30634.50	660956.30	144828.20
15.5	116.40	924.05	1346.30	115.40	1355.00	17712.70	635559.70	122125.90
16.0	107.65	675.75	674.20	124.10	1072.70	2587.00	571321.45	107405.45
16.5	124.60	535.80	419.50	128.20	987.45	1439.95	504908.00	99451.20
17.0	93.80	471.40	373.10	122.55	1009.65	912.65	446637.35	93710.20
17.5	97.95	492.45	374.15	111.80	935.05	863.05	388894.95	74871.35
18.0	101.55	458.35	324.30	108.15	1008.70	945.90	338740.20	39366.60
18.5	111.25	431.70	320.10	114.90	1121.25	971.90	302571.55	15922.75
19.0	104.60	421.40	284.20	110.75	1428.55	954.30	270408.35	9142.95
19.5	105.60	377.75	301.60	101.55	1718.90	939.10	240507.90	7238.20

Table 3.6 continued

Time	0u	1u	2u	3u	4u	5u	6u	7u
20.0	111.80	369.95	276.50	119.45	1959.15	876.90	223001.50	6391.65
20.5	115.85	308.65	307.70	114.85	2317.35	834.85	218803.50	5667.70
21.0	101.55	286.10	342.05	122.55	2766.05	792.25	216925.85	3118.55
21.5	95.90	267.55	420.15	118.45	3213.55	695.45	213853.35	2645.65
22.0	96.40	222.00	453.40	124.10	4035.60	597.80	213530.20	2677.20
22.5	103.10	217.90	469.85	124.60	4544.45	505.55	209389.80	2635.10
23.0	114.85	211.25	472.55	122.05	4385.30	463.05	199518.80	2942.95
23.5	100.50	186.55	323.05	126.15	4912.40	454.70	176343.30	3399.10
24.0	104.05	211.70	317.05	130.20	4831.60	379.15	144722.60	3454.15

Table 3.7 Bioluminescence measurement data for artificially induced bioreporters inoculated on the surface of polyampholyte hydrogels. The hydrogels were not rinsed before the bioluminescence measurement

Time	0	1	2	3	4	5
0.0	0.0	0.0	0.0	0.0	0.0	0.0
0.5	0.0	0.0	0.0	0.0	0.0	0.0
1.0	0.0	0.0	0.0	0.0	0.0	0.0
1.5	252.75	5863.65	1464.85	2750.90	1039.50	366.50
2.0	376.70	7191.75	1764.65	3266.20	1206.90	542.75
2.5	678.05	10163.65	3291.40	7037.25	1645.95	1026.30
3.0	1350.95	16067.20	7078.75	19295.15	2450.40	2192.05
3.5	2175.55	25157.45	14764.45	44614.95	4024.30	4283.10
4.0	3142.60	39786.45	27547.70	70350.55	7390.80	7740.65
4.5	4680.90	67485.55	47205.95	88461.75	12495.15	13086.35
5.0	7157.75	88662.90	75866.10	105345.10	18027.85	21714.25
5.5	11229.70	116692.20	111423.90	128972.00	21692.40	35444.00
6.0	15951.60	132635.00	135081.35	166381.90	24510.70	56389.65

Table 3.7 continued

Time	0	1	2	3	4	5
6.5	22054.95	142368.50	162040.30	194528.75	29492.90	86026.65
7.0	25865.25	151607.25	187706.80	209425.55	31085.40	113076.95
7.5	35453.65	166409.45	206010.50	211400.25	30798.35	132437.10
8.0	44543.55	186749.40	203834.65	222440.10	29048.10	147585.45
8.5	49230.20	210725.65	203853.15	227157.60	27680.40	170564.80
9.0	52767.70	219846.35	202582.90	220815.30	26570.50	202795.60
9.5	55055.20	232410.55	199871.80	211231.75	25532.35	219293.15
10.0	54977.20	248361.10	196458.90	199280.80	24282.45	216235.20
10.5	51840.00	259908.40	181558.00	189770.90	22587.75	204490.30
11.0	47643.75	262924.55	171345.85	179468.25	20458.75	192507.60
11.5	43204.05	245538.10	156634.55	169973.30	17711.65	183565.70
12.0	38586.50	163349.75	146576.05	160994.75	14883.55	178450.10
12.5	34109.05	158718.15	129808.10	154804.45	11880.00	171365.50
13.0	30815.75	151693.65	114738.90	140488.15	9589.95	163123.90

Table 3.7 continued

Time	0	1	2	3	4	5
13.5	28443.35	141205.55	36194.10	124991.80	6862.50	152404.50
14.0	20825.20	134621.30	11950.15	108872.95	3699.90	146274.45
14.5	12485.25	127454.15	4028.40	91938.15	1028.45	135231.85
15.0	11447.05	121032.90	2137.00	75041.60	135.30	124319.45
15.5	10795.10	120383.35	450.30	41221.20	80.90	115465.65
16.0	8112.25	116894.25	251.10	6995.55	86.55	105963.80
16.5	5773.50	102990.05	229.60	647.30	64.55	93718.95
17.0	4178.85	6730.10	193.70	240.45	80.40	75243.90
17.5	1933.45	1521.60	163.45	196.30	68.15	42219.00
18.0	637.60	401.90	130.10	208.10	67.60	4596.20
18.5	412.00	213.15	81.45	226.10	69.60	563.95
19.0	315.45	181.90	77.30	247.70	66.10	295.40
19.5	227.10	159.35	60.45	247.65	68.10	288.70

Table 3.7 continued

Time	0	1	2	3	4	5
20.0	174.20	190.15	69.70	181.95	67.60	292.35
20.5	135.25	212.70	74.75	134.75	66.60	320.10
21.0	122.95	210.20	73.20	96.80	81.40	307.75
21.5	116.80	210.70	66.10	82.45	81.40	230.20
22.0	108.60	157.85	87.10	69.65	78.35	152.65
22.5	96.80	123.00	71.15	88.10	69.65	105.00
23.0	111.15	77.85	93.20	70.65	68.65	86.10
23.5	95.25	85.05	73.20	73.25	75.80	80.45
24.0	86.55	84.55	78.85	82.45	72.20	75.30

Table 3.8 Bioluminescence measurement data for artificially induced bioreporters inoculated on the surface of PEG-DMAEM hydrogels. The hydrogels were not rinsed before the bioluminescence measurement

Time	Sample#1	Sample #2	Sample #3	Sample #4	Sample #5	Sample #6	Sample #7
0	1819.5	8139.4	1462.4	1774.1	355.8	907.7	15058
0.5	2461.2	10568.5	1999.3	2305.8	857.4	4698.3	54687
1	4473.7	19606.1	3560.7	4933.2	1879.3	14895.5	202718.2
1.5	8504.4	41750.8	7521.4	10740.2	4233.5	36997.4	343918.7
2	14503.6	70990.1	12830.8	18855	8426	75309.1	407200.6
2.5	22368.6	110211	19392.7	29948.7	15289.7	130481.7	239881.2
3	33136	158823.3	27762.7	43107.7	23644.3	143407.5	123625.9
3.5	46767.7	208792.5	38994.4	62714.3	32233.7	23724.2	71433.9
4	25619.5	176479.6	55675.9	86883.2	40130.1	7535.9	41966.1
4.5	14404.1	69498.7	77256.7	130910.7	49542.5	3645.1	36766.5
5	14793.8	50165.7	108159.1	99919	61972.8	2177.8	20535.1
5.5	10871.6	47555.5	122909.4	50054.7	76388.9	1306.4	6418.1

Table 3.8 continued

Time	Sample#1	Sample #2	Sample #3	Sample #4	Sample #5	Sample #6	Sample #7
6	2699.3	49975.5	54045.7	15355.5	92129.3	875.6	2206.3
6.5	795.2	52770.9	23140.3	3995.9	127967.4	767.5	1054.9
7	400	47266.1	13984.8	953.9	83545.1	681	645.7
7.5	261.5	26677.6	4353.5	336.4	9866.1	669.6	399
8	227.6	8586.2	1007.8	181.4	5318	738.4	338.4
8.5	188.6	2283.1	422.6	130.1	2743.6	842.5	302.5
9	158.9	937.3	290	101.5	1736.7	1026.2	324.1
9.5	130.1	520.3	216.3	115.8	996.2	1174.2	298.4
10	111.7	352.8	202.9	97.3	676.8	1398.7	331.3
10.5	125	289.2	240.9	102.5	601.6	1666	358.9
11.5	130.1	280.9	226.5	119.9	413.4	2433	331.2
12	137.3	261.4	225.5	108.6	409.3	2848.3	333.3
12.5	133.2	306.6	240.9	141.4	374.4	3292.4	332.2
13	150.7	361	265.5	111.7	370.2	3773.8	381.5

Table 3.8 continued

Time	Sample#1	Sample #2	Sample #3	Sample #4	Sample #5	Sample #6	Sample #7
13.5	141.4	333.3	315.8	147.6	368.1	4321.2	323
14	144.5	392.8	317.8	136.3	418.5	4923.5	337.3
14.5	116.8	385.6	324.1	161.9	431.9	5671	288.1
15	138.3	427.8	366.2	261.4	416.5	6113.2	347.7
15.5	148.6	480.3	386.8	252.2	494.6	6836.3	396.9
16	130.1	504.9	364	249.2	502.6	7492.3	396.9
16.5	148.5	515.1	392.8	194.8	551.2	8189.3	446.4
17	142.4	570.8	443.2	162.9	593.4	8674	503
17.5	145.5	603.7	416.5	166	615.1	9668.1	491.6
18	179.4	689.1	463.9	156.8	699.3	10347.6	502.6
18.5	164	752.9	456.7	168.1	716.8	10996.6	522.4
19	163.9	786.7	527.4	197.9	742.6	11408.9	589.1
19.5	168	862.3	486.4	207	789	12083	582.2
20	151.6	871.6	507	171.1	772.5	12444.6	568.6

Table 3.8 continued

Time	Sample#1	Sample #2	Sample #3	Sample #4	Sample #5	Sample #6	Sample #7
20.5	155.8	965.3	477.2	176.3	859.1	13149.8	566.5
21	171.2	1051.1	554.2	212.2	865.1	13702.6	630.5
21.5	180.3	1048.8	536.7	188.6	972.6	14375.2	635.6
22	174.2	1213.2	561.4	192.6	870.5	14772.9	617
22.5	166	1230.9	564.5	191.6	967.4	15146.6	695.4
23	187.5	1325.8	525.4	205	874.8	15243	727.1

Table 4.1 Steady state potential data for 8.66mM HEMA DMAEM hydrogels
Note: Right compartment is the reference compartment which contains 154mM NaCl at all times

S.no	Nacl conc. in left compartment (in mm)	Log(c1/c2)	Potential (in mv)
1	1.54	-2	17.1
2	4.87	-1.5	12.2
3	15.4	-1	5.8
4	48.7	-0.5	2.6
5	154	0	-0.1
6	487	0.5	-2.1
7	1540	1	-4.1

Table 4.2 Steady state potential data for 27.44mM HEMA DMAEM hydrogels

S.no	Nacl conc. in left compartment (in mm)	Log(c1/c2)	Potential (in mv)
1	1.54	-2	48.5
2	4.87	-1.5	40.5
3	15.4	-1	23.9
4	48.7	-0.5	9.4
5	154	0	0
6	487	0.5	-5.3
7	1540	1	-9.1

Table 4.3 Steady state potential data for 86.6mM HEMA DMAEM hydrogels

S.no	Nacl conc. in left compartment (in mm)	Log(c1/c2)	Potential (in mv)
1	1.54	-2	65.1
2	4.87	-1.5	54.2
3	15.4	-1	34.8
4	48.7	-0.5	15.2
5	154	0	0.2
6	487	0.5	-8.6
7	1540	1	-13.7

Table 4.4 Steady state potential data for 273.86mM HEMA DMAEM hydrogels

S.no	Nacl conc. in left compartment (in mm)	Log(c1/c2)	Potential (in mv)
1	1.54	-2	62.4
2	4.87	-1.5	52.8
3	15.4	-1	32.3
4	48.7	-0.5	11.8
5	154	0	-0.1
6	487	0.5	-6.8
7	1540	1	-9.4

Table 4.5 Steady state potential data for 866.01mM HEMA DMAEM hydrogels

S.no	Nacl conc. in left compartment (in mm)	Log(c1/c2)	Potential (in mv)
1	1.54	-2	49.2
2	4.87	-1.5	37
3	15.4	-1	22.9
4	48.7	-0.5	8.8
5	154	0	-0.2
6	487	0.5	-3.1
7	1540	1	-5.5

Table 4.6 Steady state potential data for 8.66mM HEMA MEATAC hydrogels

S.no	Nacl conc. in left compartment (in mm)	Log(c1/c2)	Potential (in mv)
1	1.54	-2	46.3
2	4.87	-1.5	44.8
3	15.4	-1	27.9
4	48.7	-0.5	11.2
5	154	0	0.3
6	487	0.5	-5
7	1540	1	-8.4

Table 4.7 Steady state potential data for 27.4mM HEMA MEATAC hydrogels

S.no	Nacl conc. in left compartment (in mm)	Log(c1/c2)	Potential (in mv)
1	1.54	-2	72.4
2	4.87	-1.5	55
3	15.4	-1	34.1
4	48.7	-0.5	14.6
5	154	0	0.1
6	487	0.5	-9.1
7	1540	1	-14.4

Table 4.8 Steady state potential data for 86.6mM HEMA MEATAC hydrogels

S.no	Nacl conc. in left compartment (in mm)	Log(c1/c2)	Potential (in mv)
1	1.54	-2	54.9
2	4.87	-1.5	44.1
3	15.4	-1	23.7
4	48.7	-0.5	9.5
5	154	0	-0.2
6	487	0.5	-5.8
7	1540	1	-8.6

Table 4.9 Steady state potential data for 273.86mM HEMA MEATAC hydrogels

S.no	Nacl conc. in left compartment (in mm)	Log(c1/c2)	Potential (in mv)
1	1.54	-2	50.8
2	4.87	-1.5	31.4
3	15.4	-1	16.2
4	48.7	-0.5	6.8
5	154	0	-0.3
6	487	0.5	-2.2
7	1540	1	-5.9

Table 4.10 Steady state potential data for 866.6mM HEMA MEATAC hydrogels

S.No	NaCl conc. in left compartment (in mM)	Log(C1/C2)	Potential (in mV)
1	1.54	-2	50.6
2	4.87	-1.5	33.1
3	15.4	-1	16.4
4	48.7	-0.5	7.8
5	154	0	0.1
6	487	0.5	-3
7	1540	1	-3.5

Vita

Arun Balasundaram was born on January 5th 1982 in Tamilnadu, India. He graduated from University of Madras, India with a bachelor's degree in Electrical and Electronics Engineering. He then attended University of Tennessee, Knoxville and earned his Master's degree in Engineering Sciences with an emphasis in Biomedical engineering.

Vita

Arun Balasundaram was born on January 5th 1982 in Tamilnadu, India. He graduated from University of Madras, India with a bachelor's degree in Electrical and Electronics Engineering. He then attended University of Tennessee, Knoxville and earned his Master's degree in Engineering Sciences with an emphasis in Biomedical engineering.